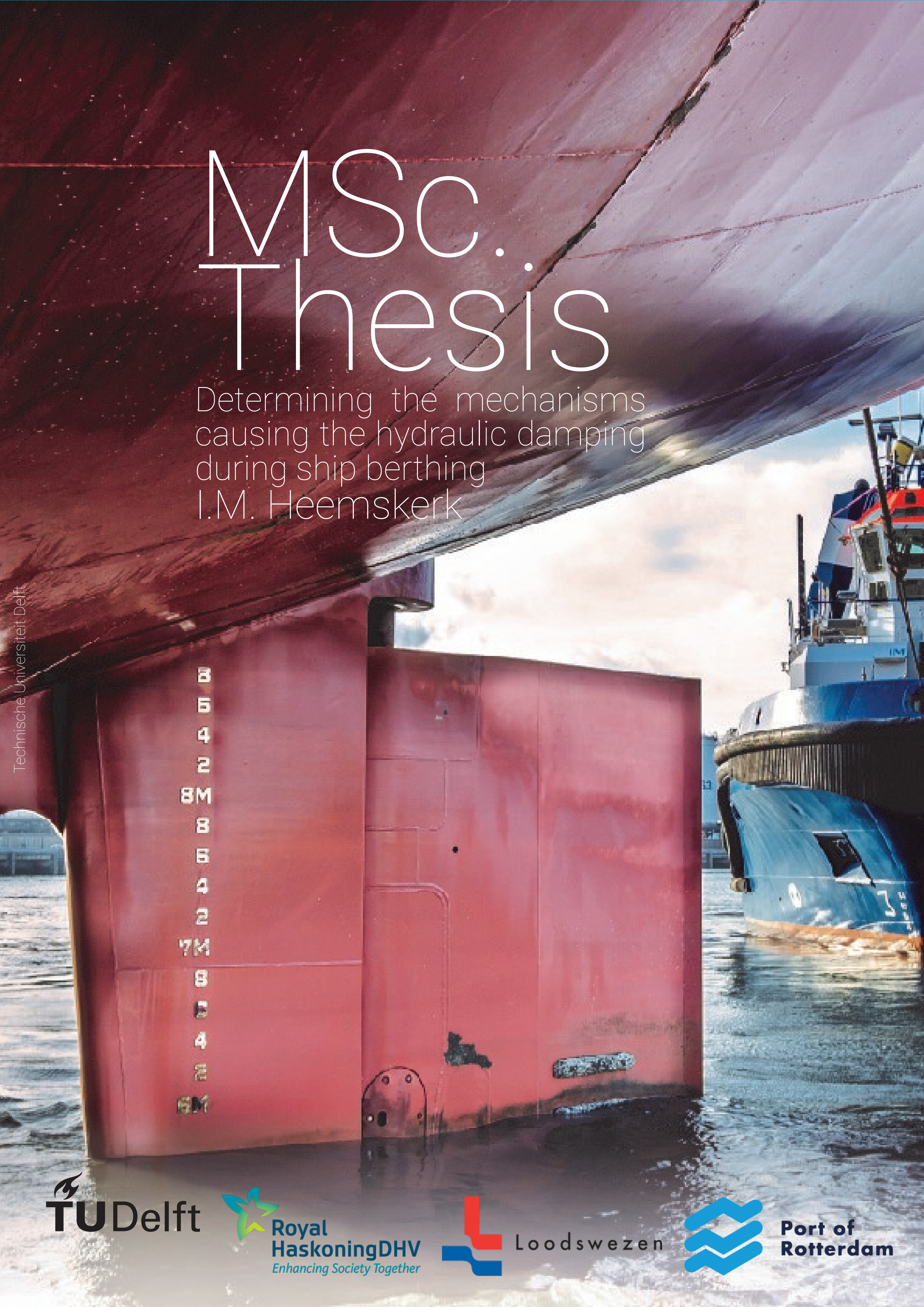

MSc. Thesis

Determining the mechanisms causing the hydraulic damping during ship berthing

I.M. Heemskerk

Technische Universiteit Delft

TU Delft | Royal HaskoningDHV Enhancing Society Together | Loodswezen | Port of Rotterdam

MSc. Thesis

Determining the mechanisms causing the hydraulic damping during ship berthing

by

I.M. Heemskerk

to obtain the degree of Master of Science
at the Delft University of Technology,
to be defended publicly on Thursday May 28, 2020 at 14:00 pm.

Student number:	4312740	
Project duration:	May 1, 2019 – May 28, 2020	
Thesis committee:	Prof. dr. ir. W.J.S. Uijttewaal,	Delft University of Technology,
	Dr. ir. R.J. Labeur,	Delft University of Technology,
	Ir. E.J. Broos,	Port of Rotterdam & Delft University of Technology,
	Ir. P. Groenewegen,	Royal Haskoning DHV,
	W. van Buuren,	Dutch Pilotage Service.

TU Delft

Preface

This master thesis concludes my time at Delft University of Technology and completes my Master of Science program in Civil Engineering with the specialization 'Hydraulic Engineering'. The research was carried out at the Port of Rotterdam in joint collaboration with the Dutch Pilotage Service and Royal Haskoning DHV.

The last 12 months have definitely been a journey. They have been very educational and they showed me where my strength lies and where my passion is. Developing and executing my own field experiments and manoeuvres with the largest vessels in the Port of Rotterdam is something that I would never thought I would get the chance to. It was very exiting, but also very challenging and stressful. I am very happy with the end result that you have in front of you and I hope you enjoy reading my final work before I officially become an Hydraulic Engineer.

I could not have done this without the help of many people and will therefore take a moment to thank them. I want to express my gratitude to my thesis committee for their feedback, knowledge and help throughout the last 12 months. First of all Erik Broos, my daily supervisor, thank you for pushing me and reminding me of the fact that everything is possible if you put your mind to it. You reminded me often that my thesis was just playing with very large boats, which student would not want that? Thank you Wim van Buuren in assisting me in every possible way during the execution of my experiments. I am so happy that I got to experience the work the Dutch Pilotage Service does and I am aware that I was very lucky to accompany you during your work. Flying in a helicopter to a huge vessel in the north sea is not something that I do every day. Thank you Perry Groenewegen for your listening ear, patience and constructive feedback when writing my report. You always found the time to help me. Thank you Robert Jan Labeur and Wim Uijttewaal for your supportive criticism, your feedback, inspirational amount of knowledge and for reminding me of what a Delft engineer should represent.

Thank you Michel Ruijter for setting up and executing my field experiments with me from scratch. Without you and your expertise this research would have stranded. The EECV terminal and in particular Bjorn Gaede and Ben Arensman, thank you for your time and enthusiasm when I came along with a bunch of instruments that I just wanted to install under water around Christmas time.

To my friends, mom, dad, roommates (old and new) and especially Thijs a big thanks for motivating me, supporting me and providing the much needed distraction. You always reminded me of the fact that everything will be okay and that I eventually will get my academic title.

I wrote the final part of my thesis and this preface during the Corona crisis. At first, I was very disappointed that the much needed and deserved end of my academic career would be a bit of an anticlimax. However, I now realise that I am very lucky that I got to finish my project and that the day of my graduation will be very unique and just as special as a normal graduation procedure.

With these last words I conclude my time as a student and a new chapter of my life will begin. If I look back at the last 6.5 years in Delft I do not think it could have been any better. I am ready to start a new chapter and I am very excited to develop myself as a professional Hydraulic engineer.

Enjoy reading!

I.M. Heemskerk
Rotterdam, May 2020

Summary

When a large ship enters a port the vessel is navigated by the pilots instead of the captain due to safety reasons. The final part of the berthing manoeuver is the most critical and consists of the vessel moving laterally towards the quay wall. At this point the vessel does not use its own propulsion force anymore but is pushed by the tugboats. During this lateral berthing manoeuver a resistance force can be noticed counteracting the lateral manoeuver to the quay which acts as hydraulic damping. A large force is needed to overcome this hydraulic damping which is referred to as the water cushion effect.

There are a handful of circumstances that are suspected to enhance the effect of hydraulic damping, but a substantiated conclusion is not yet drawn. To determine the key variables influencing the hydraulic damping the mechanisms causing hydraulic damping need to be comprehended and explained.

A literature review is performed to define the scope and find the knowledge gaps in hydraulic damping. It emerges that there are two hydrodynamic processes that could happen causing hydraulic damping. The first processes is a water level elevation between ship and quay due to the increased pressure when the ship approaches the berth, following the law of continuity and momentum. This water level elevation causes an extra counteracting force on the berthing vessel expressed in hydraulic damping. The second process is based on continuity without water level elevation, in combination with translation waves which originate from the acceleration and deceleration of the vessel. These translation waves travel towards the quay wall, reflect, travel back and act as a counteracting force on the ship's hull. Furthermore, the key variables that are suspected to have an influence on the hydraulic damping are identified.

Field experiments that are setup conform the conclusions drawn from literature are carried out. The field experiments consist of two parts. The first experiment investigates the vicinity of the quay wall on the magnitude of the hydraulic damping. Experiment 2 investigates the pressures and flow velocities between ship and quay during a lateral berthing manoeuver. The results obtained from the field experiments show that the counteracting force working on the vessel is significantly larger when the quay wall is in close proximity, following from the angular deceleration. This finding is contradicted by the behaviour of the lateral deceleration of the center of the vessel. This could be explained by environmental forces acting on the vessel during the first half of the berthing manoeuver. The measured pressure distribution between ship and quay shows the tidal increase measured in the port in combination with oscillations due to waves. Water level elevation due to the lateral berthing manoeuver cannot be deduced from these measurements due to the oscillations and the lack of accuracy of the hydrostatic pressure measurements. The oscillations due to waves are twice as large when a berthing manoeuver is performed compared to an empty basin.

A theoretical model, based on one of the two hydrodynamic processes is developed. The one-dimensional model represents the first hydrodynamic process, the water level elevation due to the approaching vessel causing hydraulic damping. The field experiments are simulated using the model to validate the assumptions made in the model. The model is applicable for the evaluation of the hydrodynamic forces because the simulations and the field experiments coincide nicely. The key variables and their influence on hydraulic damping are further investigated using the validated theoretical model. The model does capture the main physics during the berthing manoeuver but the environmental forces such are wave and current are not modelled for.

During experiment 1 environmental conditions played a role and during experiment 2 set up and accuracy could be improved. The water level elevation measurements were not accurate enough to substantiate the conclusions drawn. To make a clearer comparison between the model and the experimental results several adjustments could be made to the model as well as the experimental set-up. However, there is enough substantiation to draw solid conclusions.

Water level elevation due to pressure increase between ship and quay is the hydrodynamic mechanism that causes hydraulic damping during the lateral berthing manoeuver. The theoretical model captures the hydrodynamic processes causing hydraulic damping during ship berthing nicely. By performing a parameter study of the validated model the key variables enhancing hydraulic damping are found. The three key variables enhancing hydraulic damping are the under keel clearance, the ship velocity and the ship dimensions in the order of biggest influence. To quantify the key variables more precisely, further research is recommended.

Contents

List of Tables

List of Figures

Nomenclature

ADCP	Acoustic Doppler Current Profiler	
CT	Container Terminal	
DWT	Dead Weight Tonnage	
GDP	Gross Domestic Product	
GNSS	Global Navigation Satellite systems	
HoT	Height of tide	
MPU	Main Processing Unit	
PIANC	Permanent International Commission for Navigation Congresses	
PPU	Portable Pilot Unit	
RANS	Reynolds-Averaged Navier-Stokes	
RTK	Real Time Kinematic	
UKC	Under keel clearance	
α	Angle between velocity vector and the perpendicular of the quay	°
β	Ratio between under keel clearance and ship draught	-
χ	Resistance parameter	-
$\ddot{x}_j$	Acceleration	m/s^2
δH	Loss at internal flow	m
$\dot{x}_j$	Velocity	m/s
μ	Dynamic viscosity	Pa*s
ϕ	Angle between velocity vector and line between point of contact and centre of mass	°
ρ	Density of water	kg/m^3
τ	Half-life	s
ε	Total loss	
A	Wetted area	m^2
$a_{kj}(\omega)$	Added mass coefficient	-
B	Width vessel	m
$b_{kj}(\omega)$	Hydrodynamic damping coefficient	-
c	Speed of sound	m/s
C_b	Block coefficient	-
C_c	Berth configuration factor	-

C_e	Eccentricity factor	-
C_F	Frictional resistance coefficient	-
C_m	Virtual mass factor	-
C_s	Softness factor	-
c_{kj}	Restoring hydrostatic coefficient	-
D	Draught vessel	m
D_h	Hydraulic diameter	m
E_f	Absorbed energy by fender	kNm
E_h	Hull elasticity	-
E_s	Kinetic energy of vessel	kNm
E_{fen}	Fender elasticity	-
f	Friction factor	-
$f_{Doppler}$	Doppler shift	Hz
F_k	External force	N, Nm
h	Water depth	m
h_0	upstream water level	m
h_2	downstream water level	m
K	Radius of gyration of the vessel	m
L	Length vessel	m
M_s	Mass of vessel	t
M_v	Virtual mass	t
M_{kj}	Mass, moment of inertia	-
P	Wetted perimeter	m
R	Distance of point of contact to centre of the mass	m
R_F	Frictional resistance	N
R_h	Hydraulic radius	m
Re	Reynolds number	-
S	Wetted surface	m^2
s	Distance	m
t	Time	s
V	Flow velocity	m/s
V_s	Berthing velocity of vessel	m/s
x_j	Displacement	m

1 Introduction

1.1. Context

The Port of Rotterdam is the biggest port of Europe and the tenth largest port in the world with over 469 million tonnes of cargo in 2018 (Port of Rotterdam, 2018). After major developments in container ports it is now the 11^{th} biggest container port in the world with a 13.7 million TEU transfer in 2017 (Braden, 2018). The added value of the port is more than 45.6 billion euros, which is 6.2% of Dutch GDP. The port area stretches over a length of 42 kilometers and covers an area of circa 12,500 hectares. The success of Rotterdam's port lies in its ability to handle the biggest ships with world's deepest draughts. The size of the port and the immense variability in waterways requires a large, all-round group of pilots to manoeuver the vessels safely and quickly into the harbour. This is a comprehensive task, 220 pilots help on average 56000 vessels to smoothly enter and leave the port every year (*Nederlands Loodswezen*, n.d.). The area is full of terminals, refineries and chemical plants, heavily trafficked hence, safety comes first.

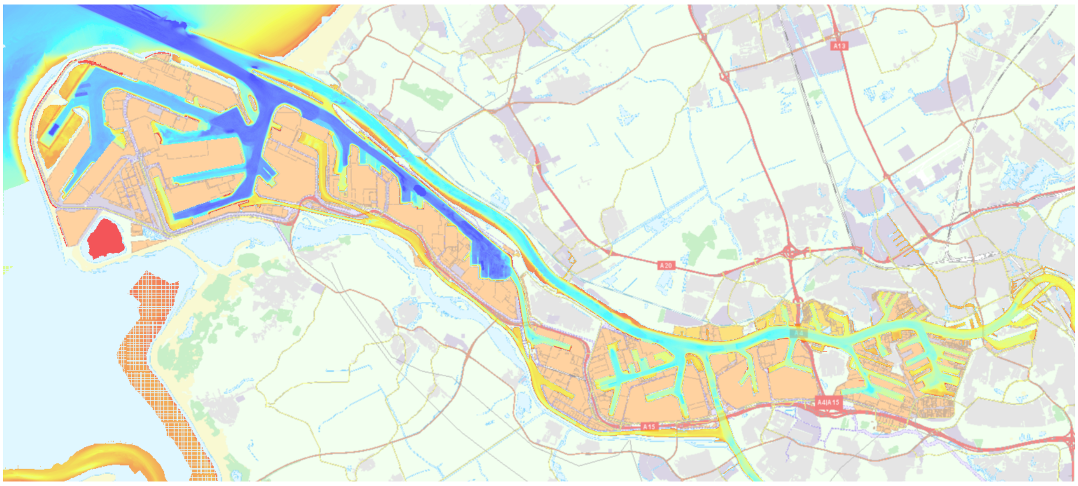

Figure 1.1: Port of Rotterdam (PoR, 2019)

A pilot enters the ship at sea via helicopter or boat and with approval of the captain, takes over the conduct of navigation. Pilots know the port by heart and are specialised in navigating and manoeuvring vessels through these waters. For larger vessels, additional tugboats are used to assist manoeuvring. The most demanding part is berthing the vessel without damaging the ship's hull, fenders or quay. Pilots know from experience that water can behave such that it counteracts or enhances the movement of the ship. This is not a problem when expected, a pilot can anticipate or even make use of these extra effects. One of these effects is the so-called water cushion. Water is 'trapped' water between ship and quay acting as a cushion, absorbing kinetic energy. There are many theories on the behaviour of a water cushion, but there is no clear answer on the development of the water cushion yet.

When a vessel decelerates and accelerates through water it drags a certain amount of mass with it, called the virtual mass or added mass. This virtual mass is actually a hydrodynamic force on the ship due to inertia, counteracting the lateral movement of the ship and therefore will be referred to as hydrodynamic added mass. During berthing, the ship stays as parallel as possible to the quay wall and moves laterally through the water. If the ship comes closer to quay, the pilot notices that the velocity decreases up until a point that part, or even all of the kinetic energy is absorbed and the ship comes to a halt or nearly a halt. When the pilot tries to push through this barrier, he notices that a lot of power from the tugboats is needed to manoeuver the ship against the berth. This barrier is hydraulic damping and referred to as the water cushion. It could be treacherous if the cushion suddenly vanishes, the vessel will impact the quay with larger forces than intended, potentially damaging the ship. The pilot usually starts to feel the cushion, if present, from approximately 10 to 1 meters away from the quay wall. When the pilot has pushed through this cushion and the ship is safely berthed, the effect is not vanished yet. When the pilot wants to unberth the vessel, the inverse cushion can still play a role and act as a suction force between quay and ship complicating the deberthing manoeuver.

The understanding and therewith prediction of the hydrodynamic counteracting forces is relevant for the pilots during berthing manoeuvers and is relevant for fender design. If the pilots know the driving forces of the presence of a water cushion, they can anticipate on the effect during the berthing manoeuver. This contributes to a safer berthing manoeuver and less chance of incidents. For fender design, the understanding and predicting of the hydraulic counteracting forces can contribute to substantiating the many assumptions used in the kinetic energy method. If the amount of assumptions is reduced and the hydrodynamic processes happening during the berthing manoeuver are better understood, the correction factors can be revised. This leads to a safer and more economical design. Revising of the method is also needed for design values to match pilots predictions.

1.2. The problem

The focus of this research is on the water cushion during berthing and therefore the inverse cushion effect is not within the scope of this research. After thoroughly reviewing literature and consultation with the pilots it became clear that the water cushion effect is not fully understood. There are terminals where the cushion effect is always noticed by pilots. There are also a handful of terminals where the cushion effect is never noticed by pilots and terminals where it is not sure if the cushion effect will be noticed. To anticipate during berthing, it would be a great addition if the pilot knows what processes are the cause of the rising of the water cushion. With this knowledge the pilot can predict the effects depending on the specific circumstances.

The effect of the water cushion is also taken into account in the design guidelines of fenders (PIANC, 2002)(Hafenbautechnische Gesellshaft (EAU2012), 2012)(British Standards Institution (BS6349-2), 2019). In design guidelines the required energy absorption by the fenders is reduced by 10% if the quay wall has a closed configuration. When the quay wall has a closed configuration it is assumed that a water cushion will develop, absorbing part of the kinetic energy. This value is based on empirical data and experience over the years and not on the actual process of the water cushion. Besides, the design guidelines contain a value for added mass, defined as the mass that travels with the vessel during acceleration and deceleration during berthing. This added mass contributes to the actual mass of the vessel, increasing the force on the marine structure. In reality, this added mass is a lot more complex than the stigmatization of water traveling with the vessel.

1.3. Objective

The objective of this research is to understand the hydrodynamic mechanisms causing the presence of a water cushion during berthing. Consequently, this research will provide an insight in the hydrodynamic processes contributing to the trapping of water between ship and quay. To meet the objective of this research, the flow behaviour around a lateral berthing ship should be investigated. Based on the objective, the following research question is specified.

Which mechanisms cause hydraulic damping between ship and quay during berthing and how can they be explained?

To answer the research question, a number of sub-questions are formulated:

- How does the flow behave around a berthing ship and how can this behaviour be explained?
- What are the key variables causing hydraulic damping and how do they affect the flow behaviour around a berthing ship?
- In what way is the movement of the ship influenced by the hydrodynamic forces acting on the ship?
- How can the forces acting on the ship generated by the hydrodynamic flow during berthing be determined and modelled?

1.4. Research method & thesis outline

This research consists of four major phases to obtain an answer to the research questions and eventually achieve the objective of this research. First, the scope is defined through the literature review in chapter 2. The literature review is also used to gain insight in the flow behaviour around a lateral berthing ship. Second, field experiments are set up conform the knowledge gap emerged from the literature review in chapter 3. In chapter 4 the results of the experiments are presented and analysed. The third step is developing a theoretical model of hydrodynamic processes and validating this model using the results from the field experiments. This is done in chapter 5. The last phase is discussing the obtained results (Chapter 6), drawing conclusions and giving recommendations for further research in Chapter 7.

1.4.1. Literature review

The first step of this research is an extensive literature review. The concepts and knowledge gained in this literature study are used to determine the relevance of this thesis, available knowledge, previous research and serves as a background for following phases. In the literature review insight is gained in:

- The hydrodynamic processes that play a role during vessel berthing
- The variables interesting for determining water cushion effects
- The different methods to evaluate hydrodynamic processes of a berthing vessel
- Problems with the approach used in design guidelines

1.4.2. Field experiments

The second step in the research are the field experiments. The knowledge gaps that surfaced from the literature review are investigated with field experiments using a large vessel. After the literature review and deliberation with the pilots, two experiments are developed and a suitable quay wall and type of ship are chosen for futher investigation. The arrivals of suitable ships at suitable quays are very limited in December 2019 hence the choice for only one ship at one quay. This quay wall in combination with the ship are chosen because the water cushion effect will most likely occur. The field experiments are done to measure the flow around a berthing ship and measure the influence of the quay wall on the hydraulic damping. Furthermore, the field experiments are done to validate the theoretical model.

1.4.3. Theoretical model

Next to the field experiments, a theoretical model is developed. The theoretical model is validated using the results of the field experiments. Consequently, the assumptions made developing the one-dimensional model are investigated and therewith the generic applicability of this model on lateral berthing manoeuvers. In addition, if the one-dimensional model suffices, a parametric study is performed to investigate the influence of the key variables that appeared from the literature review.

1.4.4. Implementation

The final phase of the research is drawing conclusions from the field experiments and the validation of the theoretical model. The reliability of the results is discussed, the research questions are answered and recommendations for further research are given. In addition, recommendations are made for redefinition of the PIANC design factors conform the conclusions drawn from research.

2
Literature review

2.1. Introduction

In the literature review the berthing process and the physics of the berthing process are thoroughly described. This is done by analyzing the hydrodynamic processes that play a role during vessel berthing. The influence of the key variables during ship berthing on the hydrodynamic flow is investigated and elaborated to the variables interesting for water cushion effects in the guidelines of fender design. Furthermore, the different methods and models discussed in literature to evaluate the hydrodynamic processes are explained. The existing methods that are used to determine the hydrodynamic forces on the ship and thereby the forces acting on the ship's hull, quay and fenders are:

- Mathematical modelling
- Scale model tests
- The Kinetic Energy method

Finally, the problems with the approach used in the guidelines for fender design are assessed.

When a vessel enters a port, a chain of events is set into motion. First thing being safely boarding a pilot to take over conduct of navigation with permission of the captain. These maritime pilots navigate and manoeuver vessels through the port and ensure safe berthing. In addition, tugboats are used for larger vessels to assist the manoeuvering during sailing and berthing in the harbour. The common procedure for berthing manoeuvres in the Port of Rotterdam is for the tugs and the pilot to position the vessel at a certain distance from the berth, as parallel and centered to the quay as possible. The vessel is kept into place while mooring ropes are lowered overboard into the boats of the boatmen. The boatmen pick them up and bring the ropes to the quay where they manually attach the ropes to the mooring bollards. For certain ships the mooring ropes are thrown directly onto the quay via a second lighter rope, so no boats are necessary between the vessel and the quay. When the mooring ropes are secured, the tugboats push the ship to the quay and at the same time the ship starts bringing the mooring ropes in, moving closer to the berth (*Nederlands Loodswezen*, n.d.).

Berthing is considered safe when the vessel is brought to a halt against the berth and there is no damage to the ship's hull, fender or quay wall. This is only possible when the fender system or quay wall can absorb and dissipate the kinetic energy of the vessel until the vessel has come to a halt (Eskenazi & Wang, 2015). The vessel could bounce back on the fender due to fender characteristics and after correction of the pilot and tugs, a second sometimes even stronger impact could take place (Saurin, 1963). The focus of this research will be on the initial impact of the vessel and quay wall.

The berthing manoeuver of a vessel contains multiple complicated phenomena. The parameters to be considered are ship geometry, approach velocity, approach angle, hull elasticity, berthing site, fender structure, under keel clearance, water cushion between ship and quay wall, forces applied by tugboats, waves, current, wind and rotational and translational motions of a ship (PIANC, 2002). This research focuses on vessel berthing and in particular the presence of the so-called water cushion and its effect on vessel berthing.

A water cushion is considered to be water 'trapped' between ship and quay. This water cushion absorbs kinetic energy and therefore acts as a cushion between ship and quay by dampening the lateral velocity of the vessel close to the quay. When a ship approaches its berth, the ship is positioned parallel at a certain distance to the berth. Starting from that position, the ship does not use its own propulsive force anymore and the berthing manoeuver is set into motion by tugboats. The tugboats position themselves at the side of the ship, opposite of the quay wall, so they can push the ship laterally towards the quay. First, the tugboats set the ship into motion and afterwards the tugboats apply force to keep the ship at constant velocity. When the ship starts moving, the water around the ship needs is set into motion as well. The resistance of the fluid to the accelerating motion acts as a counteracting force on the lateral movement of the ship. These forces that resist changes in water velocity are inertial forces, and act upon a body that is accelerating or decelerating (Demenet, 2018). In addition to the inertial forces, the ship experiences resistance forces due to viscous effects on the ship's hull and due to turbulent flow as a result of the water flow around the ship. There is a significant difference between the inertial forces and the resistance forces. The inertial forces only play a role during accelerating or decelerating. The resistance forces play a role during accelerating, decelerating but also at constant velocity. The inertial forces and resistance forces together are the hydrodynamic forces acting on a moving ship. Inertial forces are often simplified and schematised as some volume of water moving with the object called hydrodynamic added mass or virtual mass. In reality however, all fluid will be accelerated to various degrees (Lisy & Tothova, 2004). In ship hydrodynamics, the virtual mass is usually added to the actual mass of the ship and together they represent the effective mass of the ship for further applications. However, this method is derived for deep water and does not account for the nearby presence of confining walls or the seabed which could influence the effect of the virtual mass on the manoeuver.

Before a a vessel berths, the pilot decides the rate of turn and berthing velocity dependent on multiple variables. The pilot takes into account ship dimensions, ship mass, under keel clearance, current, wind, type of quay wall, tug assistance and does this conform design values, but also from experience. The pilots use portable pilot units (PPU) and on board computers to obtain all this information. When a water cushion is present, the pilot notices that the vessel looses lateral velocity while the tugboats apply the same power to the vessel. It is even possible that the vessel comes to a halt completely while the tugboats are still applying power. The pilot notices that a lot of power is needed to push through this barrier.

From deliberating with the pilots it becomes clear that if the pilot can predict the presence of a water cushion, the pilot can anticipate the effects during the berthing manoeuver. Moreover, if the driving forces of the presence of a water cushion are understood, the water cushion effect can be implemented in fender design to obtain a more accurate and economical design.

There has been research on kinetic energy absorption and contributing factors such as berthing velocity and berthing angle, but little has been investigated on water cushions and the driving forces thereof. Because the focus of this research is the rising of a water cushion and therefore the process before impact on the fender structure, the amount of absorption of the marine structure will not be reviewed in detail and will only be referred to as appropriate.

2.2. Hydrodynamic processes around a berthing ship

A ship has six degrees of motion during sailing. Three motions of translation called heave, sway and surge and three motions of rotation called yaw, pitch and roll. This is shown in figure 2.1.

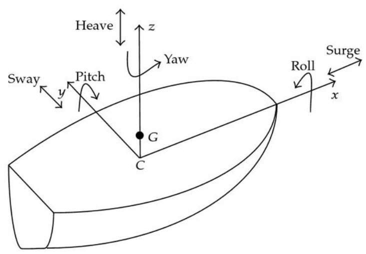

Figure 2.1: Six degrees of freedom of a ship (Ibrahim & Grace, 2010)

Because the ship moves mainly in the horizontal plane, at low speed and in shallow water, the two most important motions are yaw and sway.

2.2.1. Pure sway motion: two-dimensional flow behaviour

An ideal berthing manoeuver would be a pure sway motion. In case of yaw the vessel will not stay entirely parallel to the quay wall and the flow profile around the ship will change. In an ideal sway motion the ship pushes through water and a positive pressure field develops at the leading side of the ship. This positive pressure field remains present while the ship keeps moving laterally. This pressure field results in a pressure gradient over the vertical and in a two-dimensional approach, two things can happen. The water flows upward which results in a water level elevation or the water flows downward and flows away under the keel of the ship. Chen et al. (1997)(2000) developed and validated a Reynolds-averaged Navier-Stokes (RANS) method for time-domain simulations of a berthing ship. With this model, Chen et al. (1997) conclude that the behaviour of the water flow as a consequence of the vertical pressure gradient at the leading side of the ship depends on the behaviour of the free surface. For low Froude numbers the free surface remains almost entirely flat, pushing the water downwards through the gap resulting in high flow velocities under the ship. These high under keel flow velocities cause a large circulating flow in the wake region behind the ship. At higher Froude numbers, the water is not forced through the under keel gap but is pushed upwards resulting in a rising water level. This coincides with lower under keel flow velocities and pressure gradients. In conclusion, the lateral movement of a ship, the amount of water escaping under the keel depends mainly on the Froude number. The Froude number determines the behaviour of the free surface.

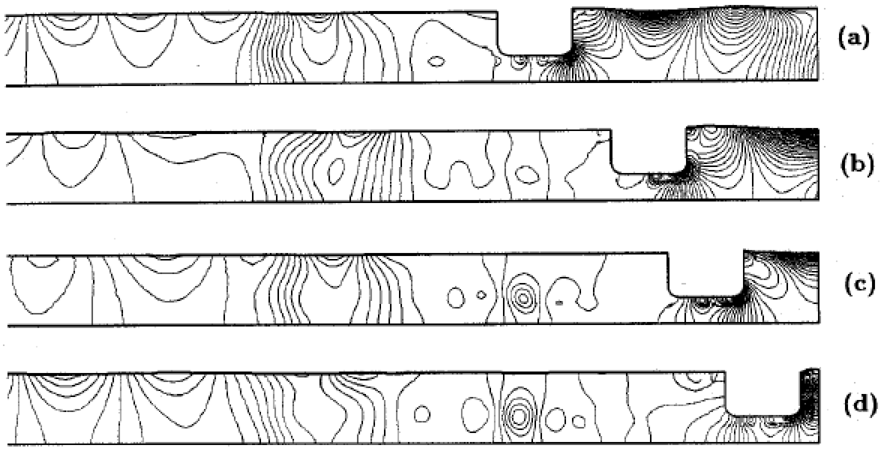

Figure 2.2: Pressure contours berthing ship, Fr = 0.03 (a) $t = 2.2$, (b) $t = 2.4$, (c) $t = 2.5$, (d) $t = 2.6$ (Chen et al., 1997)

In figure 2.2 the two-dimensional flow behaviour around a berthing ship in a fully sheltered harbour is modelled. A low Froude number, $Fr = 0.03$ and a turbulent flow case, $Re = 10^6$ are used. For completeness the velocity vector plots are shown in figure 2.3. From figure 2.2 it is seen that a pressure field is present in front

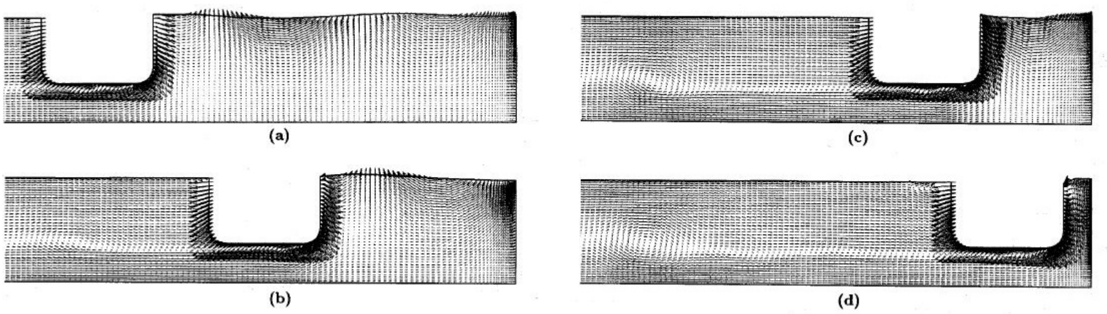

Figure 2.3: Velocity vector plots berthing ship, Fr = 0.03 (a) $t = 2.2$, (b) $t = 2.4$, (c) $t = 2.5$, (d) $t = 2.6$ (Chen et al., 1997)

of the lateral moving ship. The positive pressure field travels to the quay wall during the berthing manoeuver and eventually reflects on the quay wall, travels back to the ship's hull and reflects again. This results in a complicated free-surface elevation. Moreover, high pressures are seen at the bulge of the ship. Because the Froude number is low (0.03) the water does not move entirely upwards following the high pressures but is also forced downwards and escapes through the under keel gap. In figure 2.3 it is seen that longitudinal flow velocities are present under the keel and a circulation pattern in the wake behind the vessel is present. The most important observation from 2.3 is that the pressure field over the entire ship's draught between ship and quay is clearly visible and caused by both the waves reflecting from the quay wall as the incoming waves the lateral moving ship produces when the ship approaches the quay. This high pressure field leads to water movement. Because the Froude number is small, the water can not move upwards, rising the free surface. The water needs to flow through the under keel gap, resulting in high under keel flow velocities. The water cushion effect is clearly visible here. Apparently, the water cannot escape between ship and quay fast enough under the keel, indicating that there is a maximum possible under keel flow velocity.

2.2.2. Pure sway motion: three-dimensional flow behaviour

In Chen and Huang (2000) the RANS method is elaborated, applied and validated for a three-dimensional vessel. For simplicity the free surface effects are neglected, this is justified because the Froude number for this specific research is less than 0.005 as stated in paragraph 2.2.1. In figure 2.4 it is seen that a large pressure field is present close to the ship's hull in front of the laterally moving ship, similar to figure 2.2, only now three-dimensional. This pressure field generates a gradient in vertical direction inducing vertical flow either in the form of water level elevation or under keel flow. This is treated in section 2.2.1 for a two-dimensional approach. Because the flow is treated in 3 dimensions, this pressure field also causes a gradient in horizontal direction resulting a longitudinal flow. This longitudinal flow enables the escaping of water via the bow and stern.

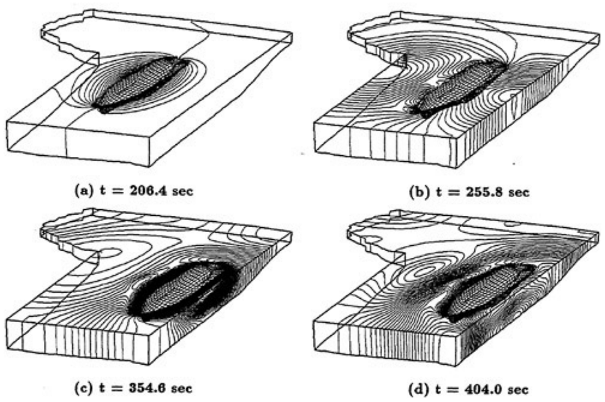

Figure 2.4: Free surface pressure contours in close vicinity of the quay wall (Chen & Huang, 2000)

In figure 2.5 the free surface velocity factors are shown for a berthing ship. A recirculating flow pattern is clearly visible at the stern of the vessel. With a lateral berthing vessel, the pressure between ship and quay causes under keel flow and flow via the bow and stern. The ratio of water flowing around the bow and stern of this vessel is estimated at 30% and the remaining 70% flows under the keel. This ratio will most likely depend on the under keel clearance and the hull shape.

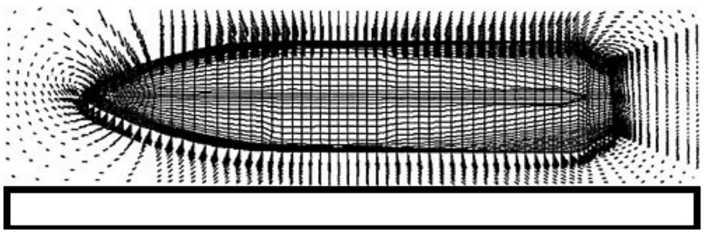

Figure 2.5: Free surface velocity vectors in close vicinity of the quay wall (Chen & Huang, 2000)

To investigate the unsteady three-dimensional flow behaviour more, the velocity vector plots are shown as well in figure 2.6. It is seen that due to sharp corners of the keel a flow separation and reattachment pattern in the direction of the ship's motion is caused. A circulation flow in the wake of the ship at mid-ship is present too when the ship approaches the quay as seen in figure 2.6 a. If one looks at figure 2.6 b it is seen that the flow patterns differ significantly at the stern of the ship in comparison to the flow patterns midships. A recirculation pattern is present which is caused by the skeg of the ship. The under keel flow velocities at the stern are significantly lower than the under keel flow velocities at midships. A plausible explanation would

Figure 2.6: Velocity vector plots of a ship approaching a quay wall (Chen & Huang, 2000)

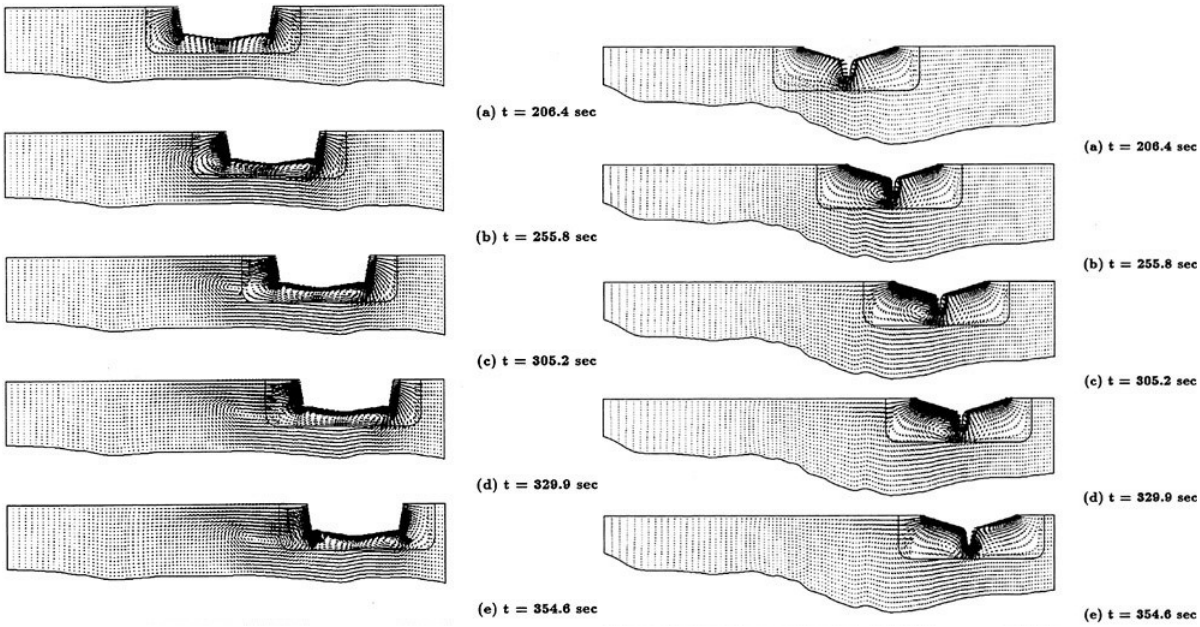

(a) Cross section at mid ship

(b) Cross section at stern

be the fact that the distance to the bottom at the stern is much larger than the distance to the bottom midships. Another explanation is that at the stern the water flows partly around the stern instead of under the keel. The fact that the path to be covered by the water flow under the keel at midships is bigger than the path under the keel at the stern could also contribute to the explanation. As concluded in the two-dimensional approach, the most important observations are the high pressures between ship and quay and the high under keel flow velocities. The most important difference in the evaluation between the two-dimensional and three-dimensional simulations is the fact that in the two-dimensional approach all the water needs to escape under the keel, resulting in very high under keel flow velocities and high pressure between ship and quay. In the three-dimensional approach a percentage of the water can escape and run around the bow and stern, resulting in less high under keel flow velocities as seen by the shorter velocity vectors in figure 2.6 a. Chen and Huang (2000) used a vessel with a length-to-width ratio of 4.38 and a length-to-draught ratio of 25.7. The vessels investigated in this research have a length-to-width ratio in the order of $5-10$ and a length-to-draught ratio in the order of 17. This means that the results of this study should be interpreted with caution.

Wang et al. (2017) performed a numerical study using the RANS method on the effect of water depth on the hydrodynamic forces and flow velocities around a berthing ship in vicinity of a quay wall quite recently. The numerical method used is validated successfully with measurements. Interesting in this study is that the free-surface, the quay wall and shallow water are all taken into account. The hydrodynamic forces and lateral flow velocity distributions are investigated during acceleration ($t' = 0-1$), constant velocity ($t' = 1-3$), deceleration ($t' = 3-4$) and rest ($t' = 4-6$) of the vessel (figure 2.7). This is simulated for situations in close vicinity of the quay wall and for different under keel clearances. The time is displayed as the ratio between the time, the width of the ship and the lateral berthing velocity ($t' = t/(B/V_s)$). This study has a lot of similar results as found in Chen and Huang (2000). The water tries to escape between quay and ship through the under keel gap resulting in very high velocity distributions in the under keel gap (figure 2.7). Furthermore, the free surface elevation between ship and quay during deceleration is larger for shallow water than for deep water (figure 2.8), contributing to the theory that with high pressures between ship and quay during lateral berthing, the presence of the bottom causes large flow velocities in the under keel.

From this research it was also concluded that with decreasing water depth the hydrodynamic forces due to inertia and friction increase rapidly on the ship (figure 2.9). The hydrodynamic forces, working laterally on the ship are displayed as the ratio between the hydrodynamic lateral forces and the kinetic energy of the hydrodynamic mass. This gives a non-dimensional hydrodynamic lateral force, $C_y = \frac{F_y}{\frac{1}{2}\rho V_s^2 B^2}$. The water depth is displayed as the ratio between the depth of the water and the draught of the ship ($h' = h/D$).

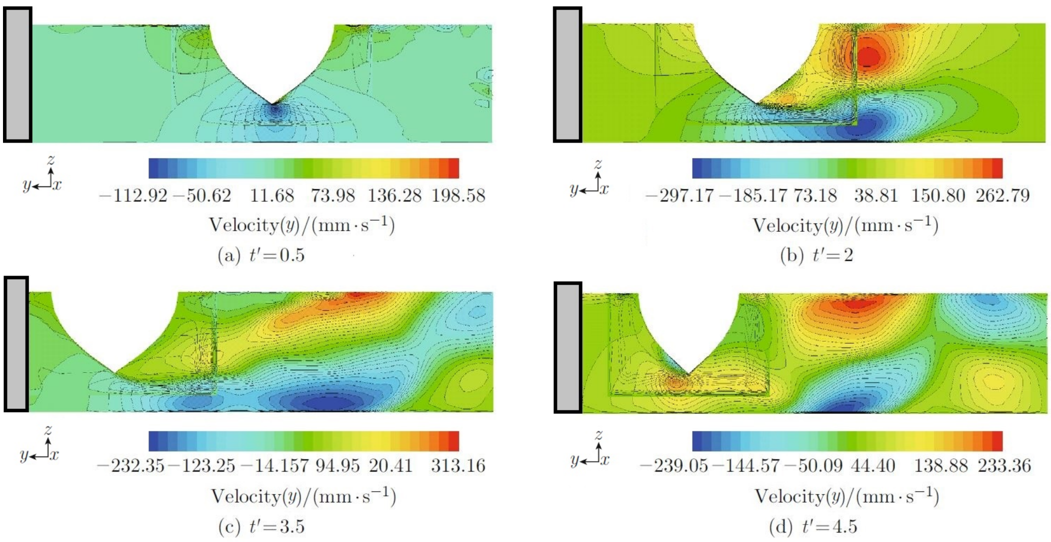

Figure 2.7: Lateral flow velocity distributions at a lateral berthing manoeuver (Wang et al., 2017)

Figure 2.8: Wave elevation contours at acceleration phase (Wang et al., 2017)

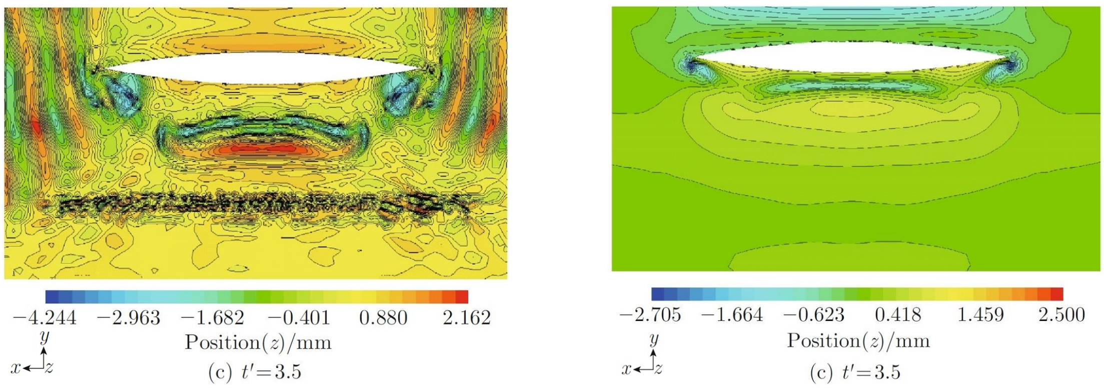

(a) Shallow water

(b) Deep water

In the rest phase the water bounces back and forth between ship and quay, hence the oscillating signal from $t' = 4.0$. The influence of the depth on this phenomenon is that the observed forces on the ship's hull are larger for smallest depth and even push the ship away from the quay, seen as the positive C_y, which can be explained as due to a strong reverse flow as seen at ($t' = 4.3$). This force counteracting the lateral movement of the ship towards the quay is what pilots call the water cushion effect. The same phenomenon does not happen for a larger water depth, the force stays below zero. This could be explained by the large under keel space which allows the water to return with low flow velocities. In figure 2.9 the water cushion effect is clearly visible and directly related to the under keel clearance. According to Grim (1955) the amount of hydrodynamic added mass during berthing increases quickly when the under keel clearance decreases. This starts when the under keel clearance has an order of magnitude equal to the ship's draught. In a recent study Roubos, Groenewegen, and Peters (2017) found no water cushion in results for berthing of large container vessels in several ports. A hypothesis is that the under keel clearance of these vessels was not small enough to produce a water cushion between quay and ship. This is in line with the observations of the pilots. According to Chen et al. (1997) and Chen and Liu (1999) maximum hydrodynamic forces occur when under keel clearance decreases, with further decrease the hydrodynamic forces decrease again. An explanation could be that due to the reflection of the water at the quay, the hydrodynamic forces act on the ship's hull in counteracting direction, decreasing the total hydrodynamic forces working towards the quay.

In Wang et al. (2016) the non-dimensional hydrodynamic forces ($C_y = \frac{F_y}{\frac{1}{2}\rho V_s^2 B^2}$) on the vessel are investigated with respect to four different distances from the quay wall. The vessel performs a lateral berthing manoeuver,

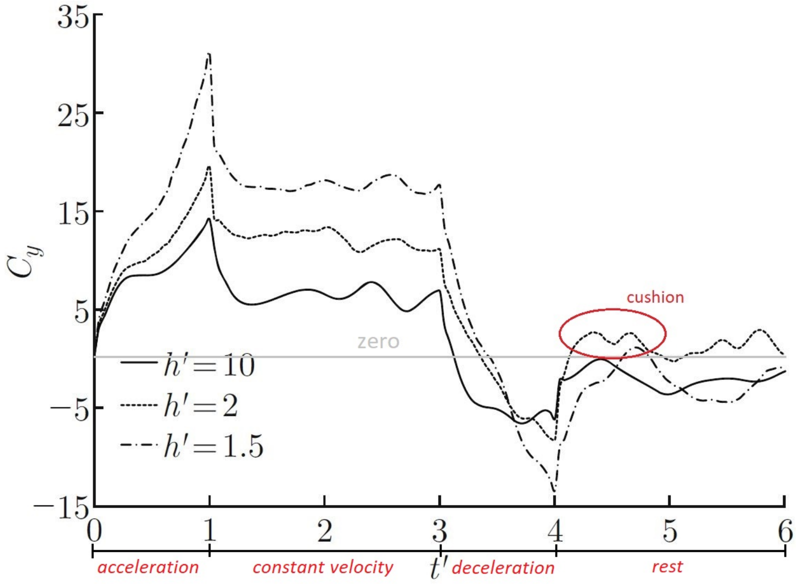

Figure 2.9: Influence h/D on lateral hydrodynamic forces acting on the ship in the vicinity of a quay wall (Wang et al., 2017)

and the distance to the quay wall after performing this manoeuver is investigated. The final distance to the quay wall is the ratio between the final distance of the quay wall, during the rest phase, to the width of the vessel ($s' = s/B$). The velocity profile of the vessel during the berthing manoeuver is the same as in figure 2.7 and 2.9. This means that the vessel accelerates ($t' = 0-1$), has a constant velocity ($t' = 1-3$), decelerates ($t' = 3-4$) and is in rest ($t' = 4-6$). The overall water depth is quite deep, so influence of the bottom of the harbour can be neglected. Figure 2.10 compares the lateral hydrodynamic forces at different final quay wall distances. From this figure it is seen that during the acceleration phase ($t' = 0-1$) the hydrodynamic forces behave almost similarly for different quay wall distances. During constant speed ($t' = 1-3$) the distance to the quay is starting to play a role and especially during deceleration ($t' = 3-4$) and rest ($t' = 4-6$) a significant influence of vicinity of the quay wall is noted. The lateral hydrodynamic forces for the different final quay wall distances differ. When the vessel stops, the water moving with the vessel still has velocity and due to inertia flows further towards the quay wall. The reflection of this current on the quay wall is a plausible explanation for the peak lateral force at $t' = 4.3$. For the distances close to the quay wall the water due to inertia bounces back and forth between ship and quay influencing the hydrodynamic forces on the ship and resulting in complex interactions. The distance far away from the quay ($s' = 50$) also shows an oscillating behaviour, however this oscillating behaviour is less pronounced and more elongated due to the longer distance between ship and quay.

If one looks at the the small final distances from the quay wall ($s' = 0.5, s' = 1, s' = 1.5$) conclusions can be drawn on the hydrodynamic forces during the ship's movement. As stated in the beginning of this section the inertial part of the hydrodynamic forces are often simplified to virtual mass. From figure 2.10 hypotheses can be set on the behaviour of virtual mass during lateral ship movement in the vicinity of a quay wall. Inertial forces are only present during acceleration and deceleration and friction forces are always present. If one looks at constant ship velocity ($t' = 1-3$), the hydrodynamic forces only consist of frictional forces. At $t' = 1$ the vessel stops accelerating and the hydrodynamic forces drop with almost 60%. A cautious conclusion can be drawn that at the end of the acceleration 60% of the hydrodynamic forces are caused by inertia and 40% by friction. When the vessel starts decelerating the inertial forces start to play a role again. Because of the deceleration the inertial forces change direction, working towards the quay with the movement of the ship, whilst the frictional forces still work against the movement of the ship. This results in a decrease in hydrodynamic forces acting on the ship because the inertial forces and frictional forces counteract each other. During acceleration the increase in hydrodynamic forces is $C_y = 15$ while during decelerating the total decrease in hydrodynamic forces is $C_y = 18$. A hypothesis for the fact that the hydrodynamic forces do not behave similar for acceleration and deceleration is the vicinity of the quay wall. Furthermore, if one compares the acceleration from $t' = 0-0.2$ and the deceleration from $t' = 3-3.2$ it is seen that during deceleration a faster increase in hydrodynamic forces is seen, substantiating this hypotheses. It is not possible to draw a conclusion on the

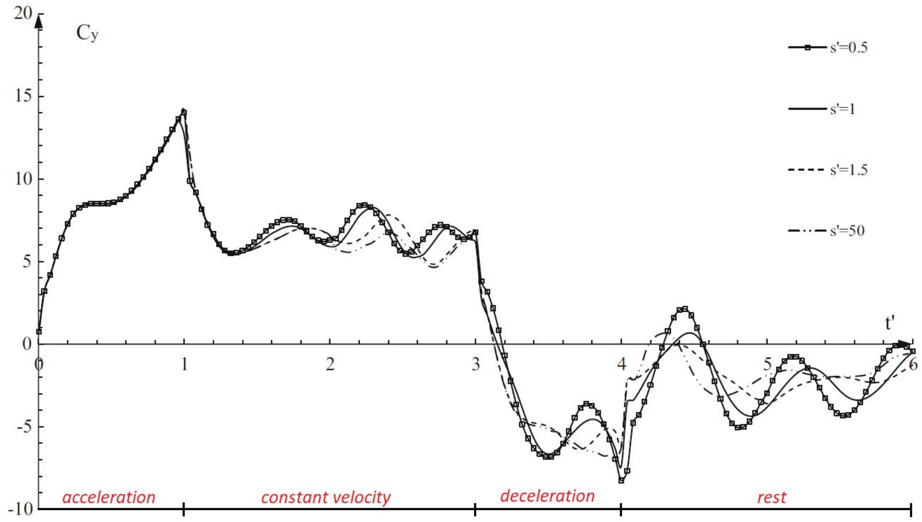

Figure 2.10: Influence final quay wall distance on lateral hydrodynamic forces in shallow water (Wang et al., 2016)

virtual mass during deceleration because the inertial forces and resistance forces counteract each other. The behaviour at rest, from $t' = 4 - 6$, is completely due to inertial forces, thus virtual mass. The oscillating behaviour of the hydrodynamic lateral forces are caused by the reflection of the hydrodynamic mass at the quay wall and at the ship's hull. The explanation of the peak at $t' = 4.3$ is the first reflection of the current on the quay wall acting as a force acting against the lateral movement of the ship. It is important to keep in mind that the researches presented in this paragraph ((Wang et al., 2016) (Wang et al., 2017)) are executed for a Wigley hull ship, which is a ship that is widely used in experimental and numerical studies. The length-to-width ratio is 10, the length-to-draught ratio is 16. This means that the results of the studies should be interpreted with caution, the difference in ratios are expected to influence the hydrodynamic processes.

In Chen et al. (1997) and Chen, Liu, Huang, and Davis (1999) it is seen that maximum hydrodynamic forces were not found for minimum quay wall clearance. An explanation could be that due to the effect of the water cushion at minimum quay wall clearance, the hydrodynamic added forces decrease again, which is in line with previous studies.

After this thorough review of the influence of a quay wall and the bottom a few conclusions can be drawn. The hydrodynamic forces during the acceleration of the vessel are influenced by the presence of the basin bottom and not only the vicinity of a quay wall. Depending on the distance of the ship to the quay wall as well as the presence of the quay wall causes a force counteracting the lateral movement of the ship which resembles the water cushion. The hydrodynamic forces during constant vessel speed, the deceleration phase and the rest phase are influenced by the vicinity of the quay wall as well as the bottom of the basin. At slow vessel speeds the inertial forces have the largest share in the hydrodynamic forces. The water between ship and quay returns around the bow and stern or under the keel. The ratios depend on the hull shape and the under keel clearance. It is expected that for the large sea-going vessels investigated in this research around around 30% of the water returns around the bow and stern and 70% through the under keel gap during berthing. This is expected because large sea-going vessels have approximately the same length-to-width ratio as the vessel used in (Chen & Huang, 2000).

2.2.3. Influence of yaw on the lateral berthing manoeuver

During the berthing manoeuver in previous paragraphs purely sway motion is assumed. In reality this is not often the case and small deviations from the perpendicular due to the pushing of the tugboats take place. When the ship deviates from it's perpendicular line the flow behaviour around the ship is influenced. If the ship deviates from the perpendicular, a longitudinal pressure gradient is expected causing an amount of water flowing along the ship's hull. This is followed by a change in bow and stern flow as seen in figure 2.11.

Because of an additional longitudinal flow it is expected that a smaller amount of water needs to flow through the under keel gap. If this is the case, this could mean that the pressure between ship and quay is not as big in comparison with a pure sway motion. This also means that less water is 'trapped' between ship and quay at the final meters of the berthing manoeuver. Naturally the hydrodynamic forces on the ship due to the

Figure 2.11: Longitudinal flow due to approach angle

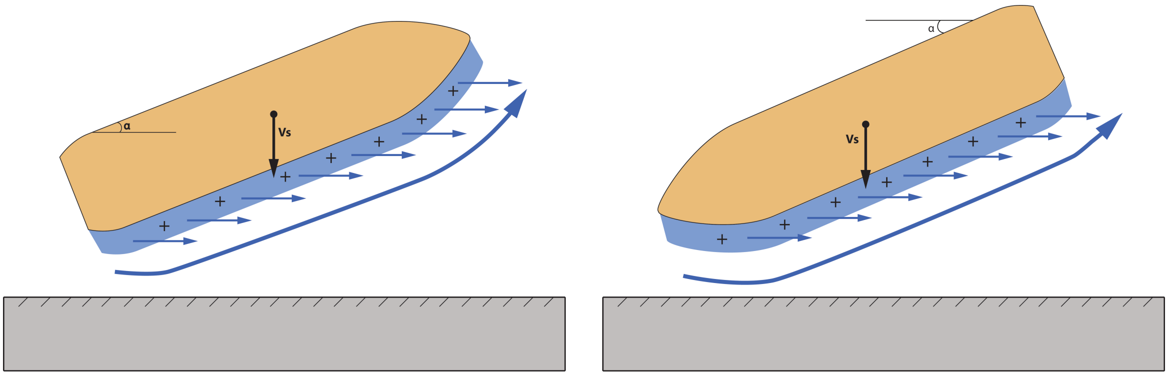

(a) (b)

reflection of the water against the quay wall and the ships hull are expected to decrease.

According to Trelleborg marine systems (2016) the typical values of the deviation of the ship from the perpendicular are 0° < α < 15°. The larger angles are used for smaller ships, smaller ships have less mass and are therefore easier to manoeuver and turn during berthing without the use of tug assistance. The pilots in the Port of Rotterdam aim to berth the ship as parallel to the quay wall as possible. However, if an angle is for example only 5°, the difference in distance to the quay wall for a ship of 320 meters long is already approximately 28 meters. This is a large space to let the water escape and it is questionable if the hydrodynamic effects counteracting the lateral movement are still noticeable then.

2.2.4. Influence of surge, roll, heave and pitch on the lateral berthing manoeuver

Sway and yaw are the most important ship motions during parallel ship berthing. In this paragraph the remaining four ship motions and their interactions with the hydrodynamic flows working around the berthing ship are discussed. Surge of a ship is induced by propulsive force or due to current. A force is needed to set the ship in a forward motion. If the vessel still has some forward velocity during the berthing manoeuver, this will influence flow pattern around the ship. The ship will have a flow pattern in longitudinal direction probably influencing the high pressures seen in a pure sway motion.

Roll, heave and pitch motions are induced by significant waves, current, and vessel speeds. Wind could cause roll motions as well for ships with larger lateral wind areas. Due to the fact that the parallel berthing manoeuver takes place in shallow and confined waters in the Port of Rotterdam at velocities in the order of centimeters per second, the motion of the ship is minimum. The flow patterns and thereby forces around the ship compared to the mass and size of the ship do not induce significant roll, heave and pitch motions in shallow and calm waters.

2.3. Key variables

After a thorough literature review the variables that are expected to have the most influence on the hydrodynamic processes around the berthing vessel are discussed. In addition, it is discussed how these variables influence the water cushion effect. A choice on the variables has been made conform the objectives of this research and the specifics of a parallel berthing manoeuver. The parallel berthing manoeuvers that are influenced by a water cushion effect are sea-going vessels berthing in the Port of Rotterdam. The vessels have lengths over 200 meters and due to their draught and mass and due to the water depths in the Port of Rotterdam, it is concluded that the berthing manoeuver takes places in shallow and confined waters. The berthing takes place in vicinity of a berthing construction, and berthing velocities are in the order of centimeters per second. Because of the fact that berthing is a lateral movement, parallel to the quay at very low velocities not all degrees in ship motion are significant. Heave, pitch and roll motions are caused by waves, wind and currents. Because of the fact that the berthing manoeuver is at low velocities in a sheltered basin it is not expected that the hydrodynamics and heave, pitch and roll motions experience significant interactions. In other words, it is not expected that the hydrodynamic forces are influenced significantly by these motions. Therefore the heave, pitch and roll motions are not treated as a key variable. The ideal berthing manoeuver is without propulsive force, only the tugboats pushing the ship laterally towards the quay. Therefore the surge is expected to be so small that it is not expected to have a big influence on the hydrodynamic processes around the berthing vessel and vic versa. This leaves the sway and yaw motion as important variables in the berthing manoeuver. As seen in paragraph 2.2 the fact that the berthing takes place in shallow waters influences the hydrodynamic processes around the vessel. Therefore, the water depth and thus the under keel clearance is an important variable. Besides, vicinity of a quay wall influences the hydrodynamic processes around the ship, so this is a variable to investigate as well. Due to the two tugboats applying the force to move the ship laterally it is expected that the ship experiences yawing motions during the manoeuver. Yawing motions coincide with an angle of approach which influences the hydrodynamics around the vessel. Furthermore, the ship dimensions are expected to influence the amount of water flow underneath the keel and around the bow and stern. Therefore, ship dimensions are treated as a key variable as well. As seen in paragraph 2.2.2 the forces counteracting the movement of the ship can be categorized in three groups:

- Hydrodynamic inertia forces
- Hydrodynamic resistance forces
- Moment of inertia ship

The key variables influencing the hydrodynamic processes around the berthing vessel are going to be evaluated conform these three forces.

2.3.1. Under keel clearance

From paragraph 2.2.2 it is seen that the under keel clearance is of direct influence on the hydrodynamic forces acting laterally on the ship during berthing. When the ratio between water depth and ship draught decreases, the hydrodynamic forces acting on the lateral movement of the ship increase significantly (figure 2.9). The resistance forces increase with decreasing water depth during constant speed of the vessel. During acceleration and deceleration of the ship, the virtual mass plays a significant role. The effect of the under keel clearance influences the lateral berthing manoeuver in two ways. When the vessel approaches the quay wall it decelerates, the water moving with the vessel still has velocity due to inertia and flows towards the quay wall. This moving water reflects on the quay wall and flows back towards the ship. With large keel clearance a part of this reflected current flows away under the keel and another part bounces back on the ship's hull. It is seen that when the ratio between the water depth and the draught of the ship reaches 2.0 and smaller, the return current cannot escape under the keel anymore, meaning that all the current bounces back on the ship's hull. This results in positive hydrodynamic lateral forces, counteracting the lateral movement of the ship. The ship is pushed away from the quay at one point, the cushion effect. The second effect is that under keel clearance influences the water pressure between ship and quay. With decreasing under keel clearance, the pressure between ship and quay increases. As a consequence of the increased pressure between ship and quay, the lateral forces on the ship's hull increase and the flow velocities under the keel increase.

2.3.2. Quay wall clearance

The quay wall clearance is of direct influence on the hydrodynamic forces. During acceleration the vicinity of the quay wall seems to be of no influence on the lateral hydrodynamic forces (figure 2.10). An explanation could be that the resistance force stays the same for the vicinity of the quay wall and the inertial forces are also not influenced because the inertial forces are influenced by the downstream boundary condition and not the upstream, the quay wall, during acceleration. During constant lateral velocity, deceleration and rest the distance to the quay wall does influence the hydrodynamic forces on the ship. Apparently, the resistance forces during constant vessel velocity are influenced by the vicinity of the quay wall, a phase lag between the oscillations is visible. The inertial forces during deceleration and rest are influenced by the quay wall clearance which could be explained due to the fact that the upstream boundary condition, the quay wall, influences the inertial forces of the vessel.

2.3.3. Approach angle

The angle of approach is an important feature on the hydrodynamics around the berthing ship as described in paragraph 2.2.3. Because of the length of the considered vessels the approach angle is assumed to be minimum during a berthing manoeuver. A small deviation from the perpendicular already results in a large difference in quay wall clearance at bow and stern. When there is even a small deviation of the parallel a longitudinal current can develop along the side of the ship (figure 2.11). This means that more water can escape and the pressure between ship and quay will most likely decrease. This will have an influence on the lateral hydrodynamic forces on the ship. The frictional forces will most likely increase when the vessel experiences an angle, due to the fact that the path along the ship's keel, in the line perpendicular from the quay, is longer under an angle. It is expected that the inertial forces will be influenced as well.

2.3.4. Ship dimensions

Water cushion effects rise at all size of vessels but are only felt by pilots berthing large vessels at container and bulk quay walls. Vessels are defined as large when they require tug assistance and have certain dimensions dependent on the ports infrastructure. The vessels that experience water cushion effect are container vessels and bulk carriers berthing at their quay walls as indicated by the Dutch Pilotage Service. Both vessels have similar shapes midships, the profile is very rectangular. Bulk carriers in general have a very block-like shape, container vessels are considerably more cut at the bow and stern.

In paragraph 2.2.2, it is explained that water can flow around the bow and stern or under the keel. For the simulation in Chen and Huang (2000) approximately 30% of the surface flow was around the bow and stern and 70% under the keel in shallow water. It is expected that the ship dimensions and particularly the ratio of vessel width to vessel length, influence the amount of water flowing around the bow and stern and under the keel. If the vessel is relatively wide (low length-to-width ratio), the frictional forces will increase at the under keel and one would expect that more water flows around the bow and stern. On the other hand if the vessel is relatively long (high length-to-width ratio), under the keel is an easier way out for the water than around the bow and stern. If the under keel clearance increases, it is expected that the amount of water returning through the under keel gap is bigger than 70%.

The under keel flow velocity is expected to be the limit state for the amount of water flowing around or under the ship. If the under keel flow velocity maximum is reached and pressure is built up between ship and quay, the water traveling around bow and stern will increase.

2.3.5. Hypotheses

From the key variables in paragraph 2.3 and the literature reviewed in this paragraph hypotheses are being set on the presence of hydrodynamic forces counteracting the lateral berthing manoeuver of the ship. The four major variables influencing the hydrodynamic forces are under keel clearance, quay wall clearance, approach angle, ship dimensions. Moreover, the variables describing the ship's motion are important. Therefore, the fifth key variable is the position of the ship over time and therefore the velocity and acceleration through the first and second derivative of the position of the ship. The focus of this research will be on the under keel clearance, quay wall clearance, position of the ship and the ship dimensions. The approach angle is not investigated further and therefore will be set to 0° in the continuation of this research.

The under keel clearance effects cause hydrodynamic forces, counteracting the lateral berthing manoeuver towards the quay when the water depth-to-draught ratio (h/D) decreases. It is expected that when this ratio is below 2 the water cushion effect is present.

The quay wall clearance effect starts to play a significant role on the hydrodynamic processes when the ratio quay wall distance to the width of the vessel has a value of ≤ 1.5. Even for the smallest seagoing vessels investigated in this research the value of this ratio stays below 1.5 during the berthing manoeuver. Therefore the vicinity of the quay wall will influence the hydrodynamic process for sea going vessels in a berthing manoeuver. The hydrodynamic forces counteracting the lateral berthing manoeuver towards the quay are present from a ratio value of ≤ 0.5, this is the case for the ships considered during the berthing manoeuver and therefore the water cushion is going to be present for these cases.

The ship dimensions influence the amount of water flowing around the bow and stern and through the under keel gap. It is expected that 30% of the flow travels around the bow and stern and 70% through the under keel gap for shallow water berthing of vessels with a length-to-width ratio of $5-7$.

2.4. Different methods to evaluate ship berthing

2.4.1. Mathematical modeling

Mathematical modeling uses formulas to describe the process of a system. When a mathematical model is developed for ship berthing, formulas are used to explain the process and the influence of different components on the process. If the mathematical model is developed properly, predictions of the behaviour of the vessel can be made.

Several studies used mathematical modeling to draw conclusions on water cushion effects as seen in paragraph 2.2. However, that does not mean that a mathematical model demands complicated computer simulations. A mathematical model can also be a set of formulas which can be solved straight forward. For example, Hautamaki (1970) simulates the cushion effect using Bernouilli's pressure law, assuming the ship is long enough to neglect the water flow around the ship. The cushion effect is determined by assuming a balance between the amount of water flowing under the ship and a rising and falling water level between ship and quay.

With the simulation of berthing manoeuvers, a quasi-steady approach is widely used. This approach assumes that only immediate acceleration and velocity influence the hydrodynamic forces on a vessel. However, this approach can't be used when slow manoeuvers take place. In ship berthing, small deceleration and acceleration with a large mass play a role and inertia should be taken into account as well. In other words, the flow is non-stationary, it is time dependent. Therefore, the quasi-steady approach is not applicable in case of ship berthing manoeuvers (Vantorre, 1992)(Vantorre & Laforce, 1998). There are a great number of different mathematical methods to serve as input for mathematical models, only two are described here. Two often used mathematical models are time-dependent description of ship's motion and discrete time approaches.

Time-dependent approach: equations of motion & impulse response functions

One way to develop a mathematical model in ship berthing is using a time-dependent description of the hydrodynamics around a berthing vessel. This is achieved through combining the time-dependent equations of motion with impulse response functions. A vessel can experience six degrees of motion, forces acting on a vessel can therefore induce acceleration or deceleration in six different degrees. External forces acting on the ship are derived from physical phenomena and added to the equation. The hydrodynamic forces acting on a berthing vessel are calculated separately, modified to a force and added to the external forces acting on the ship. For the different degrees of freedom (j) at different time steps (k) numerical integration is needed for the hydrodynamic forces since they are time dependent and depend on the time history of the respective velocity components of the water around the ship. Therefore, the dynamics of the ship are not only determined by the instantaneous kinematics but also by the inertia effects of the ship, as explained in the paragraph 2.4.1.

To be complete, the general equation of motion in the j^{th} degree of freedom is depicted below (Newman, 2018):

$$\sum_{j=1}^{6} \left\{ (M_{kj} + a_{kj}(\omega))\ddot{x_j} + b_{kj}(\omega)\dot{x_j} + c_{kj}x_j \right\} = F_k(t) \tag{2.1}$$

$a_{kj}(\omega)$ is the added mass coefficient as a function of the frequency (ω), $b_{kj}(\omega)$ is the hydrodynamic damping coefficient as a function of the frequency (ω) and c_{kj} is the restoring hydrostatic coefficient. These coefficients are multiplied with acceleration ($\ddot{x_j}$), velocity ($\dot{x_j}$) and displacement (x_j) respectively in degree of freedom j and contribute to the force in time k. The acceleration in degree of freedom j should be multiplied with a factor M_{kj} to calculate the inertia force at time k, in other words mass or moment of inertia. The right hand side of the equation represents the external forces acting on the ship. In this research the external forces, waves, wind and current are not taken into consideration so the right side of the equation is 0. For a vessel berthing, all six degrees of freedom are coupled together by the asymmetric flows around the vessel. Not only the quay influences the hydrodynamic forces, the under keel clearance does this as well (PIANC, 2002).

Discrete time approach: long wave approximation

Another way, besides the equation of motion for mathematical modeling, is long wave theory (Fontijn, 1988). In long wave theory it is assumed that if a disturbance occurs, e.g. as a ship moves, a long surface wave is generated from either side of the ship. This long surface wave results in a different pressure distribution on both sides and therefore different hydrodynamic forces.

A mathematical model based on the long wave approach is the most straight forward model because it is a direct-time approach. A direct-time approach formulates the memory effects and kinematics of the vessel by a limited number of differential equations. The long-wave approximation assumes that the hydrodynamic forces depend only on five parameters in a pure sway motion (figure 2.12 (Demenet, 2018) (Vantorre, 1992)). The basic assumptions of the long wave theory are (Demenet, 2018):

- Ship approaches in a transverse direction at an angle of 0°with the berthing line, two-dimensional approach
- Ship's length such that flow around bow and stern is relatively small to the discharge perpendicular to the lateral motion, only motion in the two-dimensional plane
- Ship berths in shallow water resulting in high flow velocities under the keel and therefore friction forces under the vessel
- Only flow forces in the form of friction under the ship's keel are taken into account.

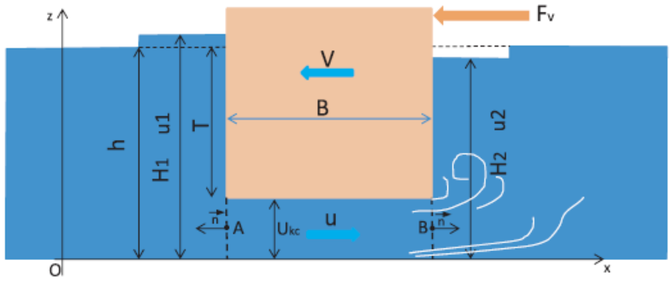

Figure 2.12: Long wave theory (Demenet, 2018)

- Vertical fluid motion negligible in comparison to horizontal fluid motion

Demenet (2018) developed a model with the long wave approximation to calculate the virtual mass factor. The values obtained were compared to the values obtained through 3D mathematical modeling and differ significantly when the under keel clearance decreases.

2.4.2. Scale model tests

The last method to be treated in this literature review are scale model tests. Several studies in vessel berthing used scale models to investigate vessel behaviour. It is especially useful for researching one specific parameter. One research has been found which investigates the water cushion effect using scale modeling (Vantorre & Laforce, 1998). According to this author the non dimensionalised cushion effect with respect to the approach velocity is determined by the under keel clearance and the quay wall clearance only. The cushion effect rises when the under keel clearance and the quay wall clearance become sufficiently small. However, yawing motion was not considered in the experiments.

Ball and Markham (1983) use scale model tests to find a relation between under keel clearance and impact force on fenders. From a certain value for under keel clearance, the force on the fender decreases instead of increases. This could be due to the presence of an energy absorbing water cushion.

Scale model tests can be used to validate a mathematical model, comprehend collected data or substantiate a design.

2.4.3. Kinetic energy method

When evaluating impact energy on a marine structure during berthing, the kinetic energy approach is most commonly used (Demenet, 2018). The kinetic energy approach determines the energy absorbed by the structure by multiplying a vessel's kinetic energy with several of factors that account for place of impact, berth type, fender deformation, hull deformation and the amount of water moving with the vessel, contributing to its mass. This approach has been used by most international standards such as PIANC, Spanish ROM, British standards and the German EAU. The kinetic energy method is based on assumptions of certain conditions (Metzger, Hutchinson, & Kwiatkowski, 2014), and when using this approach one should pay attention to the specific situation and determine if the assumptions are justified. Therefore, in design methods a so-called abnormal berthing factor needs to be applied to account for these deviations in specific conditions (PIANC, 2002) and anticipate a possible abnormal impact on the structure. This abnormal berthing factor depends on many factors such as human error, malfunctions, exceptional weather conditions, valuable cargo, frequency of berthing and many more and is used as a safety factor on the normal berthing energy. The kinetic energy method does not take into account the dissipation of energy due to contact with the structure or due to hydrodynamic effects. Below, the kinetic energy approach recommended by PIANC 2002 is discussed.

The kinetic energy (E_s) is based on the vessel's velocity (V_s) and the vessel's actual mass (M_s). Note that the hydrodynamic mass (M_v) is not implemented in this formula.

$$E_s = \frac{1}{2} M_s V_s^2 \tag{2.2}$$

When a fender is designed, it is designed to absorb a certain amount of kinetic energy. This fender energy depends on the kinetic energy of the vessel and a handful of other characteristics. The fender energy is calculated by multiplying the kinetic energy of the ship by a several factors:

$$E_f = E_s C_e C_m C_s C_c \tag{2.3}$$

This fender energy produces the berthing force, perpendicular to the quay wall. The fender absorption causes a fender reaction force. In the following sections the variables and factors are discussed.In figure 2.13 (Demenet, 2018) the movement of a ship upon initial contact as used in the kinetic energy approach is shown.

Figure 2.13: Ship berthing - one fender contact (Demenet, 2018)

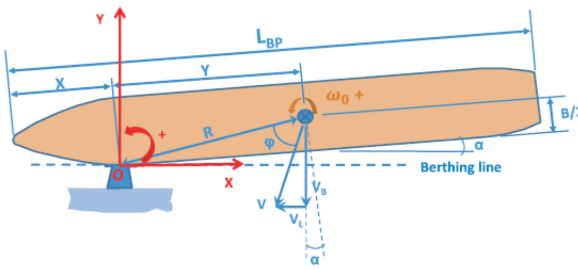

(a) Ship movement initial contact

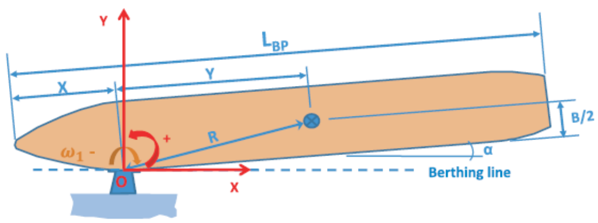

(b) Ship movement after initial contact

Mass of vessel (M_s)

The mass of the vessel is calculated with the displacement of the ship. The displacement is calculated by the volume of water displaced, multiplied by the water density and is expressed in tonne. The mass of the vessel is not to be confused with the size of the vessel. The size of the vessel is expressed in DWT. DWT is the cargo carrying capacity of a vessel including bunkers expressed in tonne (PIANC, 2002). DWT is also the input variable to obtain the berthing velocities in the Brolsma curves (Brolsma, Hirs, & Langeveld, 1977). The problem using DWT is that it is a conventional but not necessarily correct measure for expressing the size of a vessel. For example, a cruise ship has a very low DWT due to the fact that it transports people and not cargo. However, the mass of a cruise ship is significant which is important in further implementations.

Velocity of vessel (V_s)

The approach velocity is defined as the vessel speed at initial berthing contact, measured perpendicular to the berth (PIANC, 2002). The berthing speed of the ship depends on the ease of the berthing procedure. Pilots determine the berthing velocity through real time measurements and take into account a large number of factors. If one looks at the kinetic energy formula it is quite clear that the velocity of the vessel is the most influential variable in the equation, because it is squared. In PIANC (2002) the design berthing velocity is determined using the Brolsma curves as depicted in figure 2.14 (Trelleborg marine systems, 2016).
The curves show the design berthing velocities as a function of navigational conditions and vessel size.

Block coefficient (C_b)

The block coefficient, as the name suggests, represents the extent to which the ship has a block shape. The block coefficient (C_b) gives information on the hull shape of the ship. It is calculated using the ship's mass (M_s), the length (L), width (B) and draught (D) of the vessel:

$$C_b = \frac{M_s}{L * B * D * \rho} \tag{2.4}$$

Eccentricity factor (C_e)

It is highly unlikely that the first contact between vessel and fender will exactly be in the middle of the vessel. Therefore, a small berthing angle will almost always be present. The eccentricity factor accounts for this

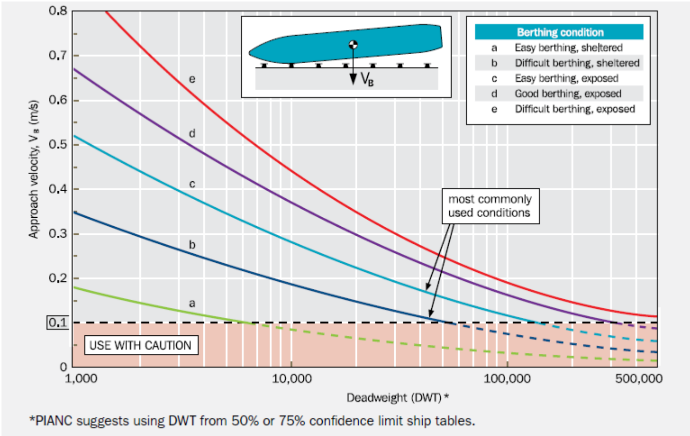

Figure 2.14: Design berthing velocity (Trelleborg marine systems, 2016)

asymmetry. Considering angular berthing the vessel will rotate around the point of contact and energy will be dissipated during that process. If the vessel does berth in the centre, no rotation will take place and C_e equals 1.0. In this case the berthing energy is absorbed by all fenders that make contact with the vessel. The eccentricity factor depends on radius of gyration of the vessel (K), the distance between the point of contact and the centre of the mass (R) and the angle between velocity vector and the line between the point of contact and the centre of mass (ϕ). The eccentricity factor is calculated with the following formula (figure 2.13):

$$C_e = \frac{K^2 + R^2 * cos^2\phi}{K^2 + R^2} \tag{2.5}$$

Where:

$$K = (0.19C_b + 0.11) * L \tag{2.6}$$

In PIANC the guidelines for berthing angles are no more than 6 degrees for vessels larger than 50,000 DWT. For smaller vessels and especially vessels without tug assistance, 10-15 degrees is proposed. These berthing angles are recommended such to account for deviations in practice and therewith safe fender design.

Softness factor (C_s)

Vessel's hull and fender can deform upon contact and consequently absorb energy. This deformation depends on the elasticity of the hull and on the softness of the fender. In other words, the ratio between the elasticity of the fender (E_{fen})and the elasticity of the hull (E_h). The softness coefficient represents part of the kinetic energy of the approaching vessel that needs to be absorbed by the structure. The other part is dissipated by the hull deformation and fender deformation.

$$C_s = \frac{E_{fen}}{E_h} \tag{2.7}$$

The softness factor presented by PIANC is between 0.9 and 1.0. In practise the softness factor is usually taken as 1.0, as fenders are usually softer than ship's hull.

Berth configuration factor (C_c)

The water cushion effect is implemented in the berth configuration factor. The type of berth structure determines this factor. If the structure is closed (figure 2.15 b), the water could be trapped in between ship and quay and acts as a cushion dissipating part of the energy. For a closed structure a value of C_c = 0.9 should be used according to PIANC (2002), some guidelines even propose C_c = 0.8 as lowest value. When the quay wall is open, the water cannot be trapped in between ship and quay and a cushion effect will not be present and will therefore not dissipate part of the energy. A value of C_c = 1.0 should be used because no energy is dissipated. Basically, if there is an easy way out for the water, the cushion effect will not rise. An easy way out for the water would be for example large keel clearance, open quay wall structure and a certain angular approach.

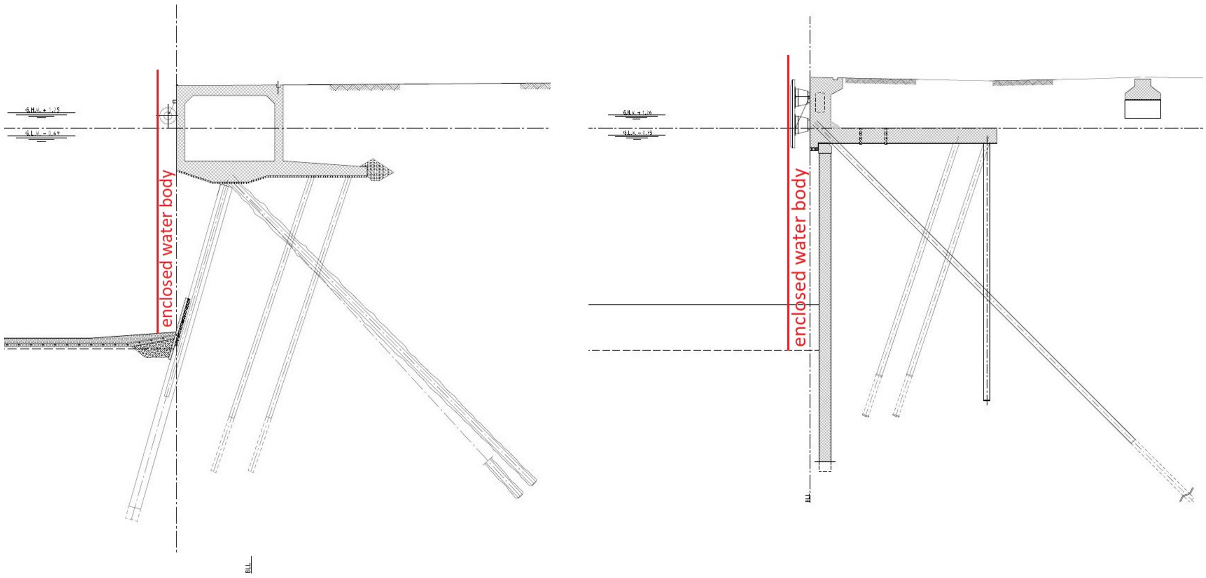

Figure 2.15: a) semi open quay wall b) closed quay wall (PoR, 2019)

Sakakibara and Kubo (2008) compared a closed quay wall, open sea and a sloped quay wall and their hydrodynamic coefficients. The heave, sway and roll motions of the ship varied significantly due to the type of quay wall and the hydrodynamic coefficients used in the equations of motion coinciding with these different configurations. Not much research has been done on this berth configuration factor and on the presence of a water cushion. After deliberating with the Dutch Pilotage Service it became clear that the water cushion effect rises at some semi-closed quay walls as well (figure 2.15 a). If there is a better understanding of the water cushion, it can be used in advantage and dissipate a part of the berthing energy. The berth configuration coefficient should be adjusted or even deleted when substantiated conclusions are drawn.

Virtual mass factor (C_m)

The virtual mass is used as the effective mass of the ship and is not equal to the actual mass of the vessel as stated in paragraph 2.2. The hydrodynamic added mass increases the energy the fender needs to absorb. In other words, this added mass contributes to the actual mass of the ship causing the effective mass to be greater than the actual mass of the ship. In the guidelines the virtual mass is taken into account in the form of a factor. The general definition of the virtual mass factor is:

$$C_m = \frac{M_s + M_v}{M_s} \tag{2.8}$$

There are several formulas to determine the virtual mass according to PIANC (2002). PIANC describes three methods. The two most commonly used formulas are defined by Shigeru Ueda and Vasco Costa. PIANC used the formulas of Ueda and Costa and compared these to the results of research. From this, new values for the virtual mass factor follow, given in table 2.1. This is the third method, called the PIANC method and is used in the Port of Rotterdam. Values for the virtual mass factor are determined by both ship characteristics and keel clearance. Which value to use depends on the keel clearance as seen in table 2.1. The values in the table are only for a lateral vessel approach. For a longitudinal vessel approach a C_m value of 1.1 is recommended. Usually, the under keel clearance is 10% of the draught of the vessel. The minimum allowed under keel clearance is 1.0 meter during sailing.
Note that when using the table (2.1), the value used for the configuration factor (C_c) should be 1.
However, it is important to note that these formulae are derived for deep water and do not take into account berthing velocity, ship deceleration or acceleration, proximity of solid structures and under keel clearance. Some research has been done on the virtual mass factor and the use thereof in the design guidelines, this is discussed in section 2.5.1

Table 2.1: Virtual mass factor

Keel clearance	C_m
> 0.5 D*	*1.5*
< 0.1 D*	*1.8*
*0.5*D < and > 0.1*D*	*linear interpolation*

2.5. Problems encountered with using the existing guidelines

2.5.1. Added mass

The term added mass in the kinetic energy method is defined as a water body moving with a ship at the same velocity during deceleration and acceleration of the ship. Another expression is the hydrodynamic sway added mass. The water body is added to the actual mass of the vessel, expressed as the virtual mass, to determine the load on marine structures. Reality however, is a lot more complicated as explained in paragraph 2.2. The added mass is actually the inertia of the water surrounding the vessel, producing a force counteracting the lateral movement of the ship. In the expression used in the design guidelines, this hydrodynamic process is lumped into one single coefficient. In reality the added mass depends on several other parameters which are not implemented in the expressions used to calculate the virtual mass factor.

Figure 2.16: Added mass berthing versus sailing (Demenet, 2018)

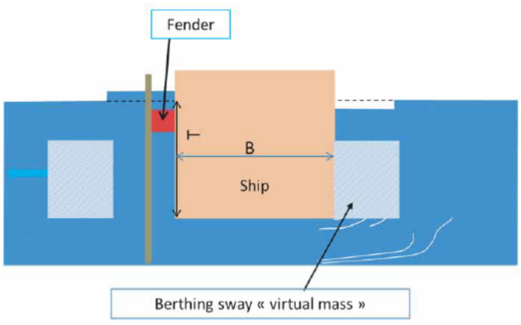

(a) Berthing sway added mass

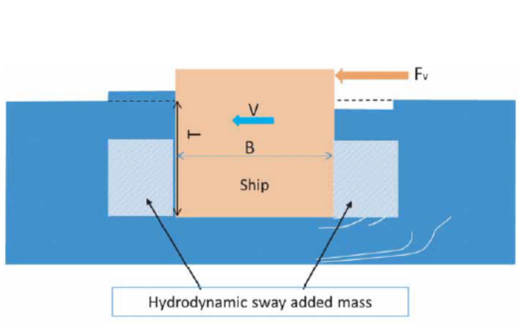

(b) Hydrodynamic sway added mass

If one takes a closer look at the table provided by PIANC for the virtual mass factor, it appears that the virtual mass factor increases with decreasing under keel clearance. This means that when the under keel clearance decreases, which is suspected to relate to the development of a water cushion not the added mass, the energy to be absorbed by the fender increases as well. This contradicts the presumption that a water cushion develops at small under keel clearances, absorb part of the kinetic energy and therefore decreases the energy to be absorbed by the fenders. The explanation PIANC gives is that the water traveling with the vessel during the deceleration before fender impact is an extra force acting upon the fenders, next to the impact of the vessel itself. This is substantiated by Chen and Huang (2000). They found that when the ship touched the fenders, the high pressure that was in front of the ship between quay and ship shifted to the other side of the ship. This is due to the inertial forces of the decelerating ship pushing the ship with large force into the fenders. The berthing facilities should not only absorb the kinetic energy of the vessel but also these hydrodynamic forces resulted from the change of momentum of the trailing water flows. This does explain the derivation of the virtual mass factor in PIANC. The pilot indicates however, that the water cushion is a barrier that needs to be pushed through to berth the ship, this means that this effect is not implemented in the design guidelines. The water cushion barrier between quay and ship can develop resulting in vessel deceleration until halt and after applying force with the tugboats acceleration before touching the fenders instead of deceleration with different hydrodynamic forces as a result. Hence, the water cushion effect should be embedded in the virtual mass factor, and not only the force of the trailing water due to deceleration needs to be considered. Besides, after the literature review it seems more logical that the berth configuration factor depends on the under keel clearance and the added mass depends on the deceleration of the vessel.

Blok and Dekker (1979) used model tests to find that the virtual added mass does not depend on the initial velocity of the vessel, which is also found in previous studies.

According to Demenet (2018) the virtual mass factor used in PIANC is not appropriate since not all water traveling with the vessel needs to be absorbed by the marine structure. A part of the water remains moving when the ship impacts the fender. There is a difference between hydrodynamic sway added mass and berthing sway virtual mass as shown in figure 2.16 (Demenet, 2018). Demenet suggests to use the term 'virtual mass factor C_m' instead of added mass coefficient and proposes several methods to define a new C_m factor. He also states that the C_m factor used in the Kinetic Energy method should be defined as the ratio of the kinetic energy absorbed by the fender to the kinetic energy the ship possesses during berthing.

The berthing consists of a swaying, yawing and surging motion. Surging is not relevant unless the approach angle of the vessel is relatively high. As shown in section 2.4.3, a distinction is made between the transverse or longitudinal approach of the vessel in determining the virtual mass factor. However, the swaying and yawing motion can occur simultaneously so the virtual mass factor should take into account both. The water mass traveling with the vessel originates from two types of motion (Blok & Dekker, 1979).

It is important to be aware that the presence of a water cushion is related to virtual mass. This virtual mass is influenced by the configuration of the waterfront structure. Therefore, the configuration of the waterfront structure should already be implemented in the virtual mass factor instead of adding a configuration factor to the energy calculation. There has been little research on this and for optimization of the PIANC guidelines this should be investigated further.

2.5.2. Hull shape

The block coefficient accounts for the shape of the vessel, it represents the extent to which the ship has a block shape. In reality there are vessels with a sharp keel as well, this is not accounted for in the block coefficient. The volume of the sharper keel is taken into account in the coefficient, the effect of the sharp hull is not. It is not known if certain hull shapes are beneficial for the behaviour of the hydrodynamics around the ship and therefore the water cushion effect. The eccentricity factor and the virtual mass factor depend partially on the block coefficient. When the block coefficient increases, the virtual mass factor decreases. These factors are used in fender design but they do not directly relate to berthing angle (Eskenazi & Wang, 2015). When the dimensions of the design vessel are not known, standard values for different type of vessels are included in PIANC. PIANC delivers eight categories of vessel: general cargo ships, bulk carriers, container ships, oil tankers, RoRo ships, passenger ships, ferries and gas carriers. If the virtual mass increases due to decrease of the block coefficient, the water cushion effects are not taken into account. Further research is needed on the influence of hull shape and the hydrodynamic forces on the ship.

2.5.3. Approach angle

The eccentricity coefficient accounts for the approach angle and that with a rotation of the ship around its point of impact with the fenders a part of the kinetic energy is absorbed. However, the eccentricity coefficient does not account for the fact that the load of the ship is not divided equally among all fenders. It is possible that the fenders in this situation experience a higher load than when the vessel does not experience an angle. Eskenazi and Wang (2015) state that the berthing angle is only reflected in the eccentricity factor. This appears contradictory because one would say that berthing energy that needs to be absorbed by the marine structure depends mainly on berthing velocity, mass of vessel and berthing angle. Implementing the berthing angle in one coefficient only, appears to be underestimating the impact of the berthing angle on the calculated kinetic energy. The eccentricity factor can be cancelled out by the value of the other factors whilst it is expected that the berthing angle is of significant influence on the flow behaviour and thus the kinetic energy. Besides, the approach angle influences the hydrodynamic processes around the vessel as seen in paragraph 2.2.3 reducing the hydrodynamic forces on the vessel, this is not implemented in the design guidelines.

2.6. Summary & Conclusion

In previous paragraphs it is concluded that the five key variables that cause the hydraulic counteracting lateral forces, the water cushion effect, are the under keel clearance, quay wall clearance, approach angles and ship dimensions. In addition, the position of the ship over time and therefore the velocity and acceleration is the fifth key variable. Theories on the phenomenon of hydraulic damping, derived from numerical models, have been developed in the past. These studies focus on one type of small ship and investigate the influence of under keel clearance and quay wall clearance on the hydrodynamic lateral forces acting on this small ship. The hydrodynamic counteracting forces have not been measured or simulated during an actual berthing manoeuver with a large sea-going vessel.

The ship dimensions, mainly the length and the width of the ship, influence the amount of water flowing around the bow and stern and flowing through the under keel gap. The under keel flow velocity is the limit for the amount of water escaping through the under keel gap. The length of the ship is the limit for the amount of water escaping via the bow and stern. The percentage of the water flowing around the vessel and the percentage of the water flowing under the vessel during the berthing manoeuver is unknown. The pressure between ship and quay, seen as a raised water level is also unknown for vessels during a berthing manoeuver. The flow velocities between ship and quay and the under keel flow velocities have been simulated through complicated mathematical models. However, these flow velocities during a berthing manoeuver with a sea-going vessel have not been measured or simulated. Therefore, the theories have not been validated.

In conclusion, the literature review presents that there are two hydrodynamic processes that contribute to the hydraulic damping between ship and quay. First, the pressure increases between ship and quay when the vessel approaches the quay wall. This pressure increase is expressed as water level elevation between ship and quay, inducing flow in the form of water runoff via the bow, stern and under keel. This water level elevation acts as a counteracting force on the vessel. Second, translation waves are produced by the acceleration and deceleration of the vessel when it approaches the quay. These translation waves reflect on the quay wall and travel back to the ship acting as a counteracting force. Which of these two hydrodynamic processes contribute the most to hydraulic damping is yet unknown.

The hydrodynamic processes causing hydraulic damping need to be investigated and explained. When the hydrodynamic process causing the water cushion is known, the key variables enhancing this process can be investigated.

3

Field experiments

3.1. Introduction

The general description of the phenomena occurring during ship berthing is rather complicated as seen in chapter 2. When the vessel has no forward velocity, thus only moves laterally to the quay a positive pressure field is present at the berthing side of the ship. When the vessel approaches the quay wall there are two scenarios. The first scenario is that the water between ship and quay cannot escape fast enough, which causes a raised water level. This raised water level adds a force to the counteracting hydrodynamic forces and causes hydraulic damping. The second scenario is that the vessel approaches the quay wall and the water can escape fast enough so no water level elevation is present. Nonetheless, due to the acceleration and deceleration of the vessel during the lateral berthing manoeuver, translation waves can occur traveling ahead of the vessel. When these translation waves reach the quay wall, they are reflected and travel back towards the vessel. This adds to the counteracting forces acting on the laterally moving vessel. These two processes require careful experimental and analytical research to determine which one plays the biggest role during the berthing manoeuver. In addition, the key variables influencing this hydrodynamic process and therefore the hydraulic damping should be investigated.

3.2. Approach

To address the knowledge gaps in hydraulic damping field experiments are set up. The first step is to determine what needs to be measured to obtain the results that can be used to complete the objective of this research. To examine the hydrodynamic process causing the hydraulic damping during the berthing manoeuver, the flow behaviour around the vessel needs to be investigated. To achieve this, the pressure and the flow velocities in three dimensions need to be measured between ship and quay during a berthing manoeuver. From the previous chapter it is seen that under keel clearance, quay wall clearance, approach angle, ship dimensions and ship position are suspected to be the key variables influencing the flow behaviour around the ship and influencing the hydraulic damping. To investigate the influence of the quay wall clearance a berthing manoeuver and a quay wall that is suitable for the evaluation of the hydraulic damping is determined. The experiment should be executed in the same way twice. Once in the vicinity of the quay wall and once in the free basin. Because of the nature of the research, the experiment should be executed with a vessel and a quay where the presence of a water cushion is most likely to appear. Therefore, vessel dimensions, depth-to-draught ratios and berthing velocities for the vessels used in the experiments are determined sufficing the ratios found from literature. To investigate the influence of these other key variables the experiments should be executed several times with varying values for the key variables. That is not feasible during these field experiments. In this research only closed and semi-closed berths and corresponding interference with flow and pressure fields around the vessel are considered. To minimize the influence of the approach angle it is key to keep the vessel as parallel as possible to the quay.

3.3. Location

The second decision that needs to be made regarding the field experiments is the location for the field experiments. Several locations are suitable due to their high probability of occurrence of the water cushion effect according to the pilots. These locations are examined further and marked as suitable if the difference in depth between the basin and the berth is smaller than 1.5 meters. In table 3.1 an overview is given of the quays that are suitable for the experiments.

Table 3.1: Overview suitable quays in the Port of Rotterdam

Quay	Berth	Basin depth (m)	Berth depth (m)	Construction depth (m)	Disadvantages	Ship dimensions
EECV Ertskade	EECV West EECV Midden EECV Oost	23,65 22,65 22,65	24,40 18,65 18,65	25,50 20,00 20,00	- Current - Waves - Depth difference berth/basin	Length > 300 m Draught > 18 m
EMO Mississippihaven	EMO 1 EMO 2 EMO 4	22,65 22,65 24,00	21,65 21,65 23,00	22,50 22,50 25,50	- Stratification	Length > 280 m Draught > 18 m
Europahaven	APM WZ APM OZ ECT DDN	16,70 - 17,68 17,40 17,40	16,00 16,65 16,65	17,00 - 18,00 18,30 18,30	- Thrust usage	Max length = 400 m
Amazonehaven	ECT DDE	17,65	16,65	18,00-18,50	- Thrust usage	Max length = 400 m
Euromaxterminal	Not considered due to large depth difference between basin and berth.					

Thrust usage influences the hydrodynamic flow field around the berthing ship. Therefore, the quays at the Europahaven and Amazonehaven are not suitable for the experiments. Only the quays at the Ertskade and the Mississipihaven are appropriate for the experiments as seen in table 3.1. The choice of the quay depends on the availability of the suitable ships and the planning of the terminal.

3.4. Set-up

The third step in the field experiments is to determine the set-up conform the approach explained in paragraph 3.2. The set-up of the field experiments is shown in figure 3.1. The two manoeuvres of experiment 1 and the positions of the instruments for experiment 2 are shown. The explanation of the positions of the instruments and the instruments itself are given in the following paragraphs.

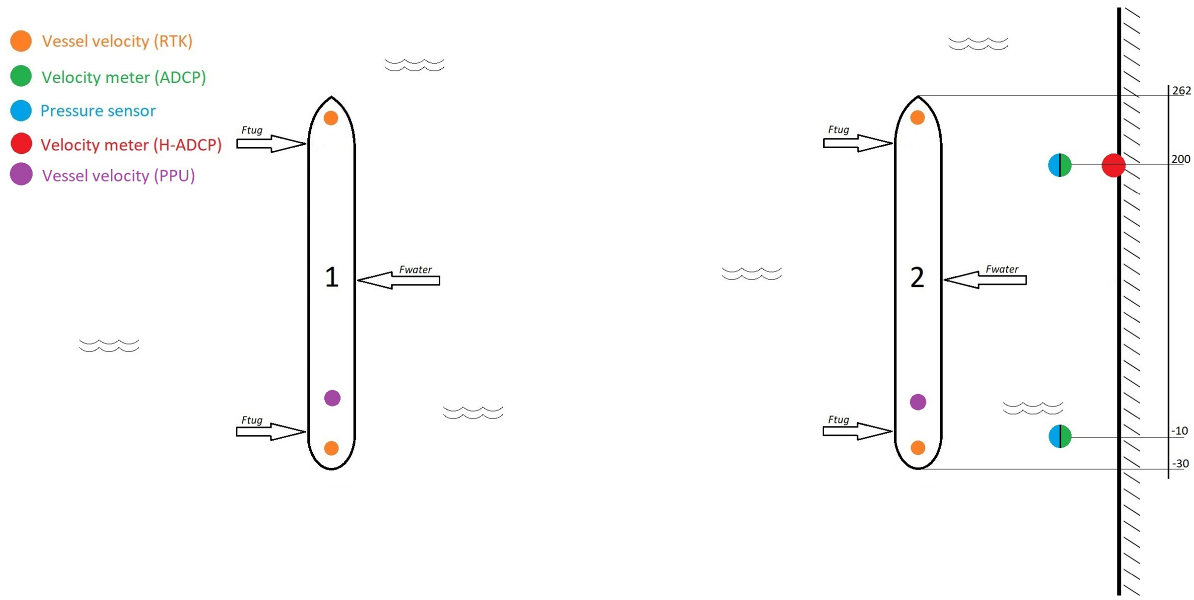

Figure 3.1: Schematisation of the experimental set-up

3.4.1. Experiment 1 - Berthing manoeuver

The first manoeuver is performed at a large distance from the quay (> 100 m), the pilot manoeuvers the vessel as parallel to the quay as possible. In the free basin, the pilot instructs the tugboats to start pushing until a lateral velocity of 6 cm/s. The pilot and tugboats keep the ship parallel during this lateral movement. When the vessel reaches the velocity of 6 cm/s the tugboats keep applying force to keep the lateral movement at constant speed. After 1 minute of constant speed the tugboats stop pushing the vessel and the ship is released. After release the ship will decelerate until the lateral velocity is 0.

For the second manoeuver the pilot positions the ship parallel to the quay at a distance of approximately 60 meters. The same procedure is carried out as for the free basin. The tugboats push until a lateral velocity of 6 cm/s and release the vessel when the distance to the quay wall is approximately 40 meters. The ship will decelerate until the lateral velocity is 0. Now, a closed quay wall is present to verify the assumptions and boundary conditions that surfaced through the theory. During the second manoeuver it is expected that the deceleration due to lateral hydrodynamic forces is faster than during the first manoeuver. This is called the water cushion effect.

During the manoeuvers of experiment 1, the exact moment when the tugboats release the vessel is timed. Besides, environmental conditions and peculiarities on the berthing procedure are documented.

3.4.2. Position, velocity & acceleration

The collecting of the position of the vessels over time is done through two real time kinematic positioning receivers (RTK) and portable pilot units (PPU). The RTK consists of two receivers that are positioned at the bow and at the stern of the vessel. From the change in position of the bow and the stern, the velocity and acceleration can be derived during the whole procedure. The PPU consists of two receivers as well, positioned at the bridge of the vessel. PPUs are used by pilots during every berthing manoeuver, the RTK used in these experiments are used additionally to test the reliability of the PPUs. Experiment 1 uses an RTK as well as a PPU to obtain the position and velocity. Experiment 2 only uses an PPU to obtain the velocity.

3.4.3. Hydrodynamic forces

The hydrodynamic forces counteracting the lateral movement of the berthing vessel consist of inertial forces and frictional forces. During the acceleration and deceleration phase of the manoeuver both forces play a role. During constant speed only frictional forces play a role. The water cushion effect is influenced by the vicinity of a quay wall and is in reality an additional hydrodynamic force that is counteracting the lateral movement of the ship. The difference in the deceleration of the vessel in vicinity of a quay wall and the deceleration of the vessel in the basin can be explained by the part of the hydrodynamic counteracting force influenced by the presence of the quay. To measure this, the position of the vessel over time and therefore the velocity, acceleration and deceleration needs to be logged. These are collected from the RTK and PPU measurements. The data obtained can produce the hydrodynamic forces over time according to Newton's second law:

$$\sum \vec{F} = m_{ship} * \vec{a} \tag{3.1}$$

By comparison of manoeuver one and two of experiment 1, the difference in maximum deceleration and therefore difference in maximum resulting forces can be obtained, which is a method to quantify the water cushion effect. The mass of the vessel remains the same during the manoeuvers and through the difference in deceleration the difference in resulting forces can be obtained and analysed.

3.4.4. Experiment 2 - Flow pattern

To investigate the hydrodynamic processes around a berthing ship, the pressure distributions and flow velocities in three dimensions between ship and quay need to be obtained. To achieve this, the fluid velocities and pressures in a watercolumn are measured at the level of the bow and stern of the ship. This is done in three directions for the entire water column at two meters distance from the quay. In addition, one horizontal velocity meter (H-ADCP) is installed at the quay to measure the surface flow velocities in two directions. The H-ADCP is used to investigate the uniformity of the flow between ship and quay. If this flow approximates uniform flow, the total amount of water flowing around the stern can be approximated through the velocity meters (ADCP) at the bottom, the distance between ship and quay and the water depth. It is stated in literature that 70% of the water flows through the under keel gap and 30% of the water flows via the bow and stern during the berthing manoeuver with vessels with a length-to-width ratio of 5-7. This needs to be validated. Furthermore, three pressure sensors that are included in the ADCPs measure the pressure build up during the berthing manoeuver. The behaviour of the pressure distribution over time gives information on the translation waves and the water level elevation due to the accumulation of water.

3.5. Final location and vessel

Taking into account the complex planning of the five different sea quays, the EECV West is suitable for the under water measurements and the berthing manoeuvers. Due to the complex planning, the measurement site for experiment 1 had to be diverted to EECV Midden and experiment 2 had to be diverted to EECV Oost at the last minute. Experiment 1, consisting of two berthing manoeuvers with one vessel, takes place at EECV Midden and is referred to as ship 1. Experiment 2 uses a vessel that berths at EECV Oost and is referred to as ship 2. The two vessels are bulk carriers and the dimensions of the vessels are shown in table 3.2. Ship 2 berths at EECV Oost, which means that the under keel clearance is a variable now and not a constant. Ship 1 berths at EECV Midden, which means that the under keel clearance varies similar to EECV Oost.

Vessel dimensions	*Experiment 1 - ship 1*	*Experiment 2 - ship 2*
Length (m)	292	292
Width (m)	45	45
Draught (m)	18.32	18.04
Lenght-to-width (-)	6.5	6.5

Table 3.2: Dimensions of the vessels that are used for the field experiments

In figure 3.2 the sectional drawing, including instruments is shown. In figure 3.3 a photograph of the quay of EECV Oost is shown.

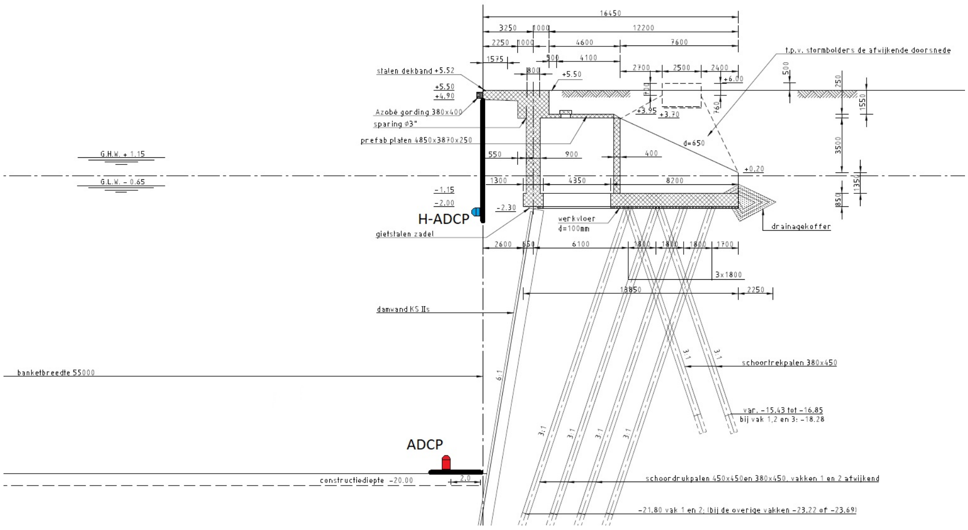

Figure 3.2: Cross section of EECV Oost with instruments (PoR, 2019)

3.6. Measurement techniques

As mentioned in section 3.4 different instruments are used in the experiments. The position of the ship is measured using real time kinematic (RTK) positioning with the use of the global navigation satellite systems (GNSS). Two receivers and one base station are needed. If the distance from three different satellites to the receiver is known, the position of the receiver is known as well. In addition, the position is measured through portable pilot units (PPU) that are used by the pilots. PPUs uses three types of GNSS positioning, dependent on the availability of the satellites. Therefore the accuracy of the PPUs fluctuates. The flow velocities around the vessels are measured with Acoustic Doppler Current Profilers (ADCP). ADCPs uses the Doppler effect of sound waves. These sound waves scatter back on particles in the water column. By measuring this backscatter the flow velocities of the particles and hence the fluid can be obtained. Three different ADCPs are used. The ADCPs used measure flow velocities in three dimensions and in two dimensions. The different instruments and their measurement techniques are further elaborated in appendix A. The accuracy and frequency of the instruments used are displayed in table 3.3.

Figure 3.3: Side view of EECV Oost quay (Cyclomedia, 2019)

	Type	*Position accuracy*	*Measurement frequency*
RTK	Trimble	0.01 m + 1 ppm horizontal & vertical	2 Hz
PPU	GPS/Glonass	4.5 meters horizontal	1 Hz
	EGNOS	0.60 meters horizontal	1 Hz
	RTK-GNSS	0.02 m horizontal; 0.10 m vertical	1 Hz
ADCP	Signature 500	± 0.3% of measured value ± 0.3 cm/s	1 Hz
	AWAC 600 kHz	± 1% of measured value ± 0.5 cm/s	0.1 Hz
	OTT	± 1% of measured value ± 0.5 cm/s	0.2 Hz

Table 3.3: Accuracy of the instruments used

3.7. Post-processing

The field experiments resulted in several datasets consisting of the position and therefore velocity and acceleration of the vessels and the flow velocities and pressures between ship and quay. In order to obtain the desired information from these data, the datasets need to be post-processed. The post-processing per instrument is described briefly in the following subsections.

3.7.1. RTK data

The Trimble RTK data consists of three datasets. The position of the two rovers at the vessel is logged at 2 Hz and the position of the base station situated on the quay is logging as well to obtain a correction signal. The Trimble Business Centre software is used to combine these three datasets. The base station is used to increase the accuracy of the positions of the two rovers. After post-processing, two datasets for the two rovers are obtained with an accuracy of 8 mm. These two datasets contain the position in the Dutch coordinate system (Rijksdriehoekscoordinaten 2008) with corresponding GPS time during the two berthing manoeuvers. To display the position in longitude and latitude the Rijksdriehoekscoordinaten are converted. This is only done for the visualization of the manoeuvers on the spatial map. For the velocity and acceleration measurements the Rijksdriehoekscoordinaten 2008 are used. The orientation of the quay is approximately 25.08°. To find the velocity and acceleration of the vessel perpendicular to the quay, the difference in position relative to the quay is obtained instead of the difference in position in the coordinate system. To obtain the velocity of the two rovers, the difference in position is divided by the time shift (0.5 s). This is done for all the position shifts to obtain the velocity. The same is done to obtain the acceleration, the velocity shift is divided by the time shift (0.5 s). The velocity and the acceleration are very scattered, therefore a moving average is applied to the datasets to find a more precise display of the velocity and acceleration during the two manoeuvers.

3.7.2. PPU data

The laptop receives the raw data from the NMS MPU and the software Qastor processes this raw data to the data that is ready to use for the pilots. The real time data that is displayed to the pilots consists of the position, heading, rate of turn, speed over ground and course over ground. From these the lateral velocities, cross track error, lateral distance and distance along track are derived and displayed (Buuren, 2014). The raw data contains a certain scatter as a result of inaccuracies. Qastor applies a Kalman filter to account for these inaccuracies. The Kalman filter is an algorithm that uses the datapoints over time and estimates the joint probability distribution over these variables for each timeframe. The variables that are produced with the Kalman filter tend to be more accurate than the single measurements alone (Kalman, 1960). The raw data is processed using the Kalman filter and the outcome of these calculations are the variables that are displayed real time for the pilots to use during the berthing manoeuver.

3.7.3. ADCP data

To obtain the correct water velocities and pressures between ship and quay from the velocity meters, the raw data needs to be post-processed first. In figure 3.4 the different possible coordinate systems for the water velocities are displayed. For the analysis of the velocities perpendicular and longitudinal to the quay, the velocities in the ENU coordinate system are the most suitable. The velocities are measured in beam coordinates. To transform this to ENU coordinates, the orientation of the instrument is very important. The AWAC and the Signature were lowered into the water from a boat to the bottom of the berth, which is approximately 18 meters deep, and therefore the orientation of the instrument at the bottom is unknown after installing.

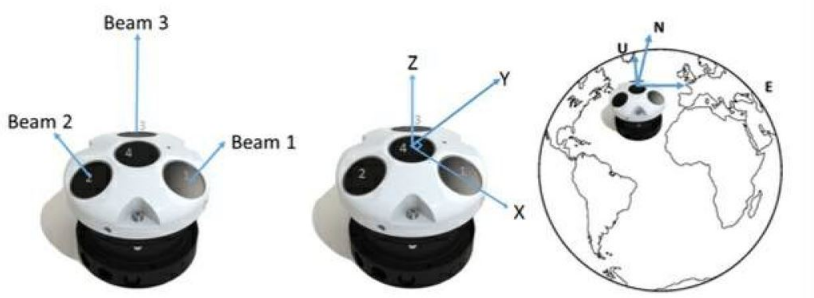

Figure 3.4: Coordinate systems for the ADCPs (Nortek Manuals, 2018)

However, the instruments do log their own orientation through attitude sensors and a compass. The OTT is installed at the quay wall structure, the orientation of the OTT is therefore known. In figure 3.5 the heading, roll and pitch of the AWAC and Signature during the berthing manoeuver of ship 2 are displayed. The heading is rotation around the z-axis, roll is rotation around the x-axis and pitch is rotation around the y-axis. The heading and pitch are positive for a clockwise rotation and the roll is positive for a counter-clockwise rotation around their axes. For the AWAC and the Signature it is seen that the heading changes during the berthing manoeuver of the ship. This means that the flow velocities are such that it causes the instrument to move.
From the heading, pitch and roll the flow velocities in the ENU coordinate system are calculated. This is done by constructing a heading matrix, a pitch matrix and using the transformation matrix unique for every instrument, which is based on tranducer geometry. From these three matrices the resulting transformation matrix is calculated and used to transform the beam velocities measured by the instrument to velocities in the XYZ and eventually ENU coordinate system. From the ENU velocities and the orientation of the quay the flow velocities perpendicular and longitudinal to the quay can be calculated.

Moreover, the amplitude counts of the beams need to be investigated. When the signals from the beams are reflected, due to for example a vessel, the signal is disturbed and the velocity profile is not reliable anymore. To investigate the reliability of the cells of the AWAC, Signature and OTT the amplitude count is investigated for the cells during the berthing manoeuver. If the amplitude count experiences a sudden increase, the signal most likely encountered a boundary and the signal is not reliable anymore (Nortek Manuals, 2018). Therefore, the reliability of the velocities per time step are known.

Figure 3.5: Orientiation AWAC 600 & Signature 500

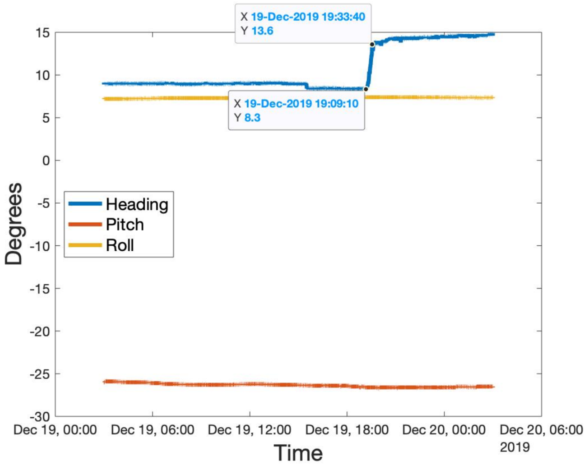

(a) Heading, pitch and roll during berthing - AWAC

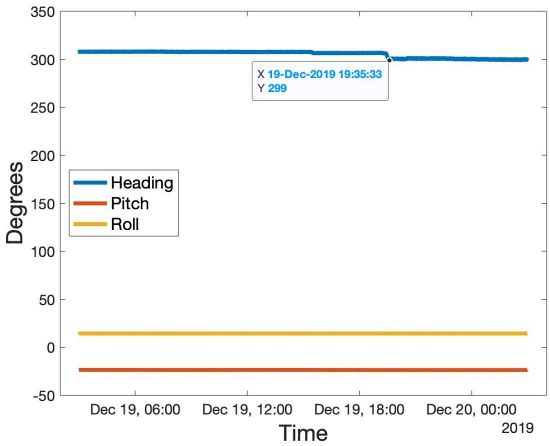

(b) Heading, pitch and roll during berthing - Signature

When the flow velocities are converted to the correct orientation, a moving average is applied to the ADCP data to discard the outliers and visualize the velocity trend. Now, the flow velocities and pressures can be visualized and analyses can be performed. It is important when analysing the velocities the reliability of the measurements is taken into account as well. This is discussed in chapter 4 during the interpretation of the experiments.

4

Results & Analyses

4.1. Height of tide and flow velocities

Information on the height of the tide (HoT), the flow velocities and the depth contours of the bottom during the experiments are needed to perform analyses. Information on the height of the tide and the velocities during the berthing manoeuvers of ship 1 and ship 2 are obtained from Port of Rotterdam authority as shown in appendix B, figure B.3 and B.4. From this information, the position of the vessel during the two experiments and the depth contours in the Port of Rotterdam, the under keel clearance is calculated and shown in table 4.1.

	Experiment 1						Experiment 2		
	Manoeuver 1			Manoeuver 2					
	Stern	Bow	Center	Stern	Bow	Center	Stern	Bow	Center
Depth (NAP)	-23.9	-22.2	-22.2	-19.7	-19	-19.3	-19.1	-19.1	-18.9
HoT (NAP)	+0.53	+0.53	+0.53	+0.80	+0.80	+0.80	-0.055 - +0.3	-0.055 - +0.3	-0.055 - +0.3
Draught (m)	18.32	18.32	18.32	18.32	18.32	18.32	18.04	18.04	18.04
UKC (m)	6.11	4.41	4.41	2.18	1.48	1.78	1.005 - 1.36	1.005 - 1.36	0.805 - 1.16
h/D (-)	1.33	1.24	1.24	1.27	1.1	1.1	1.09 - 1.11	1.09 - 1.11	1.04 - 1.06

Table 4.1: Information of the vessel and the surrounding water during the field experiments

Note that experiment 2 takes approximately 20 minutes, therefore the water depth increase due to the tide is taken into account as well. The under and upper limit is given in table 4.1, the gradient is linear. For experiment 1 the manoeuvers are only a couple of minutes, starting after the release of the vessel. Therefore tidal increase is negligible.

4.2. Experiment 1 - Hydrodynamic forces

4.2.1. PPU Data

To investigate the behaviour of the vessel during the two berthing manoeuvers, the position, velocity and acceleration are plotted over time for both manoeuvers. To pick out the data from the entire dataset that corresponds to the two manoeuvers, the logbook recorded during the two lateral berthing manoeuvers needs to be consulted (table 4.2). It is known that from the time of release until the time where the tugs push again, the vessel is not subject to external forces from the tugboats or the engine. The only forces acting on the vessel are the hydrodynamic forces.

The position of the vessel over time is measured using two different instruments. Two RTK receivers are used in addition to the the PPU. It is presumed that the data obtained with the RTK measurements, provided that the post-processing is done properly, is more accurate than the position measured with the PPU. Therefore, the RTK data instead of the PPU data is used to obtain the acceleration and deceleration of the ship. In section 4.4 a comparison is made between the PPU and RTK lateral velocity measurements to draw a conclusion on the quality of the data the PPU provides.

	Manoeuver 1	Manoeuver 2
Tugs push	05:35:20	05:47:10
Tugs release	05:40:00	06:46:38
Tugs correct	05:46:15	-
Tugs push again	05:47:10	06:53:17
Deceleration time	**00:07:10**	**00:06:39**

Table 4.2: Logbook of the berthing manoeuvers during the field experiment

4.2.2. RTK data

The RTK data log the position of the ship with 2 Hz, so every 0.5 seconds. The journey ship 1 made during the field experiments is logged. These raw datapoints are visualized by plotting them on the map of Port of Rotterdam using the Dutch spatial reference system (Rijksdriehoekscoördinaten, RD 2008). This is shown in figure C.2 and C.3 in appendix C. The position of the lateral berthing manoeuver over time of both the stern and bow sensor is visualized in figure 4.1 and C.4. From these figures it is seen that the vessel rotates while

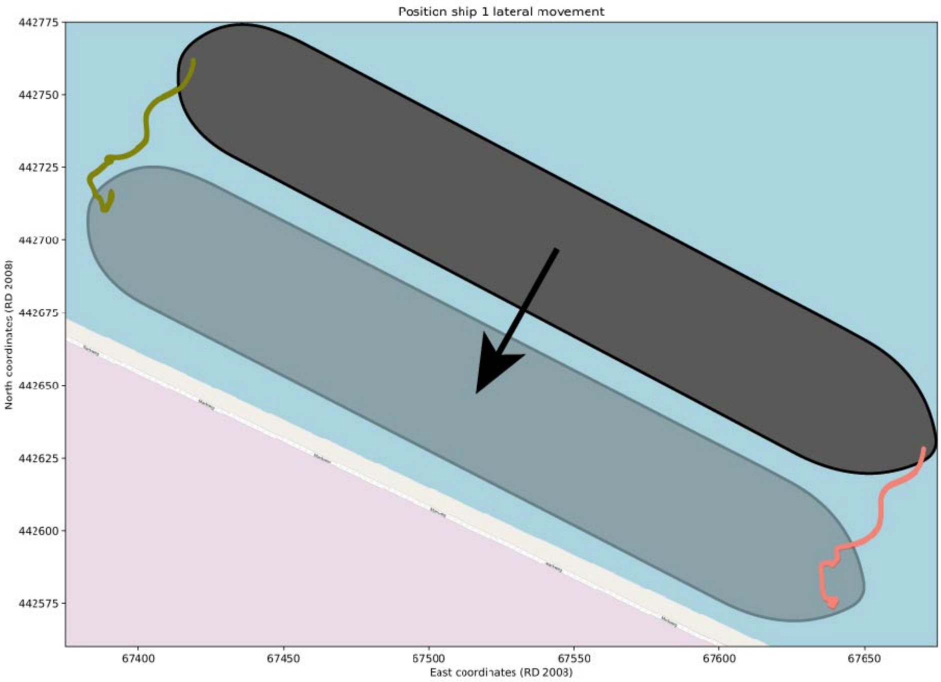

Figure 4.1: Visualization of the lateral berthing manoeuver

approaching the berth. The lateral velocity and lateral acceleration of the bow and stern during manoeuver 1 and manoeuver 2 are shown in figures C.5-C.8 in appendix C.

To make a comparison between the hydrodynamic forces acting on the vessel between manoeuver 1 and 2, the rotation and the corresponding angular velocity and acceleration of the ship are plotted as shown in figures 4.2 and 4.3. To make a comparison of the hydrodynamic forces according to Newton's second law, the center velocity and acceleration and deceleration during manoeuver 1 and 2 are plotted in figure 4.4.

Figure 4.2 shows that the angular velocity during manoeuver 1 is an almost perfect sinus shape. The velocities during the second manoeuver deviate from the velocities during the first manoeuver in the first half of the manoeuver. The second half of the first and second manoeuver is of similar shape, the second manoeuver reaches slightly smaller angular velocities and decreases much faster than the angular velocities during manoeuver 1.

In figure 4.3 the corresponding angular acceleration is compared for manoeuver 1 and 2. The angular acceleration of manoeuver 1 has a parabolic like shape. The acceleration and deceleration of manoeuver 2 oscillates more, just like the velocity. In the second half of the manoeuver, from approximately 200 seconds, the velocity of the vessels has a similar shape. If one compares the acceleration and deceleration of the second half of the manoeuver, it shows that deceleration of manoeuver 2 is much larger than the deceleration of

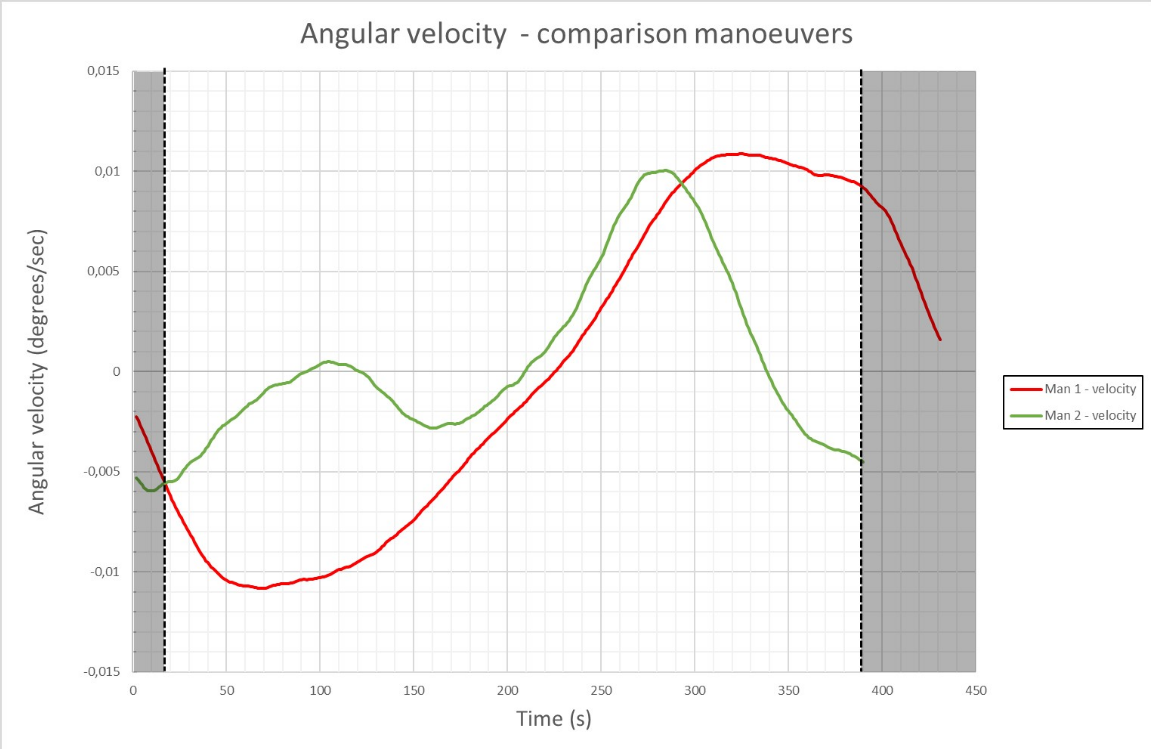

Figure 4.2: Comparison of the two berthing manoeuvers regarding the angular velocity of the ship

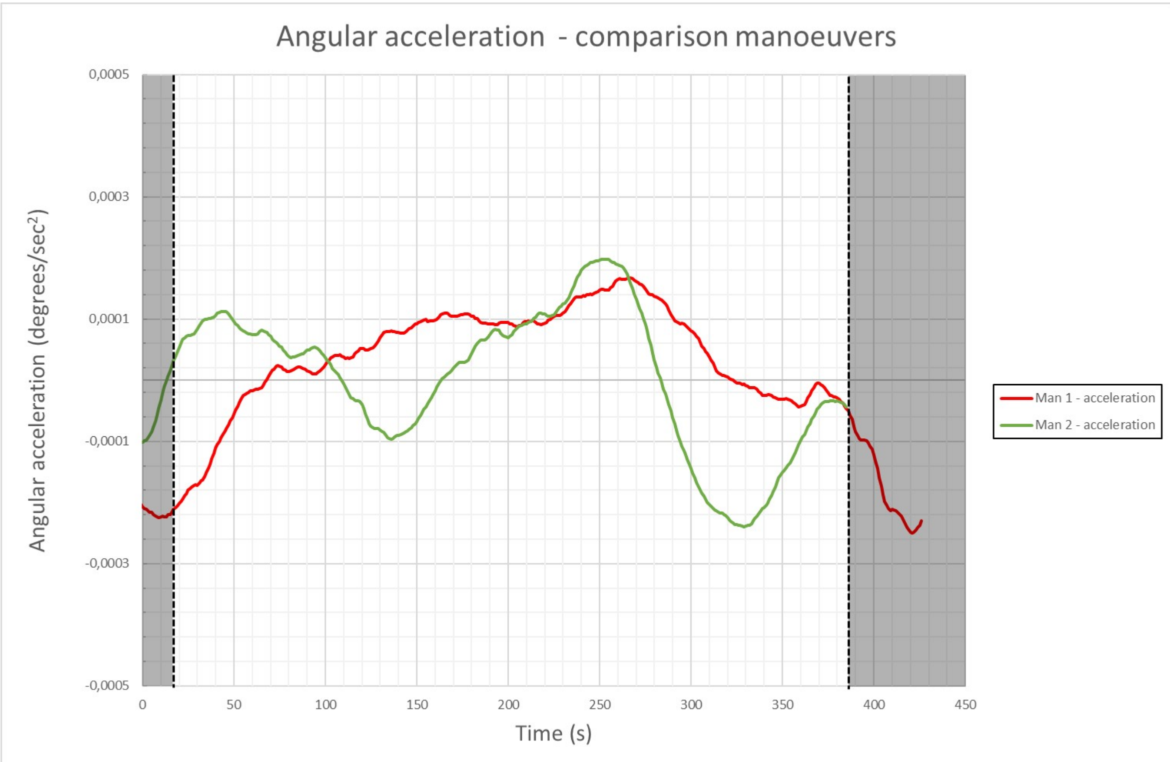

Figure 4.3: Comparison of the two berthing manoeuvers regarding the angular acceleration of the ship

manoeuver 1. The deceleration of manoeuver 1 catches up in the last 40 seconds. This cannot be compared to the deceleration of manoeuver 2, because that manoeuver is shorter. If one compares the two berthing manoeuvers from the point where the angular velocity is similar ($t = 20s$) until the point where manoeuver 2 stops ($t = 385s$) it is seen that the angular acceleration and deceleration are more pronounced for manoeuver 2. The largest deceleration is seen during manoeuver 2. In the second half of the manoeuver (from $t = 200s$) the maximum angular deceleration of manoeuver 2 is 0.0025 degrees/s^2 and for manoeuver 1 is 0.0004 degrees/s^2. This means that the maximum hydrodynamic forces acting on the vessel in the second half of the manoeuver is 6.25 times larger in vicinity of the quay wall.

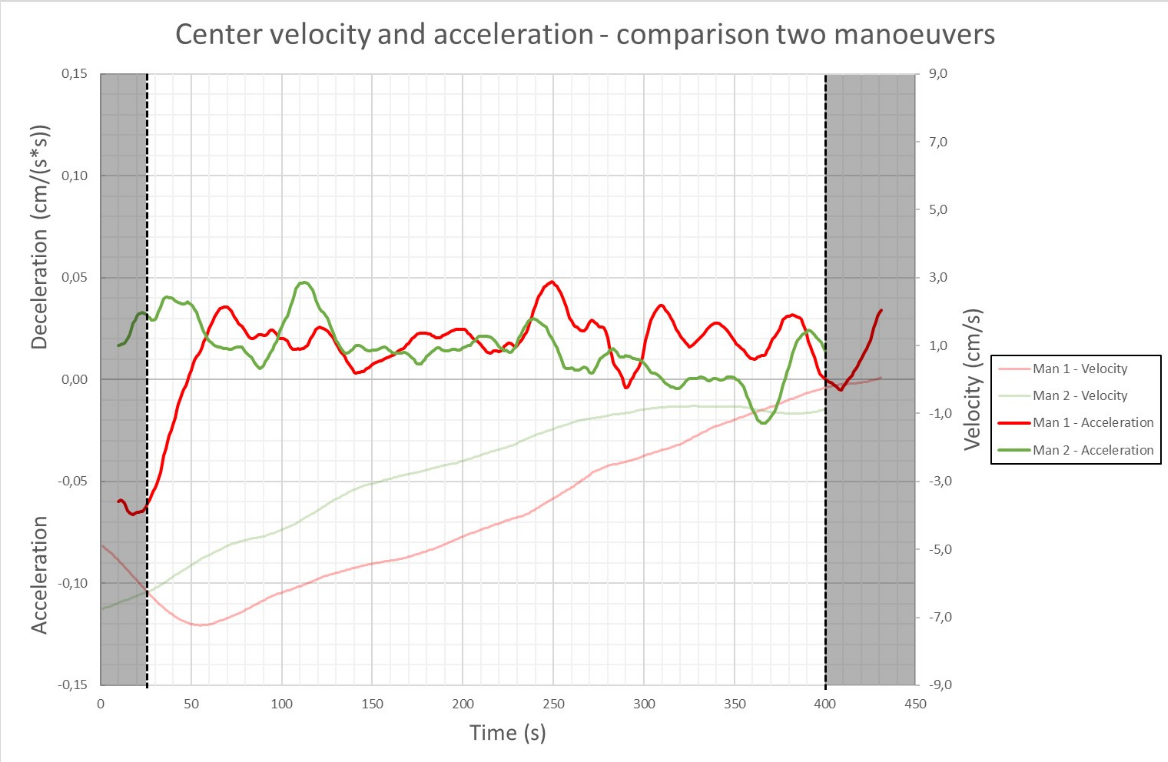

Figure 4.4: Comparison of the two berthing manoeuvers regarding the lateral velocity and acceleration of the center of the ship

In figure 4.4 the velocities, accelerations and decelerations of the center of the ship during the two berthing manoeuvers are compared. This figure shows that the velocity decrease is similar for the two manoeuvers. Manoeuver 1 shows that it reaches zero velocity before manoeuver 2. The maximum decelerations are the same for both manoeuver 1 and 2 but manoeuver 1 has an overall higher deceleration. It is necessary to take into account the flow pattern of the basin during the berthing manoeuver to explain the behaviour of the berthing manoeuver. If one looks at this flow pattern (figure 4.5 and appendix B), it is seen that the mouth of the Breeddiep attracts flow at the position of the vessel during manoeuver 1. This could be an explanation for the fast deceleration of the vessel, due to the suction force of the mouth of the Breeddiep. It could also be an explanation for the difference in behaviour of the first half of the manoeuvers in figures 4.2 and 4.3.

Figure 4.5: Flow velocity breeddiep experiment 1 - manoeuver 1

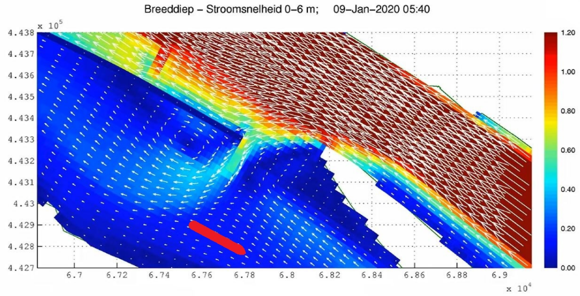

(a)

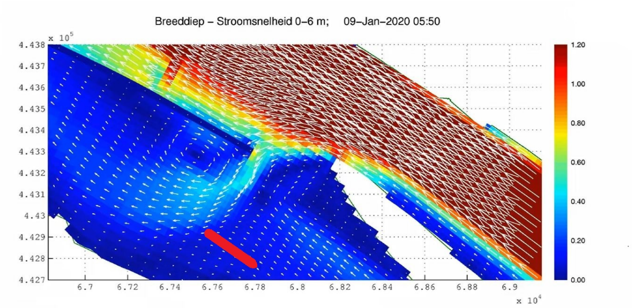

(b)

4.3. Experiment 2 - Flow pattern

4.3.1. PPU data

The bow, stern and center distance from the quay and the velocity and acceleration of ship 2 is logged with the PPU. The distance from the quay, velocity and acceleration of the center is shown in figure 4.6. The PPU graphs for stern and bow are shown in figure D.1 and D.2 in appendix D.

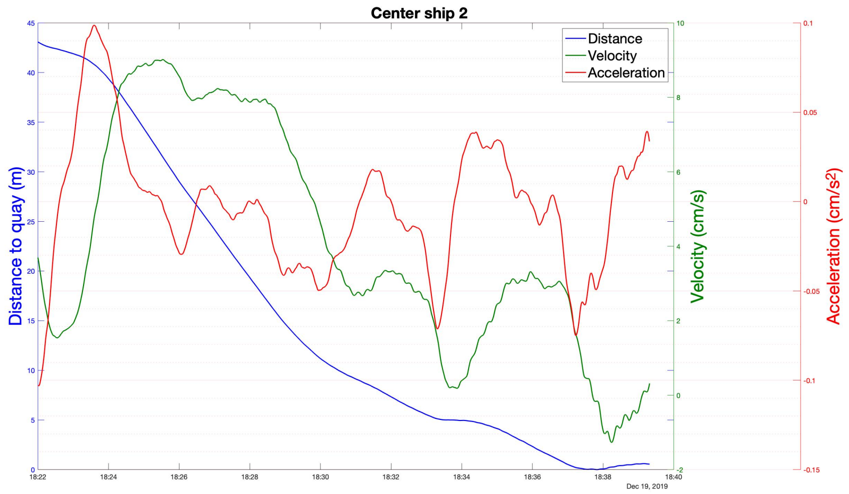

Figure 4.6: Distance to the quay, velocity and acceleration of the center of ship 2

4.3.2. Constant water level and conservation of mass

From the distance between ship and quay, the depth profile and the height of tide as shown in table 4.1, the water mass between ship and quay can be calculated during the berthing manoeuver. From the change in water mass over time the outflow can be calculated. Two extreme scenarios are investigated, first one being only bow and stern flow parallel to the quay wall and therefore no under keel flow and second, only under keel flow and neglected bow and stern flow (figure 4.8). The mean flow velocities per linear meter from the conservation of mass without water level elevation are calculated for this two scenarios and are shown in figure 4.7.

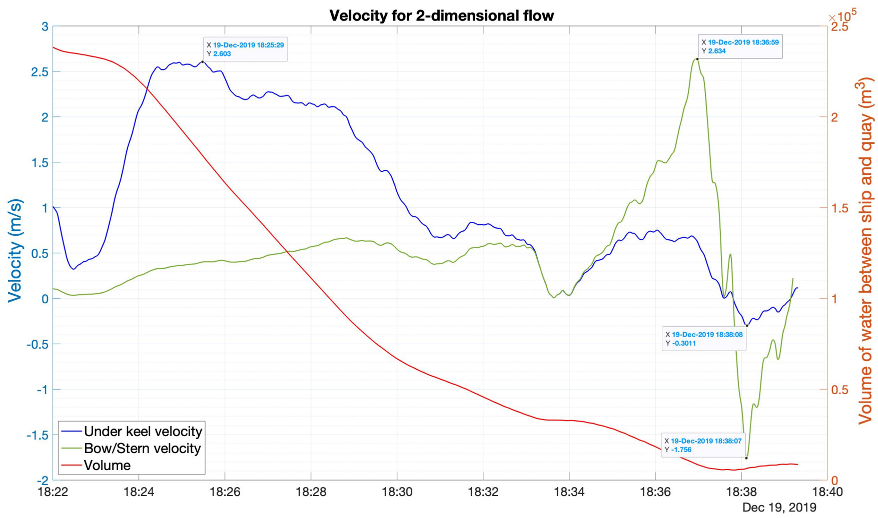

Figure 4.7: Velocities derived from constant water level and conservation of mass between ship and quay

Figure 4.7 and figures D.1 - D.3 show that under keel flow velocities are highest in the beginning of the manoeuver, at a distance of approximately 40 meters from the quay. The bow and stern velocities are highest at the end of the manoeuver, when the distance to the quay is less than 10 meters. The highest value for the under keel flow velocities is 2.634 m/s, for the bow and stern flow velocities the highest value is 2.603 m/s. Just before 18:38 GMT the flow velocities become negative, this can be explained by looking at figure D.2 and D.1. The distance to the quay increases, meaning that the vessel moves away from the quay. If the vessel moves away from the quay, the water mass between ship and quay increases resulting in negative flow velocities. The under keel velocity decreases during the manoeuver because the under keel clearance increases. The bow and stern velocity increases because the distance between ship and quay decreases.

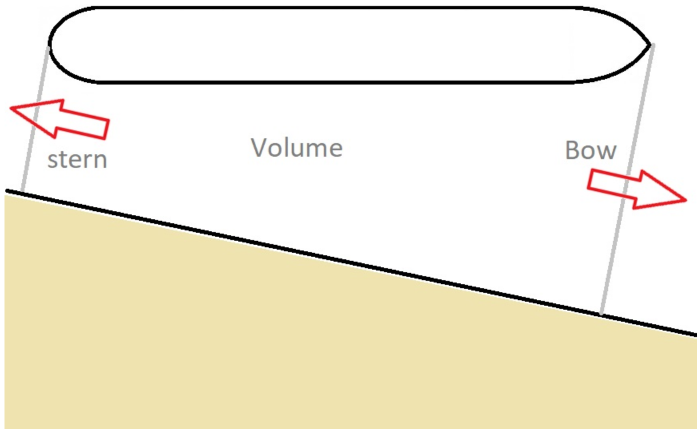

Figure 4.8: Bow and stern stern flow from constant water level and conservation of mass

4.3.3. ADCP data

First, the pressure distributions at the bow and stern are displayed, to investigate the pressure difference during the berthing manoeuver (figure 4.9).

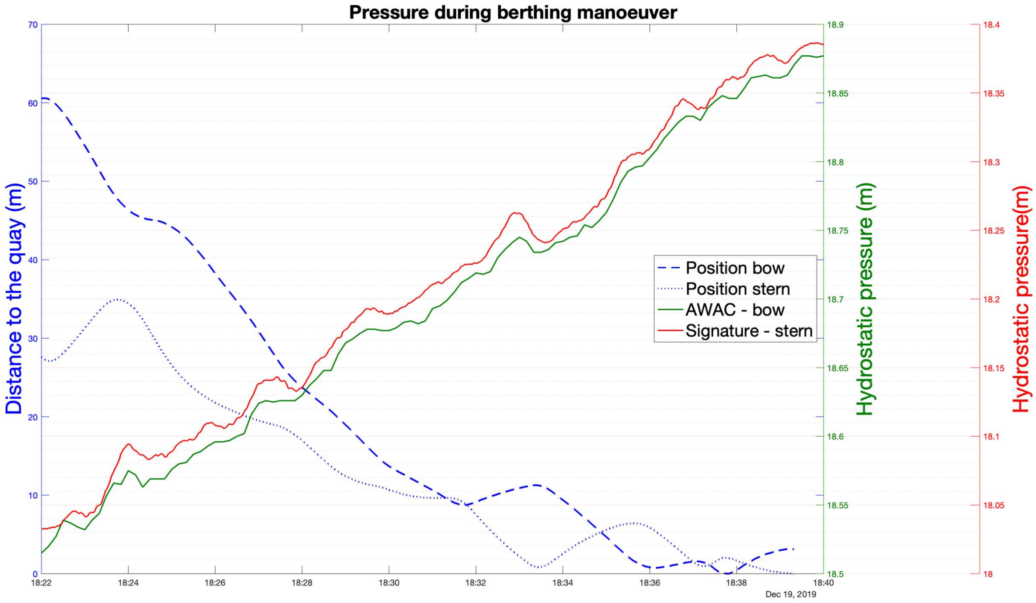

Figure 4.9: Pressure measured with the AWAC and the Signature during the berthing manoeuver

From figure 4.9 it is seen that the pressure distribution during the berthing manoeuver behaves similarly. This is peculiar because the two instruments are 210 meters removed from each other. There is a pressure difference between the two instruments, but this pressure remains similar which means that it is most likely caused by a difference in the bottom of the berth. Furthermore, the two instruments do not have the same dimensions, this also attributes to the difference in pressure measurements. If one looks closely to the distance between ship and quay for both the bow and the stern of the vessel, it demonstrates that the peaks in hydrostatic pressure from approximately 18:32 GMT seem to correspond to the peaks in distance from the quay. These peaks represent change in vessel direction. It is remarkable that when the bow and stern position are opposite, such as at 18:33 GMT the pressure behaves similarly. This is the case for all the opposite distance peaks from 18:33 GMT until 18:40 GMT. Furthermore, there are oscillations visible in the beginning of the manoeuver, when the vessel is at least 30 meters away from the quay. An explanation could be external disturbances, such as waves from passing ships. However, this could also be the cause for the oscillations at the end of the berthing manoeuver instead of the approaching vessel. Because of the fact that the pressure behaves almost identically for the bow and the stern ADCP, while the distance to the quay of the bow and the stern of the ship differs, it is not clear if the movement of the ship influences the water level elevation between ship and quay. Besides, the water level elevation oscillates with the same order of magnitude when the vessel is tens of meters away from the quay as when the vessel is within 5 meters away from the quay. This contributes to the uncertainty of the correlation between the position, velocity and acceleration of the lateral moving vessel and the water level elevation between ship and quay. From figure D.1 and D.2 it is seen however that the peaks in acceleration and deceleration correspond to the peaks in distance from the quay and therefore to the peaks in the water level elevation. In addition it is worth noting that the peaks in water level elevation do seem to have a recurrent pattern.

To investigate the possibility of translation waves counteracting the vessel it is imortant to have knowledge on how these translation waves would influence the hydrostatic pressure measurements. The velocity of translation waves in shallow water is:

$$c_0 = \sqrt{g * h} = \sqrt{9.81 * 19} = 13.65 m/s \tag{4.1}$$

If the hydraulic damping starts to play a role from approximately 10 meters distance to the quay wall, the wave has travelled towards the quay wall and back in 1.365 seconds. This means that oscillations of the water level with a period of around 1 second should be visible in the hydrostatic pressure measurements. The water level should be measured with a frequency of 4 Hz to capture the water level oscillation with a period of around 1 second. The AWAC measurements as well as the Signature measurements are not accurate enough since their measurement frequency is 0.1 Hz and 1 Hz respectively. The oscillations that would prove the occurrence of translation waves can therefore not be captured in the measurements (figure 4.10) and no conclusion on the occurrence of translation waves can be drawn.

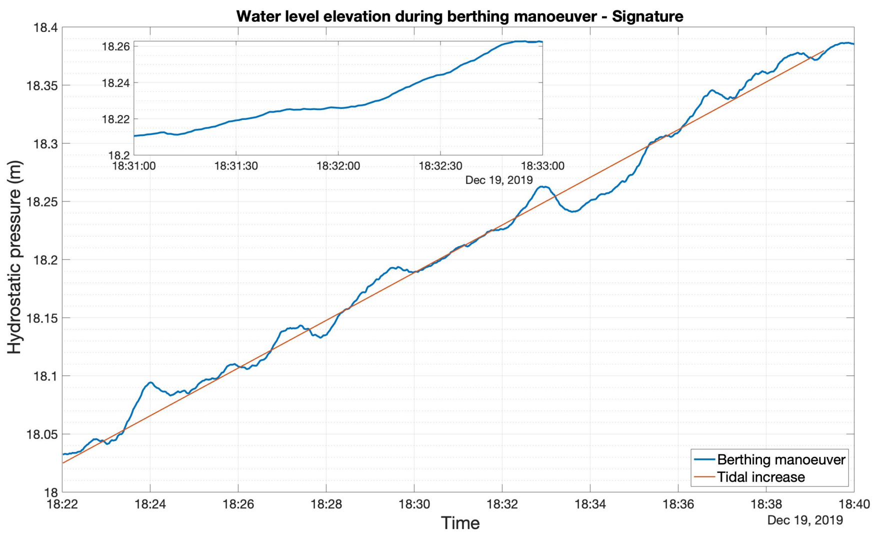

Figure 4.10: Comparison of the pressure and the measured tidal increase during the berthing manoeuver - Signature

To further investigate the pressure increase and oscillations, the water level elevation during the berthing manoeuver is compared to the water level elevation one tidal period before the berthing manoeuver. Figure 4.11 shows that the pressure distribution from the two instruments also behaves similarly. The pressure difference between the two instruments is constant and the same as in figure 4.9. Oscillations are visible again, which can be attributed to environmental disturbances. It is notable however, that the peaks seen in figure 4.9 are in the order of 0.01 meter, while the peaks in figure 4.11 are in the order of 0.02 meter. This means that the oscillations are twice as big with the presence of a lateral berthing vessel than without a vessel.

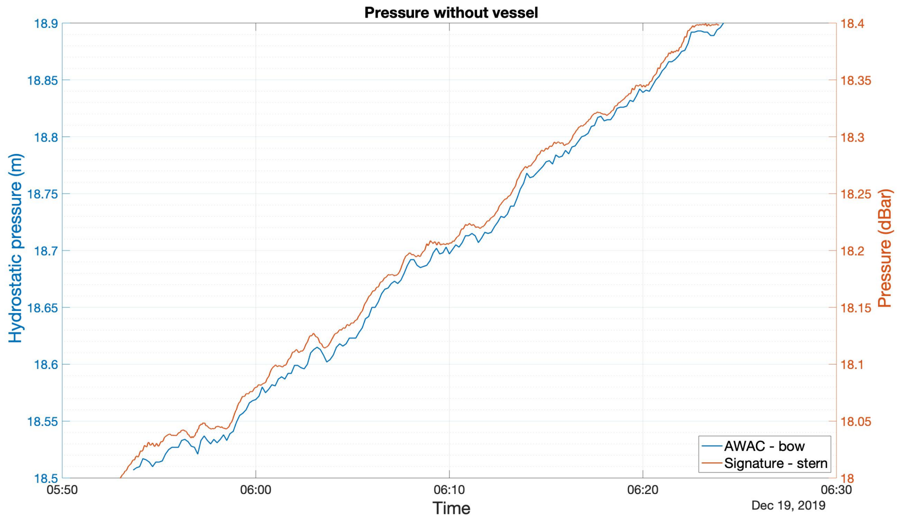

Figure 4.11: Pressure increase 19th of december 05:53 - without berthing vessel

From figures 4.10 and 4.12 it is seen that the measured water level increase follows the measured tidal increase in the port. Potential water level elevation due to the lateral berthing manoeuver cannot be deduced from these graphs due to the measured oscillations. Moreover, the tidal increase is measured and predicted in relation to mean water depth. The exact water depth (NAP) at the place of the meters is not known, therefore there is an inaccuracy in the tidal increase. Strong conclusions from the deviations from the tidal increase measured during the berthing manoeuver cannot be drawn.

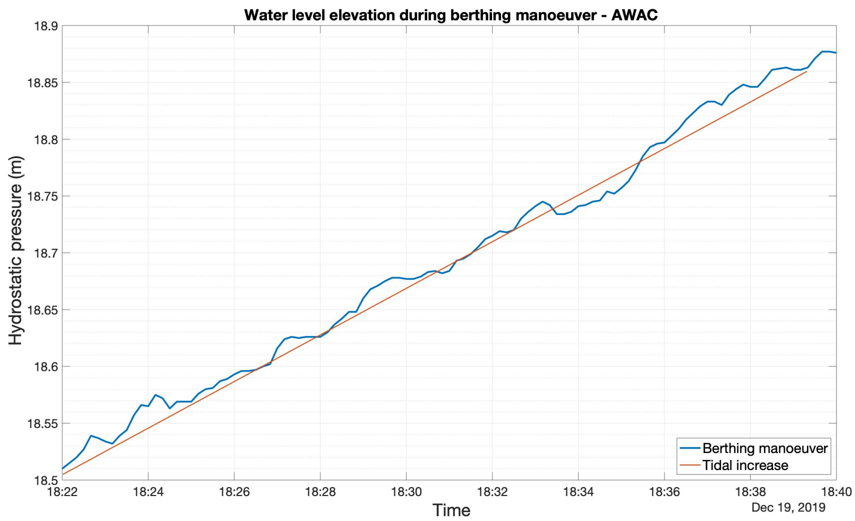

Figure 4.12: Comparison of the pressure and the measured tidal increase during the berthing manoeuver - AWAC

Second, the velocity distributions for the AWAC, Signature and OTT are investigated. The graphs for the longitudinal, perpendicular and upward velocity are shown in appendix D. In the figures in appendix D the averaged velocities per cell are plotted over time. For the AWAC this is 19 cells and for the Signature this is 38 cells. The cells are evenly distributed over the entire water column. In appendix E the reliability of the three velocity meters is investigated. The manual of the ADCPs (Nortek Manuals, 2018) learns that when the amplitude counts per time unit are plotted and there is a sudden increase, it means that the velocity meter is disturbed and the flow velocity at that time should be interpreted with caution. The disturbance at the end of the cell, is the disturbance caused by the surface. Figures E.1, E.3 and E.2 show that the upward velocity at the bow starts to be disturbed from approximately 8 meters depth to the surface, the perpendicular velocity only shows disturbances from 1 meter depth to the surface and the longitudinal velocity shows disturbances from 14 meters depth to the surface. From figures E.4, E.5 and E.6 it is seen that the upward velocity at the stern is disturbed from 18:33, the end of the berthing manoeuver. The rest of the cells do not show significant disturbances, only a few outliers. The presence of the surface is seen in the last cells, from 4 meters below surface. The perpendicular and longitudinal flow velocities show the vessel moving in to the measured water column of the velocity meters. Therefore the signal should be interpreted with caution from 18:22 - 18:35. The OTT velocity measurements from figures E.7 and E.8 show a constant disturbance around cell number 4. It is possible that the constant disturbance is from the water surface which means that the horizontal looking ADCP moved such that it tilted towards the water surface. This means that only the first 4 meters from the quay show the right water velocities.

To investigate the flow velocities over the entire water column, the averaged flow velocities per cell summed are the velocities over the entire water column. This is shown in figures 4.13 and 4.14. It is seen that the flow velocities are in the same order of magnitude of the calculated flow velocities from figure 4.7. This means that the flow velocities measured seem promising.

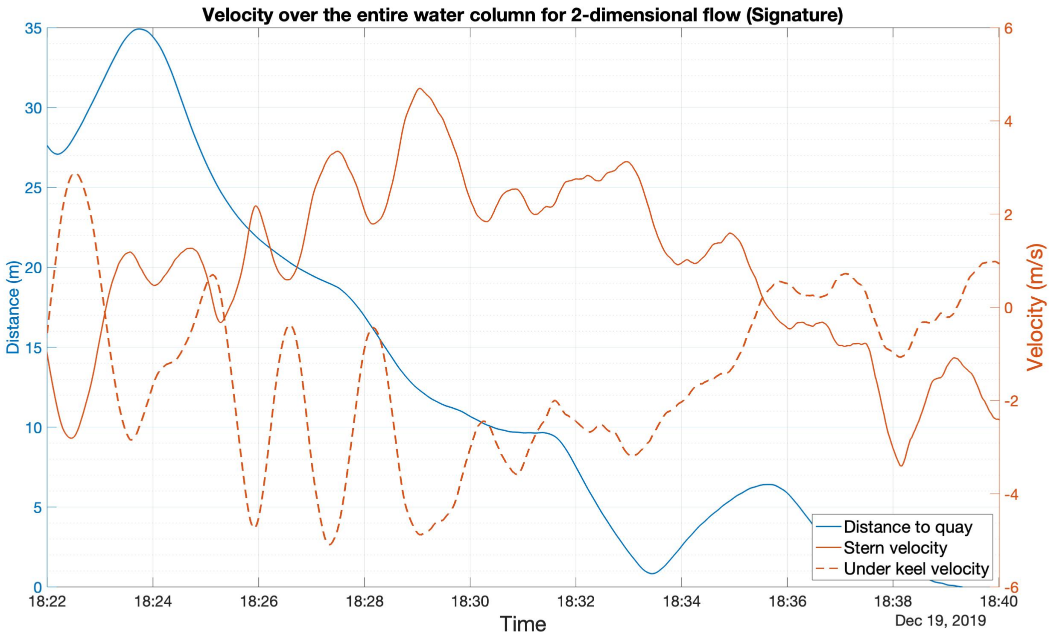

Figure 4.13: Velocities over the entire water column during the berthing manoeuver - Signature

In addition, the uniformity of the water between ship and quay is investigated. This is done analyzing the velocity profile of the OTT. The velocities longitudinal to the quay per meter distance from the quay are shown in appendix D. In figure E.9, the flow velocities per cell over time are plotted with their mean and the 95% confidence interval. To investigate the precision of the velocity per meter distance from the quay the coefficient of variation is used. The coefficient of variation is a statistical measure to classify the dispersion of datapoints. Because we want to know the uniformity of the flow from the OTT data, in other words the similarity of the velocities per meter in the water column, this coefficient is helpful in determining if the flow is uniform.

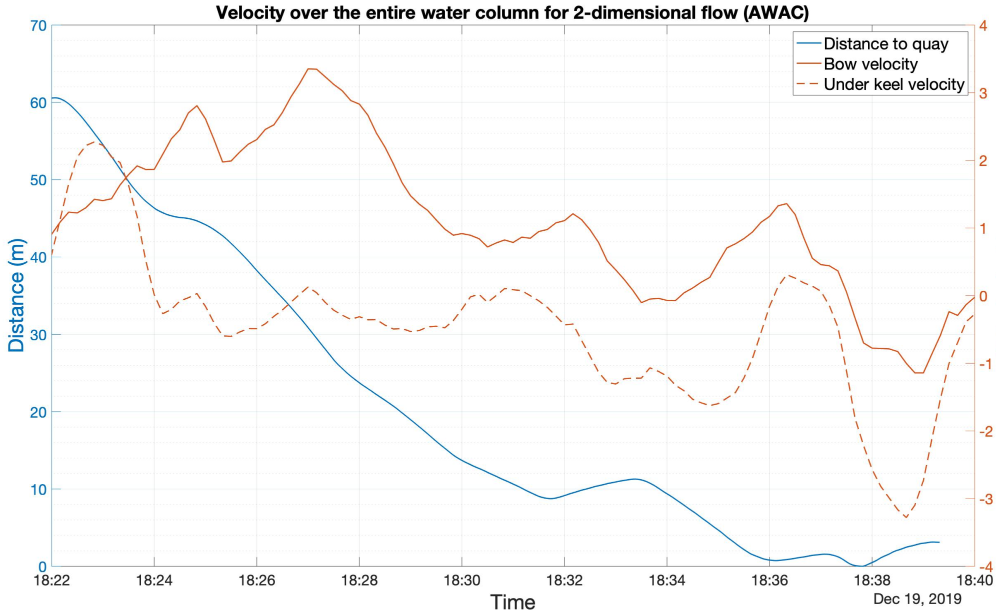

Figure 4.14: Velocities over the entire water column during the berthing manoeuver - AWAC

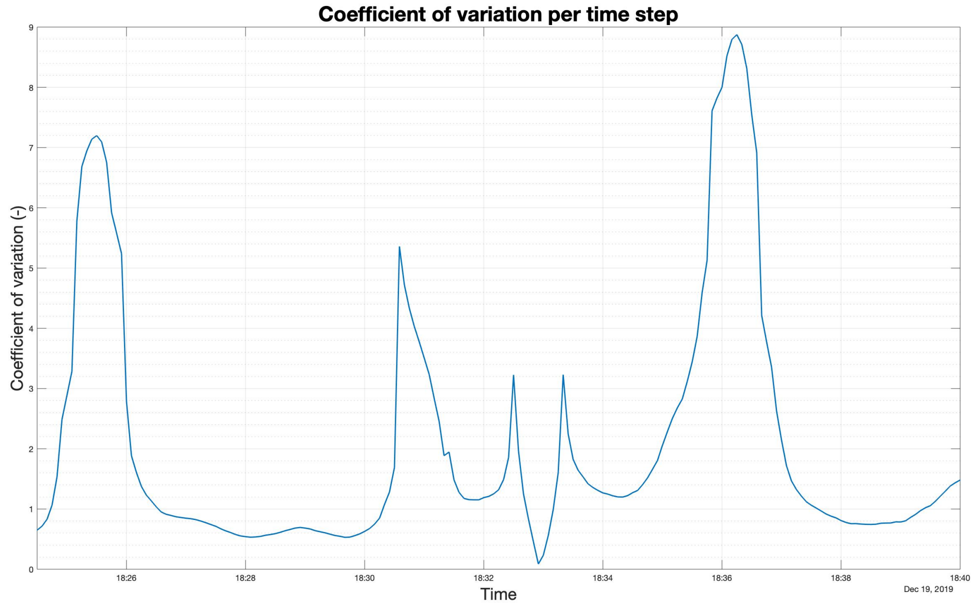

Figure 4.15: Uniformity water between ship and quay

In figure 4.15 the coefficient of variation during the berthing manoeuver is plotted. From Abdi (2010) it is seen that if the coefficient of variation is below 1 it is considered acceptable in terms of precision. From the figure it is concluded that the coefficient of variation is low enough during the berthing manoeuver from 18:26 hours until 18:30 hours to consider the flow uniform. Therefore, the percentage of water flowing under the keel and the percentage of water flowing via the bow and stern can be calculated during that time interval of the berthing manoeuver.

After thorough investigation of the reliability of the velocity meters placed at the bow and the stern, and the total volume between ship and quay during the berthing manoeuver a stable, accurate part of the berthing manoeuver and the total flow via the bow, stern and under keel is calculated. The percentage of water escaping via the keel and bow and stern during the last 30-60 meters from the quay wall is shown in figure 4.16. It appears that approximately 80% escapes via the keel and the remaining 20% escapes via the bow and stern.

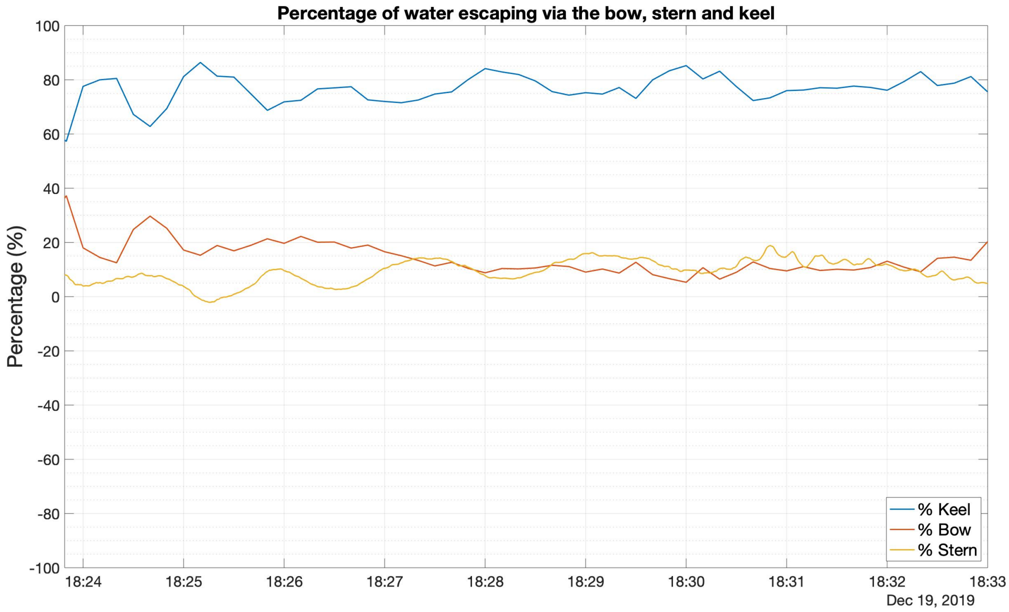

Figure 4.16: Percentage of water escaping longitudinal or perpendicular during the berthing manoeuver

4.4. Comparison RTK and PPU

Finally, the similarity between the RTK and PPU is investigated to test the accuracy and therefore usability of the PPU data used in experiment 2. From figures 4.17 and 4.18 it is seen that the performance of the PPU is very good in comparison to the RTK. For the entire measurement period, the RTK and PPU measurements correspond very precisely. To investigate the performance of the PPU further, the two berthing manoeuvers for as well the bow as the stern are investigated and shown in figures F.1 - F.4 in appendix F.

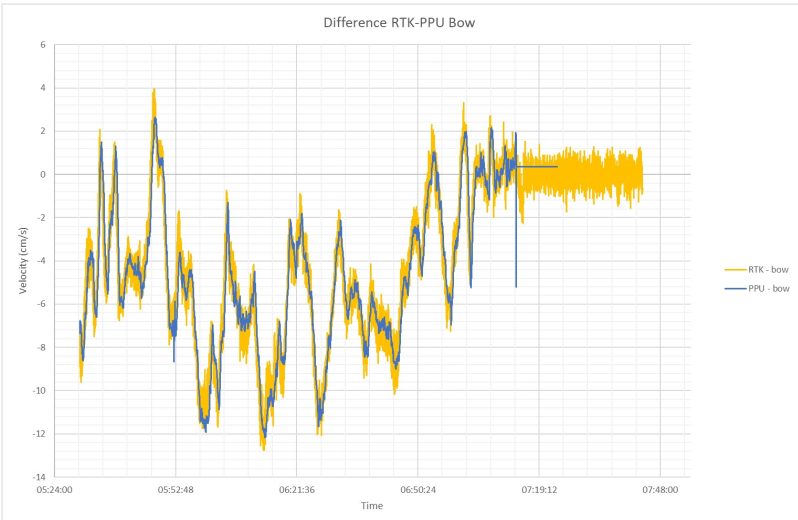

Figure 4.17: Difference in velocity measurements between the PPU and the RTK - bow

If one looks at the RTK and PPU performance during the two manoeuvers a consistent delay in the two graphs is observed. This could be explained by the fact that the RTK time is calibrated with GMT, the PPU time is not calibrated with GMT, but with the time of the computer that performs the post-processing. This computer is not calibrated with GMT frequently. This could be the reason why the PPU graph is delayed slightly. However, despite the fact that the PPU performs very well in measuring the berthing velocity and acceleration, it should be taken into account that dependent on the PPU used, the time could have a little deviation from GMT.

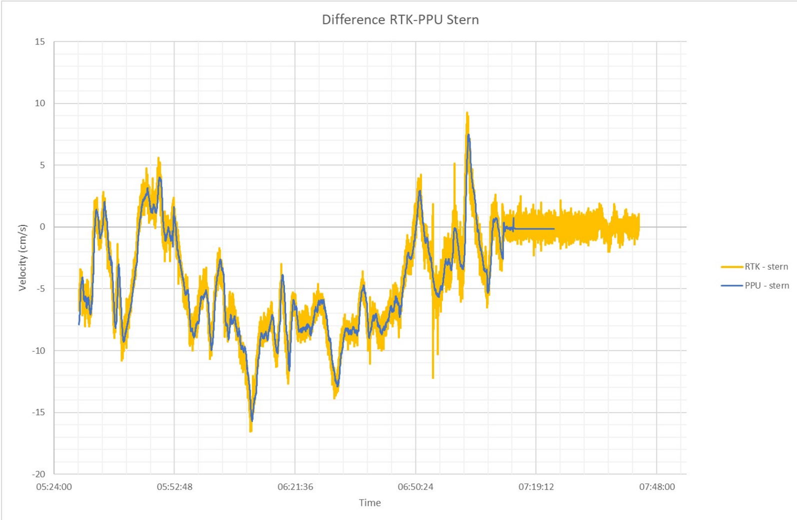

Figure 4.18: Difference in velocity measurements between the PPU and the RTK - stern

4.5. Summary

The first half of manoeuver 1 from experiment 1 is disturbed by the mouth of the Breeddiep, therefore only the second half of manoeuver 1 and 2 can be compared. From this comparison it appears that the maximum angular acceleration caused by the hydrodynamic forces acting on the vessel is 6.25 times larger when the quay wall plays a role. From the velocity and acceleration of the center of the ship the influence of the quay cannot be derived. It is seen that inertia plays a role during the first 25 seconds in manoeuver 1 and that manoeuver 1 is subject to a larger force than manoeuver 2. This is the opposite of the findings concerning the force causing the angular velocities.

From the distance between ship and quay, the water depth and the height of tide, the maximum velocities are derived using a constant water level and the principle of conservation of mass. The maximum velocities for 100% bow and stern flow are -0.3 m/s and 2.6 m/s and for 100% under keel flow -1.7 m/s and 2.6 m/s.

The water level elevation is investigated following the ADCP data. Oscillations that indicate waves are observed. The measured hydrostatic pressure increase follows the measured tidal increase in the port. It is also observed that with a berthing vessel the oscillations are almost twice as large as without a berthing vessel. The water level oscillations correspond with the acceleration and deceleration of the vessel. It is concluded that water level elevation caused by the berthing manoeuver apart from the tidal increase cannot be deduced from the hydrostatic pressure measurements due to noise in the measurements due to environmental disturbances and due to the accuracy of the instruments used. Furthermore, it is concluded that the presence of translation waves traveling from the vessel to the quay wall and back can also not be deduced from the hydrostatic pressure measurements due to the lack in in measurement precision of the instruments used.

The velocities measured with the ADCPs are promising and accurate after evaluation of their accuracy and order of magnitude. The average velocities obtained and the volume of water between ship and quay are used to calculate the percentage of water flowing via the bow and stern and the percentage of water flowing under the keel. Approximately 80% flows under the keel and the remaining 20% via the bow and stern during the last 50 meters of the berthing manoeuver.

The PPU performs very well after comparing the PPU velocities with the RTK velocities. The PPU velocities are accurate enough to use in future experiments, the RTK does not add additional accuracy to the measurements. It is important though, to consider that the delay the PPU shows from GMT is dependent on the particular PPU used and this deviation needs to be taken into account while interpreting the data obtained.

5

Modelling the characteristic flow around a berthing ship

5.1. Theoretical model parallel ship berthing

To further investigate the two processes that could cause hydraulic damping during the berthing manoeuver a theoretical model is developed. This model is a one-dimensional model and the assumptions made in this model are being tested using the results of the field experiments. Furthermore, the general applicability of this model for berthing manoeuvers is investigated. The manoeuver is assumed to be a pure sway motion so that the additional longitudinal flow induced by yawing motions does not effect the flow behaviour around the ship. The starting point for this model is a one-dimensional approach based on the first hydrodynamic process, the water level elevation between ship and quay causing hydraulic damping. The second process, translation waves oscillating between ship and quay causing hydraulic damping, is not taken into account. Because of the model being one-dimensional, only flow in the x direction is considered. This means that there is no bow and stern flow. The fluid is assumed to be incompressible. Only the water column between ship and quay and the under keel water column are modelled. The water at the trailing edge of the berthing ship is assumed to have no influence on the water pressures and velocities between ship and quay and under the keel. The model is developed using the continuity equations and Euler equations of motion. The outcomes of the field experiments from chapter 4 are used to validate this theoretical model by simulating the experiments with the model and therewith testing the assumptions made while developing this model. Moreover, the performance and therefore the general applicability of the model is analyzed.

The following model assumptions are made:

- Incompressible fluid
- The ship is infinitely long, so no bow and stern flow
- Viscid fluid effects are simplified
- The ship berths in calm shallow waters
- Hydrodynamic added mass (ship's inertia) neglected
- Trailing edge of the vessel is not taken into account
- Translation waves are not taken into account

Viscosity is not taken into account because that would change the Euler equations of motion into the Navier-Stokes equations. To solve this computational fluid dynamics is needed and this is out of scope for this elementary theoretical model. However, an approximation for the influence of ship friction is made by using a friction coefficient in the momentum equations. The friction of the quay wall and the bottom are neglected. The added mass is neglected because these elaborate effects cannot be captured using only the continuity equation and simplified Euler equations of motion.

Figure 5.1 shows the one-dimensional model of a berthing ship. In this model it is assumed that the entire water level over the column lowers uniformly when the vessel is moving towards the quay. The fluid velocities at three different locations (u_1, u_2 and u_d) are indicated in the figure. u_1 is the water velocity at the water level, u_2 is the water velocity at the bulge of the ship and u_d is the velocity under the keel. The

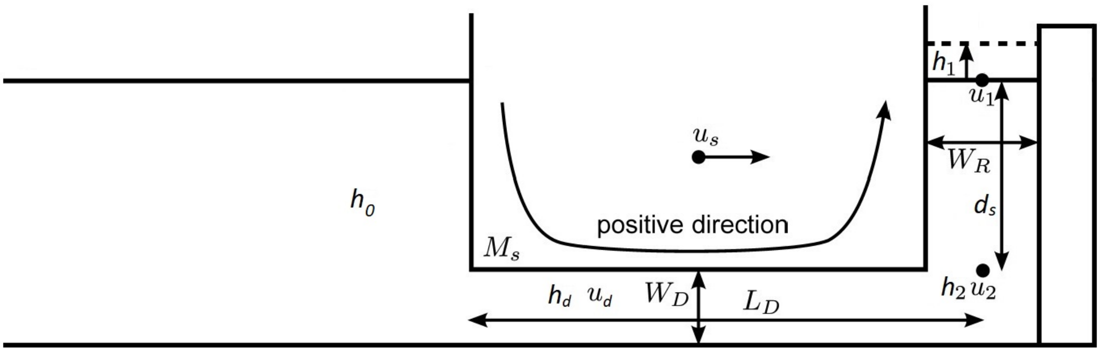

Figure 5.1: Schematisation of the one-dimension model of a parallel berthing ship

corresponding hydraulic heads are h_1, h_2 and h_d. The water level elevation between ship and quay is h_1. It is assumed that there is no energy dissipation between h_2 and h_d and that all the energy dissipates between h_d and h_0. Therefore the hydraulic head on the trailing edge of the ship is constant and equal to zero (h_0). The distance between ship and quay (W_r) is a variable and is dependent on the ship velocity (u_s). The under keel clearance is W_d. In addition, the mass of the ship (M_s), the width of the ship (W_s) and draught of the ship (d_s) are shown in figure 5.1.

5.1.1. Law of continuity

From the law of conservation of mass the bottom and right side continuity equations are respectively:

$$W_d * u_d = W_r * u_2 \tag{5.1}$$

$$\frac{dW_r}{dt} * d_s + W_r * u_1 - W_r * u_2 = 0 \tag{5.2}$$

Because the ship has a lateral velocity (u_s) and accelerates or decelerates (a_s) during the berthing manoeuver it naturally follows that:

$$u_s = u_s(0) + \int_0^t a_s(t)dt \tag{5.3}$$

Considering that the water between ship and quay, and therefore the value for the distance between ship and quay (W_r) depends on the velocity of the ship the following holds as well.

$$\frac{dW_r}{dt} = -u_s \tag{5.4}$$

5.1.2. Law of conservation of momentum

Besides the mass balance the momentum balance needs to be defined. This is done at three set locations as indicated in figure 5.1. The simplified Euler equations of motion are used. The viscid fluid effects are approximated with a ship resistance coefficients c_f. Because it is a one-dimensional model, the pressures are expressed in meters and are represented by the hydraulic heads (h). The Euler equations of motion are respectively:

$$\frac{d(u_1+u_2)}{2dt} + \frac{(u_1+u_2)(u_1-u_2)}{2d_s} + g\left(\frac{h_1-h_2}{d_s}\right) = 0 \tag{5.5}$$

$$\frac{du_d}{dt} + g\left(\frac{h_d-h_0}{W_s}\right) + 2c_f\frac{u_d^2}{W_d} = 0 \tag{5.6}$$

The equation of the motion for the ship is, where the ship is decelerated by the water level elevation between ship and quay:

$$\frac{du_s}{dt} + \frac{1}{2}g\left(\frac{h_1+h_2}{W_s}\right) = 0 \tag{5.7}$$

At the water surface the linearized kinematic boundary condition is:

$$\frac{dh_1}{dt} = u_1 \tag{5.8}$$

No energy dissipation from h_2 to h_d is assumed which means that:

$$h_2 + \frac{u_2^2}{2g} = h_d + \frac{u_d^2}{2g} \tag{5.9}$$

5.2. Mathematical validation

The model is validated by investigating the water level and velocity behaviour when the ship is assumed to have zero velocity and stays at a distance of 24.21 meters from the quay. Furthermore the advective acceleration terms have been omitted. The water level elevation between ship and quay is set to 0.5 meters above still water level. When the water level elevation is released it is expected that the water level starts to oscillate around the still water level and damp out like a spring-mass system due to the pressure terms in the equations. Furthermore, it is expected that the water velocity at the water surface between ship and quay falls behind a quarter of a period on the water level. All the potential energy is converted to kinetic energy during the oscillations since no energy dissipation is assumed in the equations. This is also behaviour of a spring-mass system. Furthermore, no energy dissipation is assumed at the bulge of the ship causing the under keel velocity to relate to the velocity at the bulge following equation 5.1. The under keel flow velocity dissipates completely since the hydraulic head in the sea is assumed to be zero. Therefore the mean under keel clearance that is returned by the model is smaller than the under keel clearance derived from 5.1. The behaviour of the model with a fixed vessel is modelled and plotted in the figures below. From these figures it is seen that the model behaves as expected for the oscillations due to an initial condition of the water level between ship and quay.

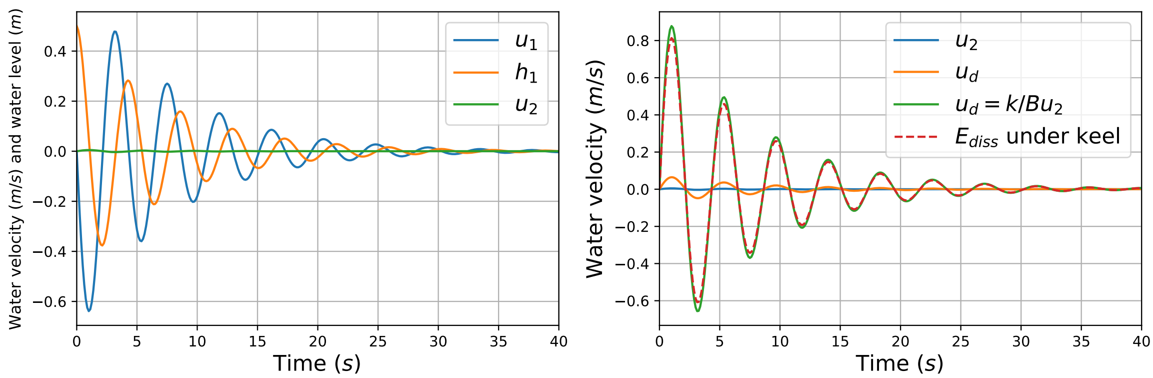

Figure 5.2: Simulation of experiment 1 - ship velocity and acceleration

Now that the model behaviour is validated, the model is expanded to the complete model by adding the advective acceleration terms, the vessel velocity and the associated changes in the continuity equations as seen in the previous sections. Now, the experiments can be simulated with the model in the following sections to test the assumptions made and test the general applicability of the model.

5.3. Experiment 1

In experiment 1, the tugboats push the ship until it reaches a certain lateral velocity. When this velocity is reached, the tugboats release the vessel which means there is no driving force anymore pushing the vessel towards the quay. The vessel will start to decelerate due to the friction of the ship and the hydrodynamic forces counteracting the lateral movement of the ship. By simulating this and comparing the simulation with the field experiments, the one-dimensional model and the assumptions made in the model are tested. The counteracting hydrodynamic forces in the model are caused by the water level elevation between ship and quay. The water level elevation causes an extra hydrostatic pressure gradient which can be translated to one force:

$$F = \frac{1}{2}\rho g {h_1}^2 \tag{5.10}$$

Following the experiments the following dimensions are used:

Vessel dimensions	*Experiment 1 - manoeuver 2*	*Experiment 1 - manoeuver 1*
Width (m)	45	45
Draught (m)	18.32	18.32
Mass (tonnes/m)	840.06	840.06
UCK (m)	1.78	4.86
Initial distance from the quay (m)	24.21	279.5
Initial velocity (cm/s)	6.75	6.046
c_f (-)	0.003	0.003
h/D (-)	1.1	1.24

Table 5.1: Vessel dimensions that are used in the simulation experiment 1

The ship resistance coefficient is derived in appendix G. Because the hydrodynamic model is developed for small distance to the quay wall, only manoeuver 2 is simulated.

5.3.1. Model validation - manoeuver 2

In figures 5.4 - 5.7 the simulation of the six variables of manoeuver 2 is plotted. In figure 5.3 the ship velocity and acceleration simulated with the model are compared to the velocity and acceleration of the field experiments. It appears that the deceleration obtained from the model behaves similarly with the deceleration from the field experiments. In the first 30 seconds the model has a slightly larger deceleration than the field experiments. The remaining part of the manoeuver the model has a slightly smaller deceleration than the field experiments. The simulation shows an exponential decay. The experiment shows an exponential decay as well, including several oscillations that are not captured with the model.

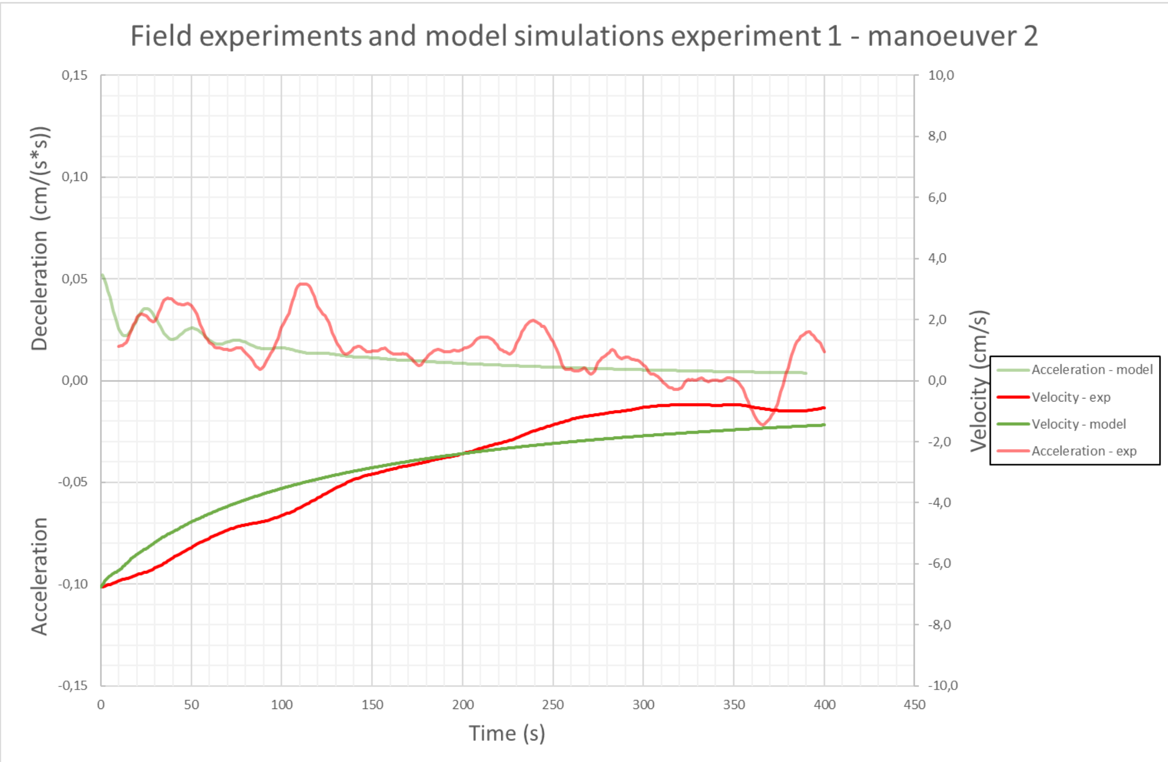

Figure 5.3: Comparison of the simulation and measurements of experiment 1 - manoeuver 2

The simulation shows that the water level elevation between ship and quay reaches a maximum of 0.4 centimeters. The water level elevation starts at 0.4 centimeters and decreases with oscillations that dampen completely after 100 seconds. The vessel reaches zero velocity after approximately 15 minutes. The flow velocity at the water level decreases with the water level elevation with oscillations. These oscillations are damped after 100 seconds. The flow velocity at the bulge of the ship starts at -5 cm/s and decreases exponentially towards zero, following the velocity decrease of the vessel. The under keel flow velocity starts at -70 cm/s and decreases exponentially towards zero following the velocity decrease of the vessel as well.

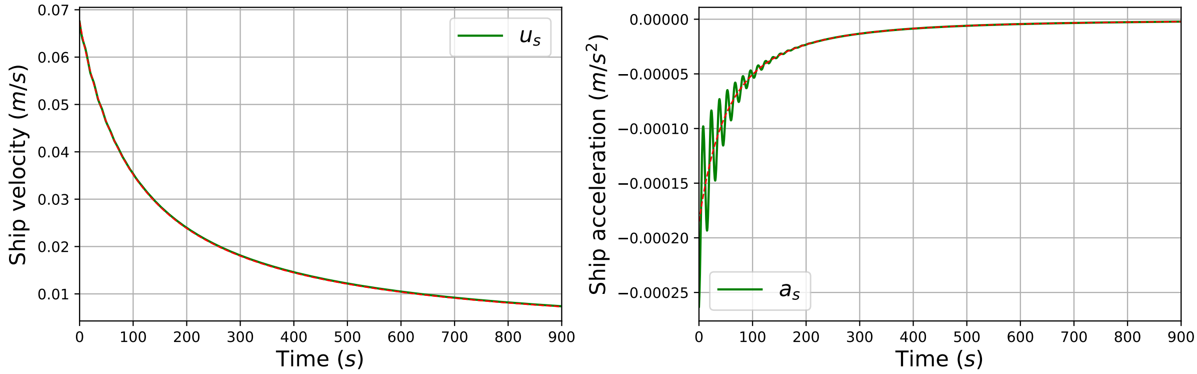

Figure 5.4: Simulation of experiment 1 - ship velocity and acceleration

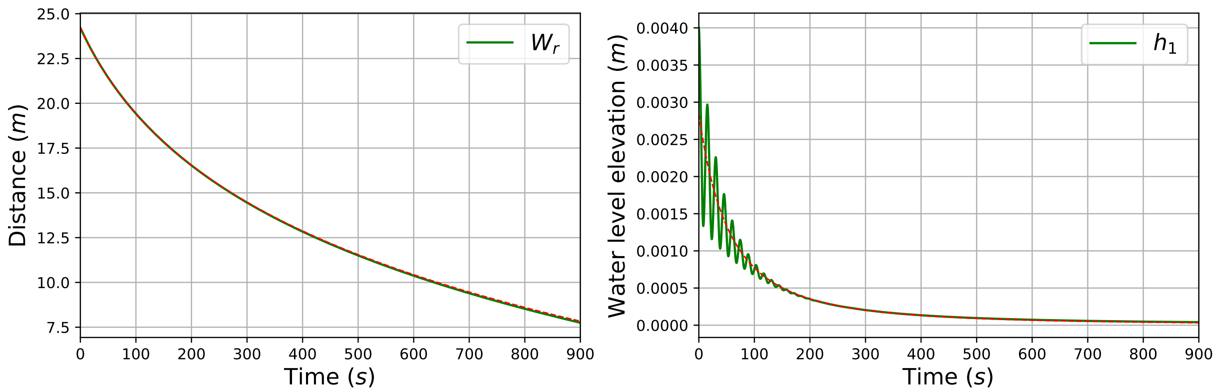

Figure 5.5: Simulation of experiment 1 - distance to the quay and water level elevation between ship and quay

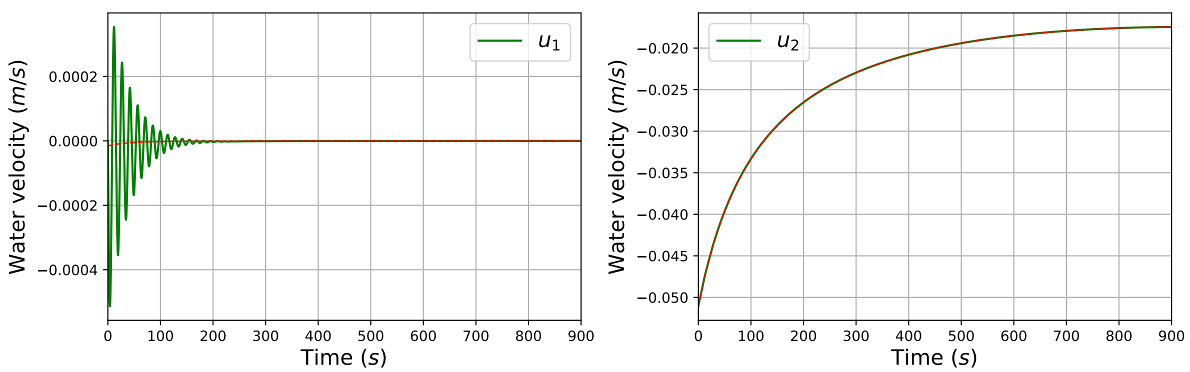

Figure 5.6: Simulation of experiment 1 - flow velocity between ship and quay

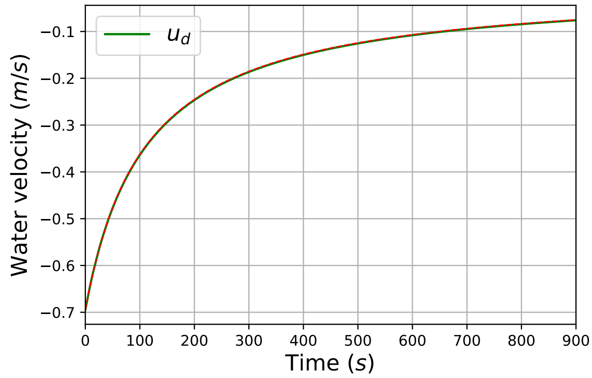

Figure 5.7: Simulation of experiment 1 - under keel flow velocity

For this numerical solution an analytical solution is approximated. In the graphs 5.4 - 5.7 the analytical solution is plotted in red, it is seen that the analytical solution performs very well with the numerical solution. The analytical solution can be applied when the velocity head between ship and quay is small enough. This applies when:

$$\frac{{W_d}^2}{W_r} << 1 \tag{5.11}$$

The velocity of the vessel can be described with:

$$u_s = \frac{u_{s0}}{1 + t/\tau} \tag{5.12}$$

Where τ is the half-life:

$$\tau = \frac{W_s}{u_{s0}} \beta \frac{1+\beta}{\chi} \tag{5.13}$$

With:

$$\beta = \frac{W_d}{d_s} \tag{5.14}$$

χ is a resistance parameter consisting of the exit losses, the wall resistance under the vessel with a hydraulic radius of half the under keel clearance.

$$\chi = \frac{1}{2} + 2c_f \frac{W_s}{W_d} \tag{5.15}$$

The water level elevation between ship and quay can be described with:

$$h_1 = \left(\frac{W_s}{g\tau} u_s\right)^2 \tag{5.16}$$

The under keel velocity can be described with:

$$u_d = -\frac{d_s}{W_d} u_s \tag{5.17}$$

5.4. Experiment 2

In experiment 2, the tugboats did not release the vessel but manoeuvred the vessel towards the quay wall. Consequently, the lateral pushing force on the vessel is unknown. However, the velocity profile of the center is known, and with this velocity profile the flow velocities between ship and quay and the under keel flow velocities can be simulated. It is important to be aware that the velocity and therefore acceleration and deceleration profile are now known. This means that the inertia of the vessel is not neglected anymore like in experiment 1. This simulation only focuses on the water velocities and water level elevation due to the approaching vessel. Therefore the assumptions used in the model are:

- Incompressible fluid
- The ship is infinitely long, so no bow and stern flow
- Viscid fluid effects are simplified
- The ship berths in calm shallow waters
- Trailing edge of the vessel is not taken into account
- Translation waves are not taken into account

The dimensions used in the simulation of experiment 2 are:

Vessel dimensions	*Experiment 2*
Width (m)	45
Draught (m)	18.04
Mass (tonnes/m)	827.22
UCK (m)	0.555-0.91
Initial distance from the quay (m)	43.075
Initial velocity (cm/s)	3.697
c_f (-)	0.003

Table 5.2: Vessel dimensions that are used in the simulation experiment 2

The under keel clearance changes during the berthing manoeuver due to the change of the tide as seen in chapter 3. The under keel clearance increases linearly and taken into account in the simulation. The vessel velocity used in the model is derived from field experiment 2.

5.4.1. Model validation

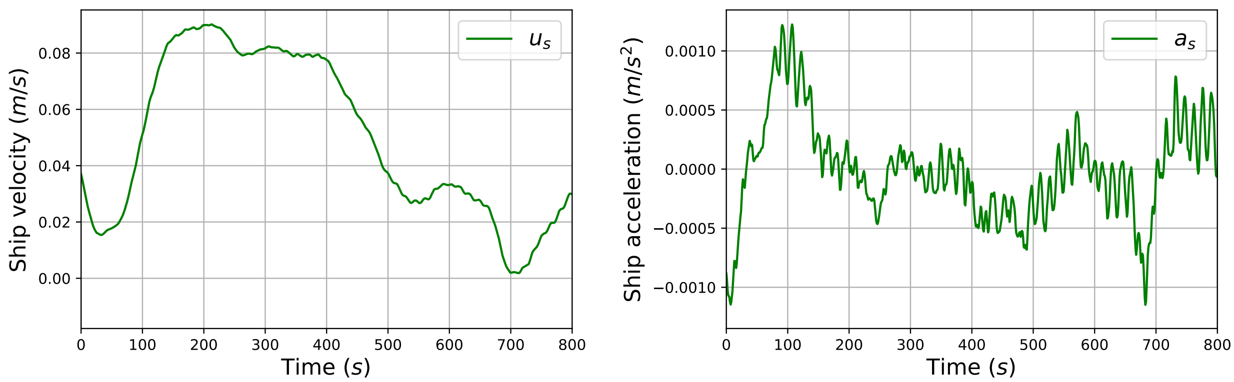

Figure 5.8: Simulation of experiment 2 - ship velocity and acceleration

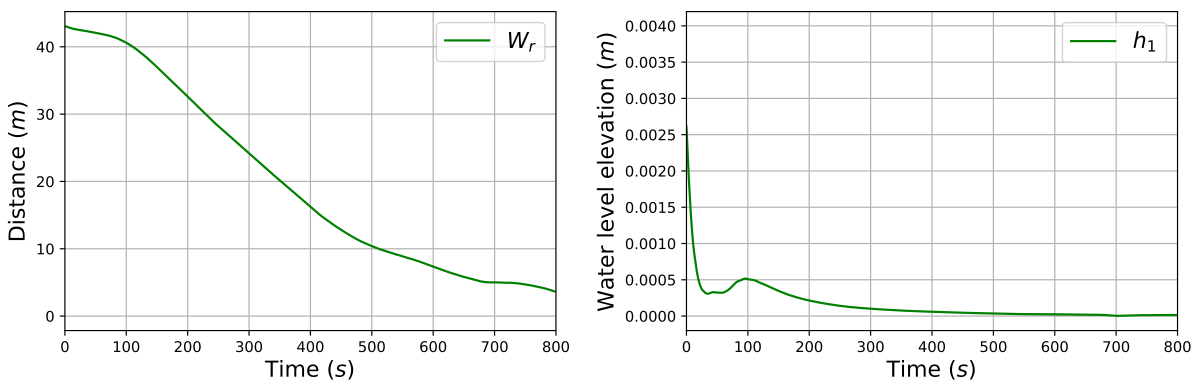

Figure 5.9: Simulation of experiment 2 - distance to the quay and water level elevation between ship and quay

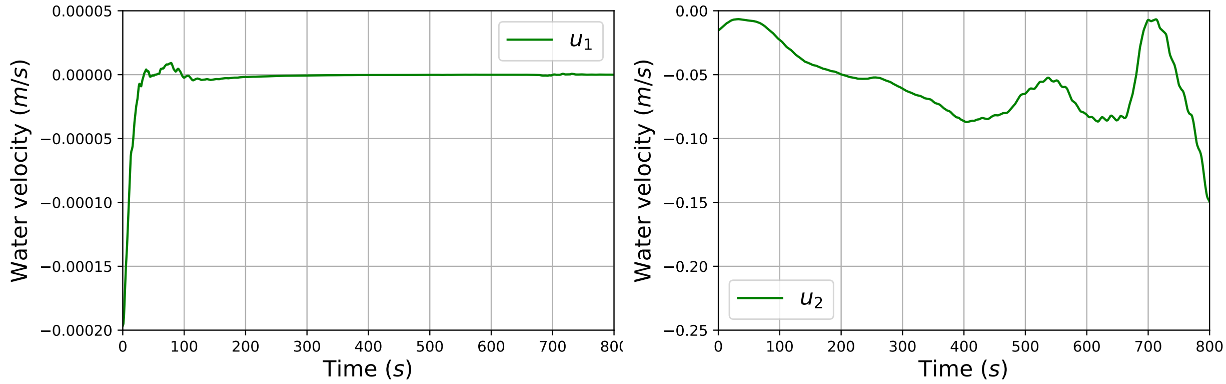

Figure 5.10: Simulation of experiment 2 - flow velocity between ship and quay

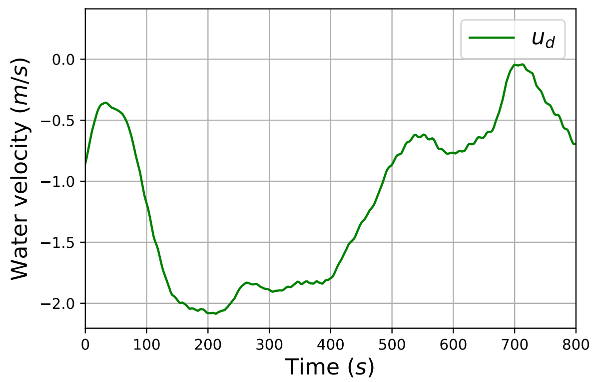

Figure 5.11: Simulation of experiment 2 - under keel flow velocity

In figures 5.8 - 5.10, experiment 2 is simulated using the one-dimensional model. The outcomes of the flow velocities and water level elevation are compared to the velocities and pressures measured during the field experiments. First, the water elevation (figure 5.9) is compared to the pressure distribution during the berthing manoeuver in figure 5.12. The pressure distribution is corrected using the lowest value of the measured pressure to obtain the water level elevation. From figure 5.12 it is seen that the water level increases with the increase of the tide in the simulation. The experiments show a tidal increase plus oscillations as discussed in chapter 4. It is seen that the behaviour of the water level elevation between ship and quay (figure 5.9) is not visible when it is compared to the water level elevation from the field experiments. The water level decrease from the simulations is in the order of millimeters and the oscillations from the experiments are in the order of tens of centimeters. Therefore, the oscillations that are obtained from the simulation dissolve in the much larger oscillations from the field experiments. The oscillations from the field experiments are not captured with the theoretical model due to the lack of measurement accuracy of the instruments used and the noise due to environmental circumstances. Moreover, it is very important to consider the fact that the two instruments are placed at the bow and stern of the ship as seen in figure 3.1. The simulation however, simulates for the center of the ship.

The flow velocities (u_1 and u_2) are compared to the upward flow velocities at the corresponding depths in figure 5.13. The flow velocities obtained with the simulations for the bulge of the ship coincide well. The order of magnitude is the same and the behaviour of the graph shows similarities as well, especially for the Signature measurements. The flow velocity at the water surface does not coincide with the field experiments. An explanation is that the flow velocity measured in the field experiment is a couple of tens of centimeters below the water surface, the velocity at the water surface cannot be measured due to scattering of the signal. Therefore the flow velocities of the simulation and the experiments do not agree and a conclusion on the surface flow velocity simulated and measured cannot be drawn.

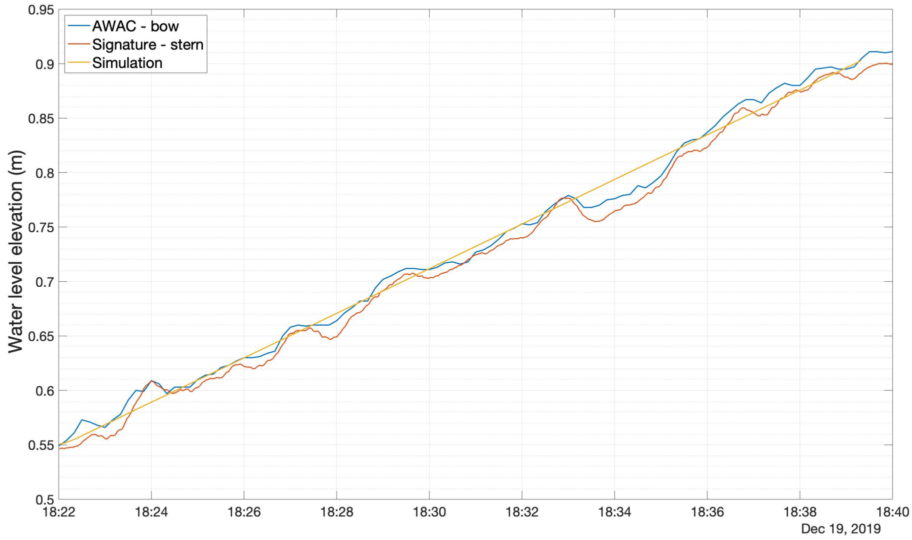

Figure 5.12: Comparison of the simulation and water level elevation measurements of experiment 2

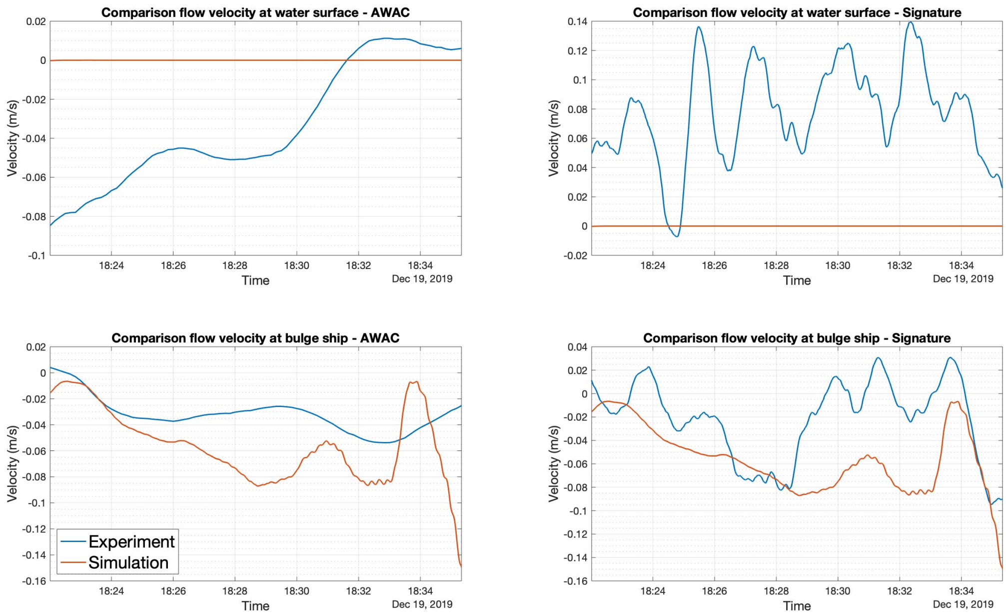

Figure 5.13: Comparison of the simulation and the flow velocities between ship and quay of experiment 2

5.5. Applicability of the model

Experiment 1 manoeuver 2 shows that the simulation and the field experiments agree nicely. However, there are oscillations in the field experiments that are not captured with the model. The behaviour of the deceleration corresponds well to the simulation and the field experiments.

The water level elevation fluctuations obtained from the simulation are not visible in the field experiments because of their order of magnitude in comparison to the order of magnitude of the oscillations in the field experiments. The accuracy of the instruments used does not suffice for the changes in water level elevation as discussed in chapter 4. In addition, the water level elevation measurements are to disturbed by large oscillations due to waves that the oscillations from the simulation are snowed under. Therefore, no conclusion can be drawn on the simulation of the water level elevation in comparison to the outcomes of the field experiments.

The simulation captures the flow velocities at the bulge of the ship quantitatively and qualitatively. The flow velocities at the water surface do not coincide. An explanation is that the flow velocity at the water surface cannot be measured correctly with the instruments, the flow velocity that is shown in the figure is a couple of centimeters below the water surface. Therefore the comparison of the simulation of the water surface flow velocity and the field experiments is inaccurate.

The conclusion of the validation of the one-dimensional model is that the simulation does represent the outcome of the field experiments decently. The only thing the simulation does not capture are the water level oscillations which are most likely waves produced by the berthing vessel. The assumptions made in the model can be verified. Therefore, a parameter study can be carried out to investigate the influence of the key variables on the hydraulic damping.

5.6. Parameter study of the model

In the parameter study the influence of the key variables obtained from the literature are investigated. The variables are tested conform the hypotheses that are set in literature.

5.6.1. Under keel clearance

From literature it is seen that the under keel clearance influences the hydraulic damping. The ratio that is used is the water depth-to-draught ratio (h/D). If this ratio is below 2, counteracting forces start to play a role. Because the vessel has a constant mass, the difference in maximum deceleration for the different under keel clearance is a way to evaluate the magnitude of the hydraulic damping.

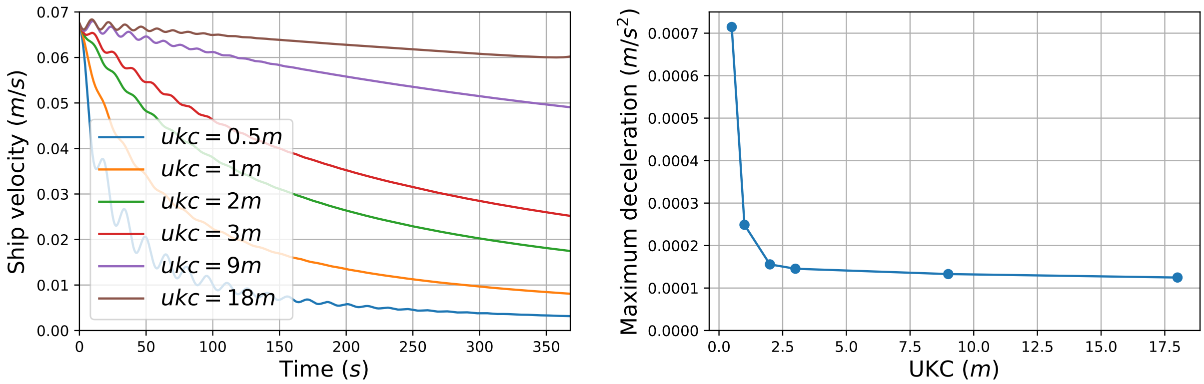

Figure 5.14: Influence of UKC on ship velocity

UKC	*h/D*	*Max. deceleration*	*% of draught*
0.5 m	1.03	-0.000715	2.7%
1 m	1.05	-0.000249	5.5%
2 m	1.11	-0.000156	11%
3 m	1.16	-0.000145	16%
9 m	1.49	-0.000133	50%
18 m	2	-0.000125	100%

Table 5.3: Influence of under keel clearance on hydrodynamic counteracting forces

From figures 5.14 and table 5.3 it is seen that the counteracting forces decrease with increasing under keel clearance. It is also seen that it does not decrease linearly but exponentially. It seems that the hydraulic damping starts to play a significant role from $h/D = 1.1$ and $ukc = 2\text{m} = 0.11D$ and smaller. Therefore, the hypotheses from literature should be adjusted slightly.

5.6.2. Ship dimensions

The ship dimensions influence the behaviour of the hydraulic damping conform literature. Because the model is one-dimensional, the influence of the width of the ship on the ship's velocity is investigated in combination with a fixed ship length. From literature length-to-width ratios of 5-10 are common for berthing large vessels that experience significant hydraulic damping. Therefore these ratios and their influence on the maximum deceleration are investigated.

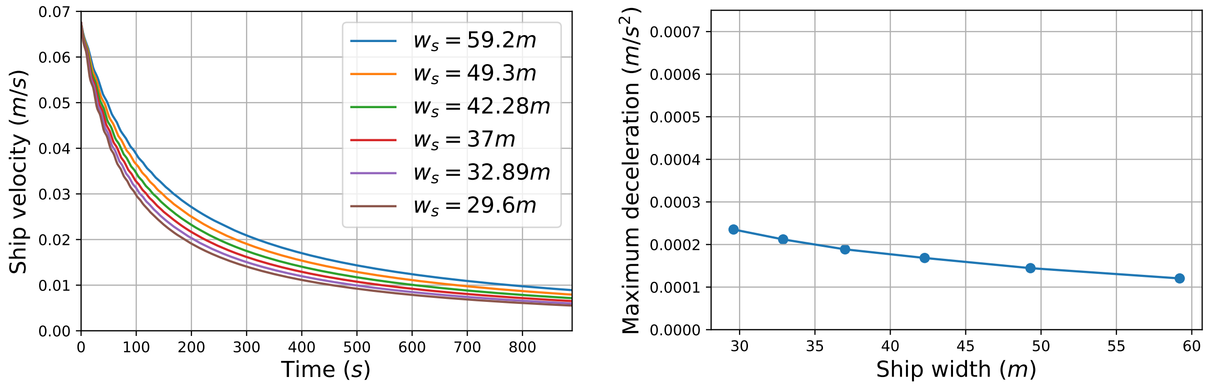

Figure 5.15: Influence of ship width on ship velocity

W_s	*L/B*	*Max. deceleration*
59.2 m	5	-0.000120
49.3 m	6	-0.000145
42.28 m	7	-0.000168
37 m	8	-0.000192
32.89 m	9	-0.000216
29.6 m	10	-0.000240

Table 5.4: Influence of ship width on hydrodynamic counteracting forces

Figures 5.15 and table 5.4 show that the maximum deceleration decreases slowly with increasing ship width corresponding to decreasing length-to-width ratios.

5.6.3. Ship position

The initial distance to the quay is tested but seen that this does not influence the ship's behaviour. The model is valid for $L/w_r < 1.5$. The initial velocity of the ship does influence the hydrodynamic forces acting on the ship. In the Port of Rotterdam approach velocities of 6-8 cm/s are standard, but in other ports approach velocities of 10-12 cm/s are widely used. Therefore the influence of the initial approach velocity is investigated.

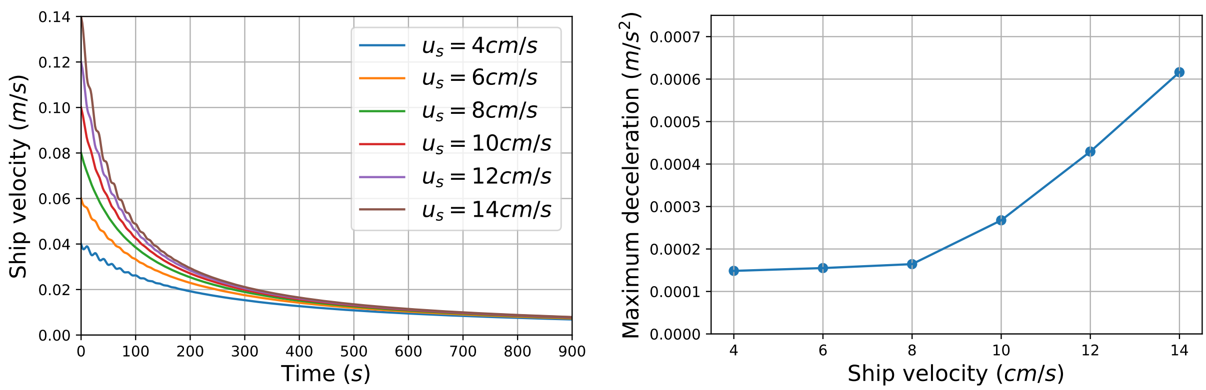

Figure 5.16: Influence of initial ship velocity on ship velocity

u_s	*Max. deceleration*
4 cm/s	-0.000148
6 cm/s	-0.000155
8 cm/s	-0.000164
10 cm/s	-0.000268
12 cm/s	-0.000429
14 cm/s	-0.000616

Table 5.5: Influence of ship width on hydrodynamic counteracting forces

Figures 5.16 and table 5.5 demonstrate that the maximum deceleration increases exponentially with increasing initial ship velocity.

5.6.4. Conclusion

From the parameter study it is concluded that the under keel clearance has the biggest influence on the hydrodynamic counteracting forces. It is seen that with decreasing under keel clearance the maximum deceleration increases exponentially. From h/D = 1.1 - 2.0 the deceleration increases linearly. From $h/D < 1.1$ the deceleration increases exponentially with a maximum at an UKC of 0.5 meters. 0.5 meters is the smallest allowed UKC during berthing manoeuvres. The second biggest influence on the hydrodynamic counteracting forces is the initial ship velocity. With increasing velocity the maximum deceleration increases exponentially. The ship width has the smallest influence on the hydrodynamic counteracting forces. With increasing ship width the maximum deceleration decreases almost linearly.

6
Discussion

Before conclusions can be drawn from the conducted research, a critical reflection on the results is required. This chapter addresses the relevance of this research, the applicability of this research in other areas and the the quality of the obtained results as well as their shortcomings.

6.1. Relevance to practice

Information on the hydrodynamic processes causing hydraulic damping is not accurately known and therefore any contribution to the understanding of these processes and the influence of the variables on these processes is considered relevant. This research contributes to the first steps in the mapping of the hydrodynamic processes during full-scale lateral berthing manoeuvers and to accurately measuring the processes playing a role in the berthing manoeuver. Furthermore, this thesis provides a starting point for future research on lateral berthing manoeuvers in indicating future research and providing experimental set-ups.

6.2. Applicability to other ports

Since this research is only conducted for two berthing sites and two similar vessels the applicability of the conclusions to other berthing sites in the Port of Rotterdam or other ports in general is questionable. It is important to consider that the environmental conditions in ports influence the characteristics of the flow behaviour in a port. The hydrodynamic processes in this study are evaluated without taking into consideration environmental influences. The conducted field experiments from this research were subject to current and therefore it is expected that the influence of current on the development of the hydraulic damping is manageable. It is expected that the main processes causing this damping are applicable to all berthing sites and ports with a closed or semi-closed quay wall. The presence of waves is expected to influence the outcomes of this research slightly, but it is also expected that the main conclusions will stay upright. However, it is expected that stratification will influence the outcomes of this research and will influence the mechanism causing hydraulic damping due to the influence of stratification on flow behaviour. Further research to the effect of stratification on berthing manoeuvers is therefore proposed. As stated before, this research did not aim to provide a complete model to simulate berthing manoeuvers or to collect data to empirically derive the key variables in hydraulic damping. The main goal was to point out and explain the dominant hydrodynamic mechanisms causing hydraulic damping during a lateral berthing manoeuver. Furthermore, the goal was to evaluate the key variables and their influence on the hydraulic damping. The first steps in completing this goal are done and more research is needed to substantiate the conclusions from this research and to investigate the influence of environmental forces.

6.3. Scientific reflection

The hydraulic damping of lateral berthing manoeuvers of large vessels has not received a lot of attention as seen from the literature review. A handful of studies do investigate the force on the quay wall structure and on the ship and the movement of the ship is also studied extensively in shallow and confined waters. However, the hydraulic damping is usually dismissed following a couple of assumptions and an entire study is not devoted to it. The findings from this study have been compared to some previous studies who do pay more attention to the flow pattern and hydrodynamic forces acting on the lateral moving vessel. From Wang et al. (2017) and Chen and Huang (2000) it came forward that no large water level elevation between ship and quay is measured due to water that cannot escape between ship and quay but oscillations due to waves that reflect on the quay wall. This substantiated in this research as well. In addition, the velocities between ship and quay are compared quantitatively to the flow velocities from Wang et al. (2017) and the flow velocities are in the same order of magnitude, namely in the order of centimeters per second. From Wang et al. (2017) (2016) it emerged that the ratio of the final quay wall clearance to the width of the vessel (s' = s/B) and the water depth-to-draught ratio (h' = h/D) influences the amount of hydraulic damping. Because the experiments conducted in this research are not executed with different water depths and distances from the quay, the results of these variables on the hydraulic damping cannot be compared to literature. The ratios s' and h' used in the field experiments are in the order of magnitude that according to literature hydraulic damping should be present. However, the influence of these variables on the hydrodynamic counteracting forces are investigated with the validated model. In the parameter study it is seen that the hydrodynamic counteracting forces increase rapidly when $h/D < 1.11$. According to literature the hydraulic damping is present from $h/D < 2$ and large from $h/D < 1.5$. This is partly substantiated, although literature overestimates the influence of the UKC slightly. Because the model is developed for berthing vessels, it does not model the situation where $s' = s/B > 1.5$. Therefore, no conclusion can be drawn on the distance from the quay, when the quay wall starts to play a role precisely.

6.4. Interpretation of the results

The interpretation of the results needs to be done cautiously. The reliability of the results coming from the experiments and the theoretical model is discussed in the following sections.

6.4.1. Field experiments

First of all, the set-up of the field experiments is discussed. The location of the quay wall is subject to environmental conditions such as current and small waves which influence the results obtained from the field experiments. Besides, an extra force acting on the vessel caused by the outflow of the Nieuwe Waterweg into the Breeddiep influences the outcomes of the field experiments. In the following subsections the influence of these factors on the results per experiment are discussed.

Experiment 1

Experiment 1 is conducted using a suitable vessel, however the results obtained from the acceleration and deceleration of the ship need to be interpreted with caution since the force that is derived from the experiment does not only consist of the hydrodynamic counteracting force. An extra force due to the current, waves and outflow into the Breeddiep influences the angular and lateral velocity of the vessel which is difficult to distinguish from the influence the hydrodynamic counteracting force influencing the position of the ship. In addition, it is known that a ship does not have an equal distribution of cargo. Therefore the center of rotation is not necessarily halfway the length of the ship while in the analyses the center of the ship is assumed to be halfway.

Experiment 2

Experiment 2 used two velocity meters placed at the bottom of the berth and one velocity meter placed at the quay wall. The exact position of the instruments is not guaranteed during placement because the instruments were lowered from a vessel. The exact coordinates of the instruments on the berth's bottom are therefore not known and the results should be interpreted carefully. In addition, there is a chance that the two velocity meters located at the bottom of the berth are placed to close to the quay wall. This is a problem because the quay wall investigated is positioned slightly backwards in comparison to the river bank. The position of the velocity meters could be so close to the quay wall that they might measure the water column that is sheltered by the quay and underestimate the mean flow velocities between ship and quay. The orientation of the instruments at the bottom in three dimensions is measured by the instrument and used during post-processing to obtain accurate velocity measurements within the coordinate system. This also accounts for position changes of the instruments during the berthing manoeuver. The horizontal velocity meter however does not measure the orientation internally and therefore the results are much less accurate than the results of the instruments placed at the bottom of the berth.

During post-processing the height of the tide as well as the bottom of the basin is used from estimates of the port authority. This means that the calculations done with this information such as the total volume of water between ship and quay and the velocity derivations from that total volume need to be interpreted with caution as well. However, it is expected the deviations from the height of tide and the bathymetry of the basin are not evident enough to have a significant influence on the results of the experiments.

Furthermore, the distance from the quay is not derived from position measurements but from the integral of the velocity of the bow, stern and center of the ship. This is less accurate than the distance obtained from position measurements. Moreover, there is a slight delay in PPU data in comparison to RTK data as seen in the last section of chapter 2.5.1. Experiment 2 is solely based on PPU data, this means that the results on the vessel's position from experiment 2 are slightly less accurate than the results from experiment 1 in general. Nonetheless, the measurements from as well the PPU as the RTk are accurate enough to drawn substantiated conclusions.

The velocity meters used in experiment 2 can be disturbed by objects in there measuring area, such as a vessel that approaches during berthing. The three instruments measure the reliability of the transmitted signals used to calculate the velocity of the water column. During the berthing manoeuver the signal shows some disturbances, these disturbances are caused by the approaching vessel and therefore no strong conclusions can be drawn from that part of the measurements. However, due to the reliability measurements of the instruments, the conclusions drawn from the reliable parts of the measurements are substantiated well.

The hydrostatic pressure measurements are not precise enough to capture the oscillations that would be caused by the translation waves travelling between ship and quay. The pressure measurements are also too disturbed and not precise enough to deduce information on the water level elevation due to the berthing ship.

6.4.2. Model validation

The hydrodynamics used in the theoretical model are based on continuity and conservation of momentum. Simulating the experiments using the theoretical model questions the assumptions made in the theoretical model. This approach however does have several limitations. Furthermore, the density of the water is assumed and not measured which can cause deviations in the model calculations. However, the density of the water used in experiment 2 is the same as the density for the water used in the simulations.The model simulates for the center of the vessel while the velocity meters are placed more than 100 meters away from the center of the vessel. Therefore, the simulation of experiment 2 cannot be validated seamlessly using the velocity meters, since the position of the velocity measurements does not match the simulation. Considering that 80% of the water flows under the keel, the deviation from the velocity meters from the center of the vessel is manageable and conclusions drawn are sufficiently substantiated. The pressure distribution during the berthing manoeuver, and therefore the water level elevation at the bow and stern is known. However, the water level elevation at the center, which is simulated, is not known. This does not provide a seamless comparison between the water level elevation in the model and in the field experiments and conclusions should be drawn carefully.

7

Conclusions and Recommendations

7.1. Conclusions

The main objective of this research is to understand the hydrodynamic processes that play a role during the lateral berthing manoeuver of a large vessel and therewith explaining the cause of hydraulic damping. To answer the main research question, a number of sub-questions is formulated and need to be answered first. In this section, the findings from this research are used to obtain the answers to these research questions.

How does the flow behave around a berthing ship and how can this behaviour be explained?
There are two processes that could take place between ship and quay during a lateral berthing manoeuver with a large vessel. First, a pressure build up between ship and quay resulting in a water level elevation which exerts a counteracting force on the vessel. Second, translation waves caused by the deceleration of the ship which reflect on the quay wall and exert a counteracting force on the ship's hull. From the experiments and the model simulations it is established that the first process is the hydrodynamic process that represents the flow behaviour between ship and quay. The simulations show similar hydraulic damping as obtained from the experiments. This is substantiated by the simulated flow velocities between ship and quay, which coincide quantitatively and qualitatively with the velocities measured. However, the pressure increase due to water level elevation is not visible in the experiments due to the lack of precision of the instruments. Only the tidal increase and oscillations due to waves are observed. The oscillations due to waves dominate the pressure distribution causing the small water level elevation to be invisible. It is cautiously concluded that the pressure with a vessel shows larger oscillations than the pressure distribution without a berthing vessel. This could be waves produced by the accelerating and decelerating vessel. However, they do not exert a significant hydrodynamic counteracting force since this can be attributed processes that are included in the model. It is necessary to mention, as stated in the discussion, that conclusions drawn from the pressure distribution should be investigated further due to the position and accuracy of the meters. Furthermore, the water level oscillations that would substantiate the translation waves theory cannot be measured due to the precision of the instruments used. In conclusion, there is enough evidence that indicates that the flow around a berthing ship is caused by a pressure build up between ship and quay resulting in a water level elevation which exerts a counteracting force on the vessel. The water that needs to escape between ship and quay flows via the under keel and via the bow and stern. Approximately 80 % flows under the keel, while the remaining 20 % flows via the bow and stern as seen in measurements. Moreover, the experiments indicate waves that are caused by the berthing ship. However, these waves do not contribute to the hydraulic damping as concluded from the theoretical model.

What are the key variables in hydraulic damping and how do they effect the flow behaviour around a berthing ship?
The suspected key variables in the hydraulic damping are the under keel clearance, approach angles, ship dimensions, quay wall clearance, and the position of the ship over time. The effect of the approach angle on the hydraulic damping is not investigated in this study.

The under keel clearance during experiment 1 and 2 is similar and the water depth-to-draught ratio varies between 1.03-1.32. The hypotheses was set that if $h/D < 2$ hydraulic damping would be present. The experiments are not conducted with two different under keel clearance. Nonetheless, the validated theoretical model is investigated and the influence of the key variables is investigated. From the theoretical model it is concluded that the under keel clearance is the variable with the largest influence on the hydraulic damping. With decreasing under keel clearance the hydraulic damping increases exponentially. When $h/D < 1.1$ the hydraulic damping is significant. Between 1.1 and 2 the hydraulic damping is there but much less pronounced. From the ratio 2 and larger the hydrodynamic damping behaves similarly.

The ship dimensions used in the experiments have a length-to-width ratio between 5-7, which means that it is expected that approximately 70% of the water escapes under the keel and 30% via the bow and stern according to literature. In experiment 2 it is seen that 80% of the water escapes under the keel and 20% via the bow and stern for a length-to-width ratio of 6.5. Other length-to-width ratios are not investigated with the field experiments. From the parameter study of the theoretical model it has surfaced that the length-to-width ratio does have an influence on the hydraulic damping. With decreasing length-to-width ratio the hydraulic damping decreased as well. This decrease behaves slightly curved. However, the effect of the ship dimensions is the least significant of all the key variables and their effects.

The quay wall clearance has been investigated during experiment 1 and it is concluded that the hypotheses of the quay wall clearance is accepted. The hydraulic damping is present when the final distance from the quay wall to vessel width ratio is below 1.5. The maximum acceleration is 6.25 times larger when the ratio is below 1.5 in comparison to a ratio much larger than 1.5. Therefore, it can be concluded that the vicinity of the quay wall influences the flow behaviour around a berthing ship. The vicinity of the quay wall exerts an extra hydrodynamic force counteracting the lateral berthing manoeuver of the vessel which is referred to as the water cushion. Further research is needed to investigate if the turning point is indeed at a ratio of 1.5. This could not be investigated with the theoretical model since the model was only developed for berthing manoeuvers in close vicinity of the quay wall.

The ship position and therefore velocity is investigated with the theoretical model. With increasing initial velocity the hydraulic damping increases as well. This curve is exponential. The initial velocity is the second most important key variable influencing the hydraulic damping. It is important to notice that the significant increase is from 8 cm/s. In the Port of Rotterdam these velocities are usually not present during the risky berthing manoeuver.

In what way is the movement of the ship influenced by the hydrodynamic forces on the ship?

The experiments and the simulations demonstrate that the hydrodynamic forces on the ship cause two changes in movement. First, the hydrodynamic forces are not equal over the length of the ship, this means that the ship experiences an angular acceleration and deceleration. The acceleration is attributed to the environmental forces. The deceleration is attributed to the hydrodynamic counteracting forces. From experiment 1 it is seen that the angular deceleration during the same manoeuver in vicinity of the quay wall is 6.25 times larger than without vicinity of the quay wall. Therefore it is concluded that the vicinity of the quay wall exerts a larger hydrodynamic counteracting force on the lateral berthing vessel. Moreover, the center of the ship also experiences a hydrodynamic counteracting force. However, the counteracting force during manoeuver 1 is bigger than during manoeuver 2 contradicting the hypothesis and expectation that the vicinity of the quay wall causes a larger hydrodynamic force on the vessel. Nonetheless, because of environmental forces the behaviour of the center can be explained, the extra force on manoeuver 1 was caused by the suction force of the Breeddiep channel. Therefore, no conclusions can be drawn on the behaviour of the center position of the vessel during the two berthing manoeuvers of experiment 1. In conclusion, the hydrodynamic forces cause the ship to decelerate and accelerate both laterally and angularly.

How can the forces acting on the ship generated by the hydrodynamic flow during berthing be determined and modelled?

The forces acting on the ship can be modelled through a one-dimensional model that is based on the continuity and momentum equations resulting in a water level elevation between ship and quay. The water level elevation between ship and quay due to these equations is the cause for the hydraulic damping acting on the berthing vessel. The field experiments show that approximately 80% of the water escapes under the keel and the remaining 20% flows via the bow and stern. Therefore, it is concluded that expanding the model to a two-dimensional model does add some accuracy to the simulations performed in this study. Nonetheless, the mechanism causing hydraulic damping can be captured using a one-dimensional model since the largest part of the water between ship and quay flows under the keel. There are more processes happening such as turbulence, waves and eddies produced by the berthing ship but these are not captured with a one-dimensional model. To capture all the processes computational fluid dynamics is needed. Furthermore, environmental processes such as wind, current and waves are not accounted for in the model. The model does

perform well in capturing the hydraulic damping as validated with the field experiments. The forces acting on the ship that are relevant in the lateral berthing manoeuver can be modelled through a one-dimensional model and the hydraulic damping and the key variables influencing the hydraulic damping are captured with this model. For more elaborate ship motions and flow behaviour around the vessel a numerical model is appropriate.
Now that the answers to the sub-questions are formulated, the answer to the main research question can be given.

"Which mechanisms cause hydraulic damping between ship and quay during berthing and how can they be explained?"

The mechanism causing hydraulic damping between ship and quay can be explained with the continuity and momentum equations in a one-dimensional model. Water level elevation due to the fact that water cannot escape fast enough between ship and quay is the phenomenon happening during berthing and therefore the cause of hydraulic damping. The water level rises due to the approach of the vessel causing the water column between ship and quay and under the keel to be accelerated. This acceleration causes consequently a lowering of the water level. The under keel clearance is the most important variable influencing the amount of hydraulic damping, followed by the velocity of the vessel and the ship's dimensions.

7.2. Recommendations

Based on the conducted research, recommendations can be made on the further investigation of hydraulic damping during lateral berthing manoeuvers. As seen from this thesis, the water cushion effect has not been studied extensively. This research is only one of the first steps that has been taken on research on the presence of hydraulic damping. The discussion and conclusions establish that there is room for improvement for the experiments carried out during this investigation. To substantiate and reinforce the conclusions from this thesis the following expansions and improvements to this research are proposed:

- The berthing manoeuvers from experiment 1 and the velocity measurements from experiment 2 should be executed in a more sheltered basin where current, waves, in or outflow of river mouths and stratification do not play a role. The perfect berthing site would be the Laurenshaven, which is very sheltered from environmental disturbances. When this is done, the hydrodynamic forces acting on the vessel can be attributed entirely to the hydraulic damping since environmental forces do not contribute.

- Experiment 1 and 2 should be executed with the same vessel for the same manoeuver. This was the initial plan for this research, due to circumstances however this was not achieved. An improvement would be that if the two berthing manoeuvers from experiment 1 would have been reinforced by the velocity measurements at the same place and time.

- A fourth ADCP at the bottom of the berth should be placed between ship and quay. This ADCP should be at the level of the center of the berthing ship so that conclusions of the one-dimensional model and the pressure en velocities obtained from the center of the ship can be compared to the simulations of the one-dimensional model to draw more accurate conclusions.

- The ADCPs should be placed more precise so that the coordinates are known. This can be done by adding weight to the construction the ADCP is secured to. Furthermore, divers are needed to ensure that the ADCPs are placed correctly.

- The water level elevation between ship and quay should be measured more precise such that the oscillations caused by the translation waves can be excluded entirely and the water level elevation due to pressure increase can be substantiated more. Water level elevation should be measured with an frequency of at minimum 4 Hz.

For further research the following recommendations are given:

- To test this one-dimensional model more and test the assumption that 80% of the water flows under the keel the under keel flow velocities during a berthing manoeuver should be measured at the center of the vessel.

- To substantiate the conclusion that translation waves are not the mechanism causing hydraulic damping a one-dimensional model should be developed using hydrostatic waves. With this model the experiments should be simulated again to see if the translation waves are indeed not causing the hydraulic damping.

- The most straightforward way to measure the hydrodynamic forces acting on the vessel during a berthing manoeuver is to place dynamometers on the two tugboats that push the vessel laterally to the quay. These dynamometers should be placed such that the force that the tugboat exerts on the ship's hull is a point force with only one contact point between the tugboat and the ship's hull. When the force exerted to push the ship to the quay is measured for the whole lateral berthing manoeuver and compared to the velocity and acceleration of the vessel, the hydrodynamic counteracting force can be derived quite accurately.

Finally, some recommendations are made for the guidelines that are used in fender design. However, these recommendations need further research, the recommendations given here are a starting point for this research:

- The water cushion effect is proven not to act as a cushion such that it absorbs kinetic energy when the vessel approaches the quay wall. The cushion effect occurs further away from the quay causing a barrier for the pilots to push trough. Therefore, the water cushion effect should not be taken into account in the guidelines, the effect is of importance before the first contact with the fenders takes place. The phenomenon that is important for fender design is the ship's inertia. This plays a role during deceleration induced by the fender impact. The fender does not only have to withstand the force due to impact velocity of the vessel but also the force due to inertia of the vessel, counteracting the deceleration of the vessel.

- Virtual mass is a force that is caused by the inertia of the vessel. This force counteracts the movement during acceleration and reinforces the lateral movement during deceleration. The virtual mass factor in the fender design guidelines should be revised. The virtual mass factor used is derived for deep water and with much larger velocities than used during berthing. Because of the conclusion derived from experiment 1, where the influence of the quay wall to the deceleration of the vessel is investigated, it seems that the virtual mass factor is too conservative. The deceleration in vicinity of the quay wall was 6.25 times larger than in the free basin. This difference in deceleration from experiment 1 is caused by two things. First, the water cushion effect exerting an extra counteracting force acting on the ship and second the inertia that is suspected to be smaller for these velocities and water depths, causing larger deceleration. This means that a part of this 6.5 times smaller force is due to smaller inertial forces. Meaning that the virtual mass factor should be decreased from the deep water virtual mass factor that is used now.

  To substantiate these presumptions, more research is needed to the inertia working on decelerating ship during a lateral berthing manoeuver in berthing waters. This can be done by manoeuvring a vessel through deep and shallow waters without vicinity of a quay wall, the same way as in experiment 1. The relation between the inertia in deep and shallow water can then be derived from the difference in deceleration of the vessel.

  To investigate the inertia working on the vessel and therefore on the fenders during the deceleration during fender impact, one could also measure the force exerted on the fenders during the first impact. With this force and the vessel's mass and deceleration, the inertial force pushing the vessel to the quay can be calculated and related to the mass of the vessel.

  The recommendations for further research for the guidelines of fender design are elaborated further in appendix H.

References

2019 Woods Hole Oceanographic Institution. (2019). *Acoustic Doppler Current Profiler (ADCP).* Retrieved from https://www.whoi.edu/what-we-do/explore/instruments/instruments-sensors-samplers/acoustic-doppler-current-profiler-adcp/

Abdi, H. (2010). Coefficient of variation. *Encyclopedia of research design, 1*, 169–171.

Ball, D. J., & Markham, A. (1983). Hydrodynamic energy transfer in shallow water ship impacts. *International Journal of Mechanical Sciences, 25*(9-10), 615–621.

Blok, J. J., & Dekker, J. N. (1979). On hydrodynamic aspects of ship collision with rigid or non-rigid structures. In *Offshore technology conference.* Offshore Technology Conference.

Braden, D. (2018). *Growth Accelerates At Top Global Ports.* Retrieved from https://www.joc.com/port-news/growth-accelerates-top-global-ports_20180816.html?destination=node/3443561

British Standards Institution (BS6349-2). (2019). *BS 6349-2.*

Brolsma, J. U., Hirs, J. A., & Langeveld, J. M. (1977). Paper on Fender Design and Berthing Velocities. Leningrad, Russia. PIANC World Congress.

Buuren, W. (2014). *Beschrijving van de NMS type ADX XR Bestandsnaam: Beschrijving AD X pagina 0 Beschrijving van de NMS type ADX XR.*

Chen, H., Chen, M., & Davis, D. A. (1997). Numerical simulation of transient flows induced by a berthing ship. *International Journal of Offshore and Polar Engineering, 7*(04).

Chen, H., & Huang, E. (2000). Validation of a Chimera RANS Method for Transient Flows Induced by a Full–Scale Berthing Ship. Twenty Second Symposium on Naval Hydrodynamics. *The National Academy of Sciences.*

Chen, H., & Liu, T. (1999). Turbulent flow induced by full-scale ship in harbor. *Journal of engineering mechanics, 125*(7), 827–835.

Chen, H., Liu, T., Huang, E., & Davis, D. (1999). Chimera RANS simulation of ship and fender coupling for berthing operations. In *The ninth international offshore and polar engineering conference.* International Society of Offshore and Polar Engineers.

Cyclomedia. (2019). *Streetsmart.* Cyclomedia Technology BV. Retrieved from https://globespotter.cyclomedia.com/

Demenet, P. (2018). The Kinetic Energy method revisited. *Journal of Applied Water Engineering and Research, 6*(1), 1–16.

Duffy, F., Eksioglu, Y., Rotenberg, A., Madsen, J., Shankardass, A., & Als, H. (2013, 1). The frequency modulated auditory evoked response (FMAER), a technical advance for study of childhood language disorders: Cortical source localization and selected case studies. *BMC neurology, 13*, 12. doi: 10.1186/1471-2377-13-12

Elger, D. F., Williams, B. C., Crowe, C. T., & Roberson, J. A. (2013). Engineering fluid mechanics. *Energy, 2*, 1–3.

Eskenazi, J., & Wang, J. (2015). Analysis of angular side berthing against a rubber Cone Fender. *Journal of Shanghai Jiaotong University (Science), 20*(5), 571–583.

Fontijn, H. (1988). Fender forces in ship berthing.

Grim, O. (1955). Das Schiff und der Dalben. *Schiff und Hafen, 7*, 535.

Hafenbautechnische Gesellshaft (EAU2012). (2012). *EAU.* Ernst & Sohn.

Hautamaki, P. (1970). Simulating Dynamic Motion Of Ship In Contact With Elastic Mooring Elements By A Nonlinear Algorithm. *WIT Transactions on Engineering Sciences, 1.*

HEXAGON positioning intelligence. (n.d.). *An Introduction to GNSS.* Retrieved from https://www.novatel.com/an-introduction-to-gnss/chapter-5-resolving-errors/real-time-kinematic-rtk/

Ibrahim, R. A., & Grace, M., I. (2010). Modeling of ship roll dynamics and its coupling with heave and pitch. *Mathematical Problems in Engineering, 2010.*

Kalman, R. E. (1960). A new approach to linear filtering and prediction problems. *Journal of basic Engineering, 82*(1), 35–45.

Kolkman, P. A. (1989). Discharge relations for hydraulic structures and head losses from different components. *Q965-C67.*

Kristensen, H. O., & Lützen, M. (2012). Prediction of resistance and propulsion power of ships. *Clean Shipping Currents*, *1*(6), 1–52.

Lisy, V., & Tothova, J. (2004). On the (hydrodynamic) memory in the theory of Brownian motion. *arXiv preprint cond-mat/0410222*.

Metzger, A., Hutchinson, J., & Kwiatkowski, J. (2014). Measurement of marine vessel berthing parameters. *Marine Structures*, *39*, 350–372.

Nederlands Loodswezen. (n.d.). Retrieved from `https://www.loodswezen.nl/Over%20ons.aspx`

Newman, J. (2018). *Marine hydrodynamics.* MIT press.

Nortek Manuals. (2018). *The Comprehensive Manual for ADCP's.* Nortek AS.

Nortekgroup. (2018). *Principle of Operation.* Vangkroken: Nortek AS. Retrieved from `file:///C:/Users/iris.heemskerk/Downloads/N3015-025-Principles-of-Operation-Signature_0918.pdf`

PIANC. (2002). *Guidelines for the Design of Fender Systems* (Tech. Rep.).

PoR. (2019). *Portmaps.* Rotterdam: Port of Rotterdam. Retrieved from `https://portmaps.ad.portofrotterdam.com/PortMaps/Index.html?viewer=PortMaps.Portmaps_UH2&LayerTheme=9#`

Port of Rotterdam. (2018). *Facts and Figures.* Retrieved from `https://www.portofrotterdam.com/sites/default/files/facts-and-figures-port-of-rotterdam.pdf?token=CJ3nvKBO`

Roubos, A., Groenewegen, L., & Peters, D. (2017). Berthing velocity of large seagoing vessels in the port of Rotterdam. *Marine Structures*, *51*, 202–219.

Sakakibara, S., & Kubo, M. (2008, 3). Effect of Structure Types of Quay Wall on Moored Ship Motions. *Coastal Engineering Journal*, *50*(1), 101–122. doi: 10.1142/s0578563408001752

Saurin, B. F. (1963). Berthing forces of large tankers. In *6th world petroleum congress.* World Petroleum Congress.

Trelleborg marine systems. (2016). *TRELLEBORG MARINE SYSTEMS Fender Application DESIGN MANUAL* (Tech. Rep.).

Trimble R10 GNSS Receiver - user guide. (2014). Sunnyvale: Trimble Navigation Limited. Retrieved from `www.trimble.com`

Vantorre, M. (1992). Mathematical modeling of fender forces and memory effects for simulation of ship manoevres in confined waters. In *Proceedings of the 10th international harbour congress* (pp. 15–19).

Vantorre, M., & Laforce, E. (1998). Experimental investigation of hydrodynamic forces acting on a ship in the vicinity of a quay wall. In *Man'98 international symposium and workshop on forces acting on a manoeuvring vessel. val de reuil, france.*

Wang, H., Li, X., Chen, L., & Sun, X. (2016). Numerical study on the hydrodynamic forces on a ship berthing to quay by taking free-surface effect into account. *Journal of Marine Science and Technology*, *21*(4), 601–610.

Wang, H., Sheng, X., Wang, S., Chen, L., Yuan, Z., & Wu, Q. (2017). Numerical study on water depth effects on hydrodynamic forces acting on berthing ships. *Journal of Shanghai Jiaotong University (Science)*, *22*(2), 198–205.

A

Instruments

A.1. Real time kinematic positioning

Real time kinematic positioning is a technique that is based on satellite positioning. Position measurement systems using satellite positioning are called GNSS, Global Navigation Satellite Systems. This system uses a constellation of satellites that sends out radio signals from space. If one has a GNSS receiver and at least three satellites, the distance to the GNSS receiver can be calculated through the sent radio signals. If the distance from three different satellites to the GNSS receiver is known, the position of the GNSS receiver is known as well. RTK positioning is based on carrier-based ranging which is much more precise than code-based positioning which is used in simpler GNSS systems (HEXAGON positioning intelligence, n.d.). RTK systems eliminate errors that GNSS systems usually have present. This makes RTK positioning very applicable, it can position with an accuracy up to 1 cm + 1 ppm.

The range from the rover station to the satellite is calculated through carrier cycles multiplied by the carrier wavelength. However, errors are still present due to delays from the signal in the ionosphere, the ionized part of Earth's upper atmosphere and delays in the troposphere, the lower part of Earth's atmosphere. Errors are also caused by difference in satellite clocks and deviations from the ephemerides, which are the trajectories that artificial objects orbit in the atmosphere. To eliminate these errors the base station is used, the base station sends out measurements to the rover station as shown in figure A.1a.

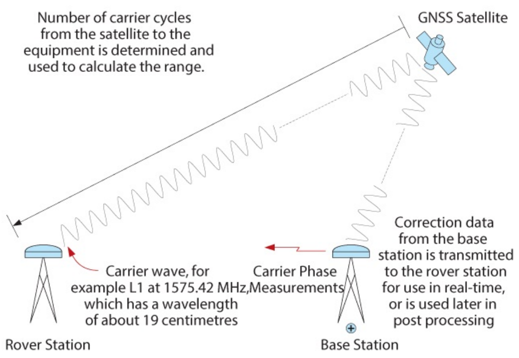

(a) Basic set-up of RTK positioning

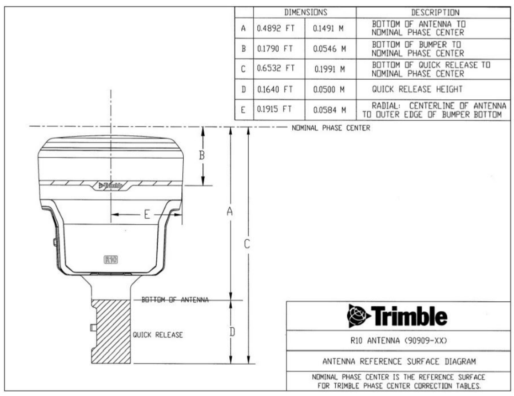

(b) Trimble R10 GNSS receiver

Figure A.1: (HEXAGON positioning intelligence, n.d.) , (*Trimble R10 GNSS Receiver - user guide*, 2014)

For the position of the vessel during the berthing manoeuver two Trimble R10 GNSS Receivers and a base station are used A.1b. This RTK system has an accuracy of ±8 mm + 0.5 ppm. The two receivers are placed at the bow and stern of the ship. The base station is placed at the quay. During the two manoeuvers the position is logged over time. Through differentiating these positions over time, the velocity of the vessel is obtained. With differentiating again, the acceleration and deceleration of the ship can be plotted over time.

A.2. Portable pilot units

The PPUs used by the pilots are based on GNSS positioning as well. The pilots use the NMS - ADX XR. The NMS is a portable navigational system which receives GNSS signals from satellites. The NMS consists of two GNSS antennas, one main processing unit (MPU) and one laptop. The MPU consists of two receivers that receive satellite signals. The satellite signals from the two antennas are processed in the MPU and these data are send to the laptop and processed to real time measurements as presented to the pilots during berthing manoeuvers. The NMS uses three types of GNSS methods for positioning with three different accuracies displayed in table A.1. Which satellite signals to use depends on the location of the NMS. As seen from the table RTK is the most accurate, when RTK signals are not available, the NMS will fall back to EGNOS signals and eventually to GPS/Glonass (Buuren, 2014).

	Position accuracy
GPS/Glonass	4.5 meters horizontal
EGNOS	0.60 meters horizontal
RTK	0.02 m horizontal; 0.10 m vertical

Table A.1: Accuracy of different sattelite signals used by the PPUs (Buuren, 2014)

In normal GNSS systems the velocity is calculated through the difference in position over a certain time. This works only if the position is measured very accurately. Because the NMS position accuracy depends on the GNSS satellite available, the accuracy fluctuates. Therefore, to obtain a velocity the Dopplershift of the satellites (antennas) and the receiver (NMS) is used. The highest accuracy achieved for the velocity is 0.74 cm/s (Buuren, 2014).

The difference in velocity between the Trimble RTK-GNSS system and the PPU is that the PPU measures the velocity of the receivers through the Doppler shift and the Trimble system calculates the velocity using the difference in position over time. As seen in paragraphs A.2 and A.1 the velocity obtained with the Trimble system is more accurate than the velocity obtained through the PPUs.

A.3. Acoustic doppler current profilers

An ADCP is an instrument that measures flow velocities in a water column. This ADCP emits sound waves with a constant frequency, called 'pings'. The sound waves reflect on moving objects, which in this case are the particles suspended in the moving water. The waves reflect, therewith change direction and travel back to the instrument. The instrument listens to the response pulse. The pulse that is transmitted is a frequency modulated pulse and is called a chirp. Multiple chirps are transmitted simultaneously and form a ping. This chirp is an acoustic sine wave with frequencies ranging from low to high (Nortekgroup, 2018). The bandwidth is the difference between the upper and lower frequencies. In figure A.2 a frequency modulated sound wave is shown. Because of the Doppler effect the frequencies of the emitted and received wave differ. This difference

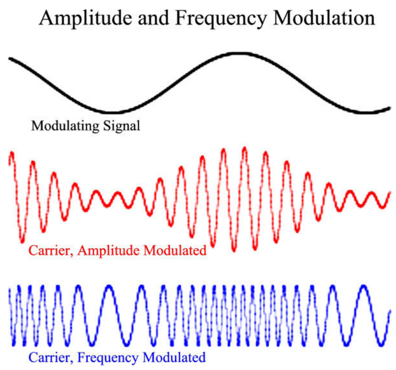

Figure A.2: Difference between frequency and amplitude modulating of a carrier wave (Duffy et al., 2013)

is used to calculate the speed of the particle using the speed of sound.

$$V = t * c * f_{Doppler} \tag{A.1}$$

Where the flow velocity is calculated through time (t), speed of sound (c) and the Doppler shift ($f_{Doppler}$). Because the suspended particles are transported by the water, their velocity represents the velocity of the moving water, this is the biggest assumption of the ADCP technique. Particles that move towards the instrument and reflect the wave produce a slightly higher frequency and particles that move from the instrument produce a slightly lower frequency. In addition, the waves that are emitted with a ping encounter both particles close to the instrument and particles far away from the instrument. The reflected waves come back to the instrument and the time between these differs as well (2019 Woods Hole Oceanographic Institution, 2019)(Nortekgroup, 2018). Using this time difference and the Doppler shift the ADCP measures speed of the particles at many different depths and therefore flow velocities at different depths.

The velocity of the particles is measured in the direction of the beam. To obtain the velocity of the water in three directions, at least three beams are needed. These beams are positioned in such a way that a triangular area is covered and within this area, the velocity in three directions is measured as shown in figure A.3b.

Figure A.3: Configuration of an ADCP (Nortekgroup, 2018)

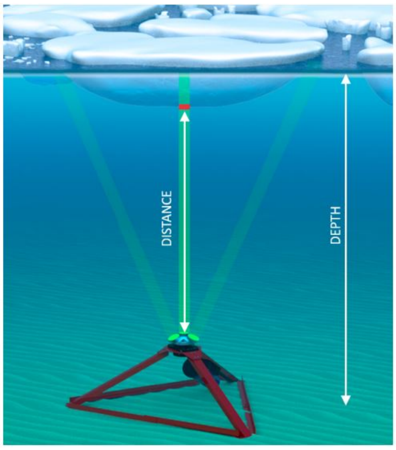

(a) Signature 500 installed on the ocean floor

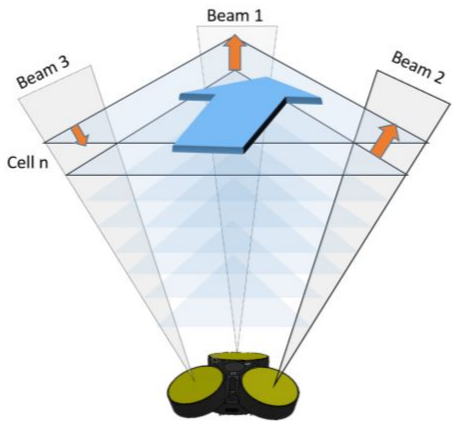

(b) Position of the beams of the signature 55 (three beams)

In this research three types of ADCPs are used to measure the flow velocities between ship and quay. These ADCPs are shown in figure A.4. The signature 500 and AWAC 600kHz are used to measure velocities in three directions over a certain depth as shown in figure A.3. Furthermore, these two ADCPs measure pressure which is used to monitor the pressure behaviour of the water between ship and quay. The OTT SLD is a side looking Doppler sensor. It also uses the Doppler shift principle but uses two beams, obtaining velocity in two directions. For the application in this research it means that the OTT SLD will measure the flow velocity perpendicular to the quay and parallel to the quay.

Figure A.4: Three different instruments used to measure flow velocities (Nortekgroup, 2018)

(a) Signature 500

(b) OTT SLD

(c) AWAC 600kHz

Sidenotes

- When the signal is reflected by the particles and send back to the ADCP, the signal received is subject to a certain amount of noise. There are different sorts of noise but the noise is averaged out by averaging the pings of the instrument and subtract a velocity out of this averaging.

- The speed of sound is dependent on the medium through which the soundwaves travel. This medium is for these ADCPs always water, but the speed of sound differs with the different densities water can possess. The density depends on the density and the salinity of the water. The ADCP uses a standard salinity and measures a temperature to calculate the density of the water and therefore the speed of sound. The temperature is a bigger influence on the density, therefore it is sufficient to specify a salinity beforehand.

- One must keep in mind that per beam the particles that travel perpendicular to the beam does not effect the doppler shift, so the velocity is only calculated for particles traveling in the direction of the beam.

B

Flow velocities and height of tides in the basin

Figure B.1: Flow velocity during experiment 1 - manoeuver 1

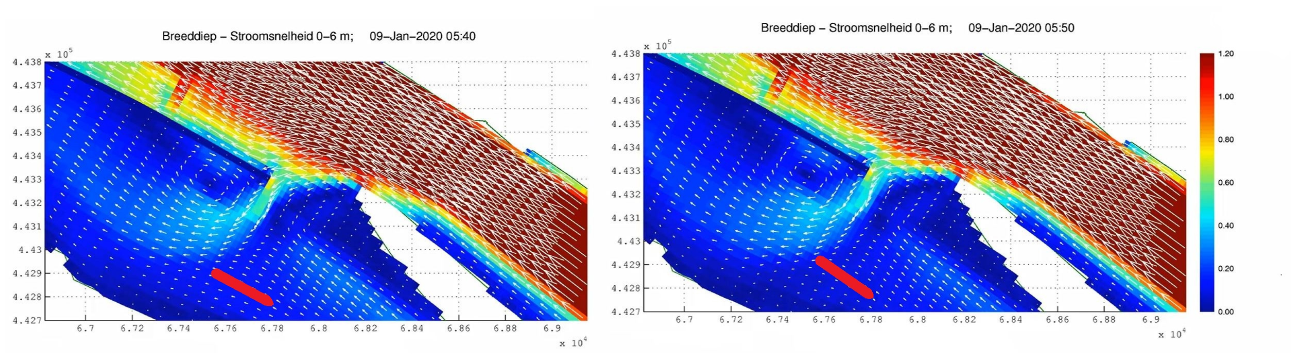

(a) (b)

Figure B.2: Flow velocity during experiment 1 - manoeuver 2

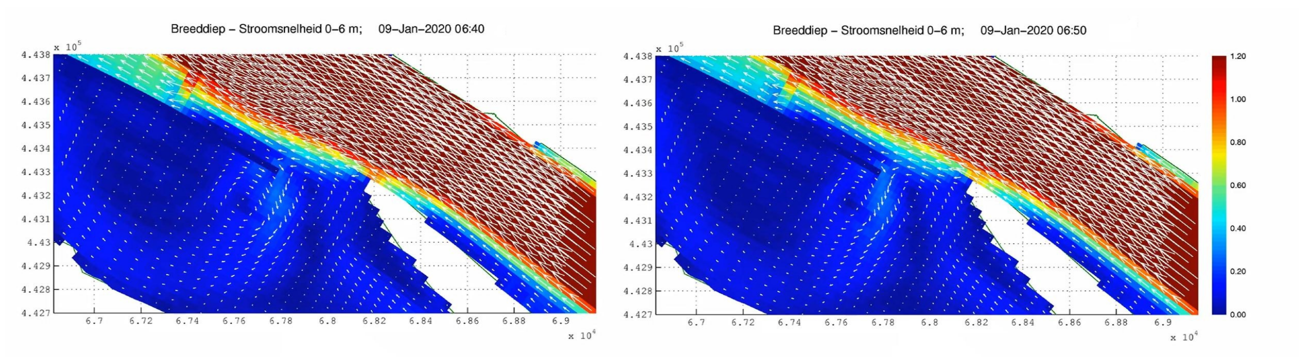

(a) (b)

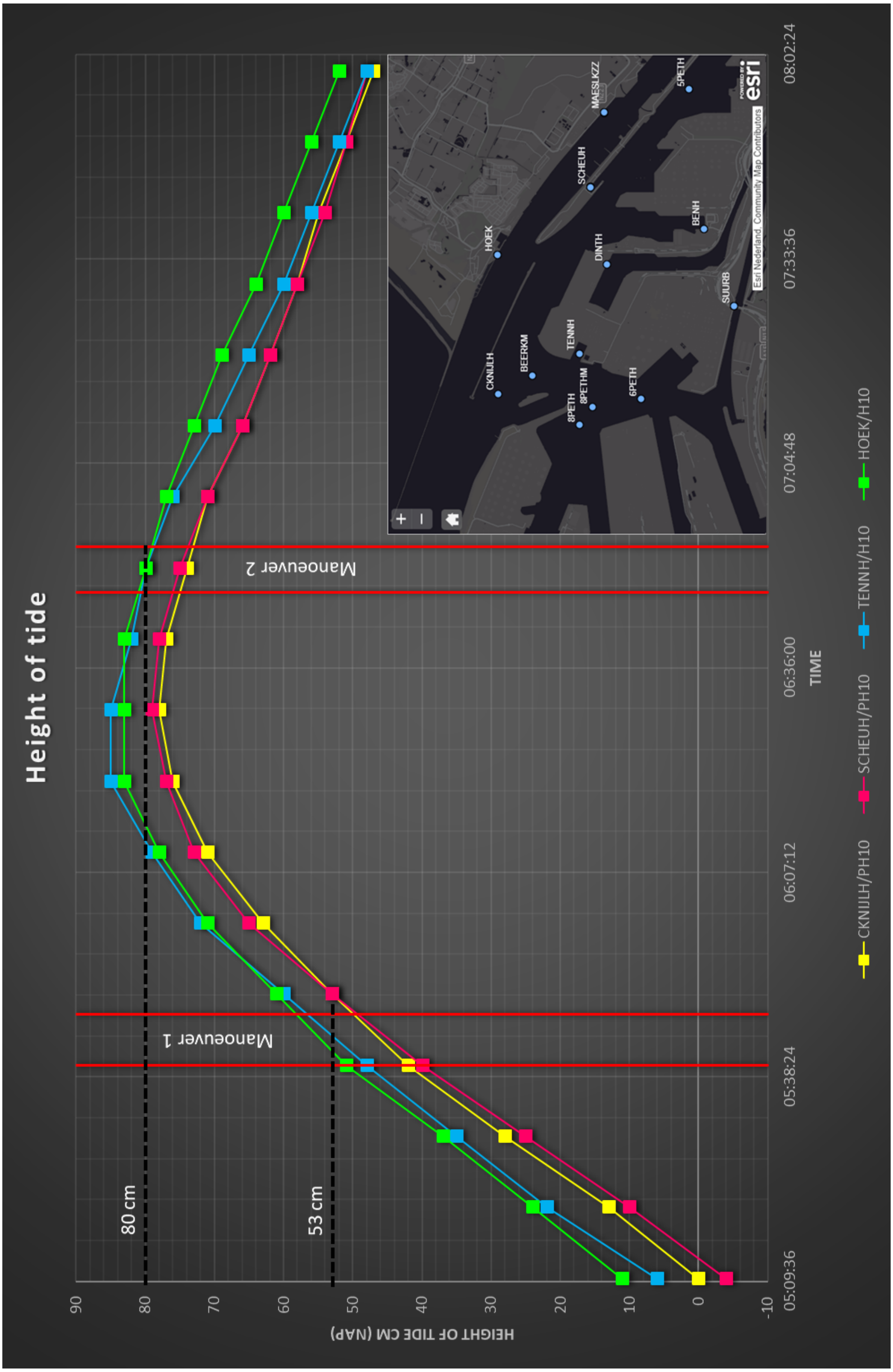

Figure B.3: Height of tide during field experiment 1

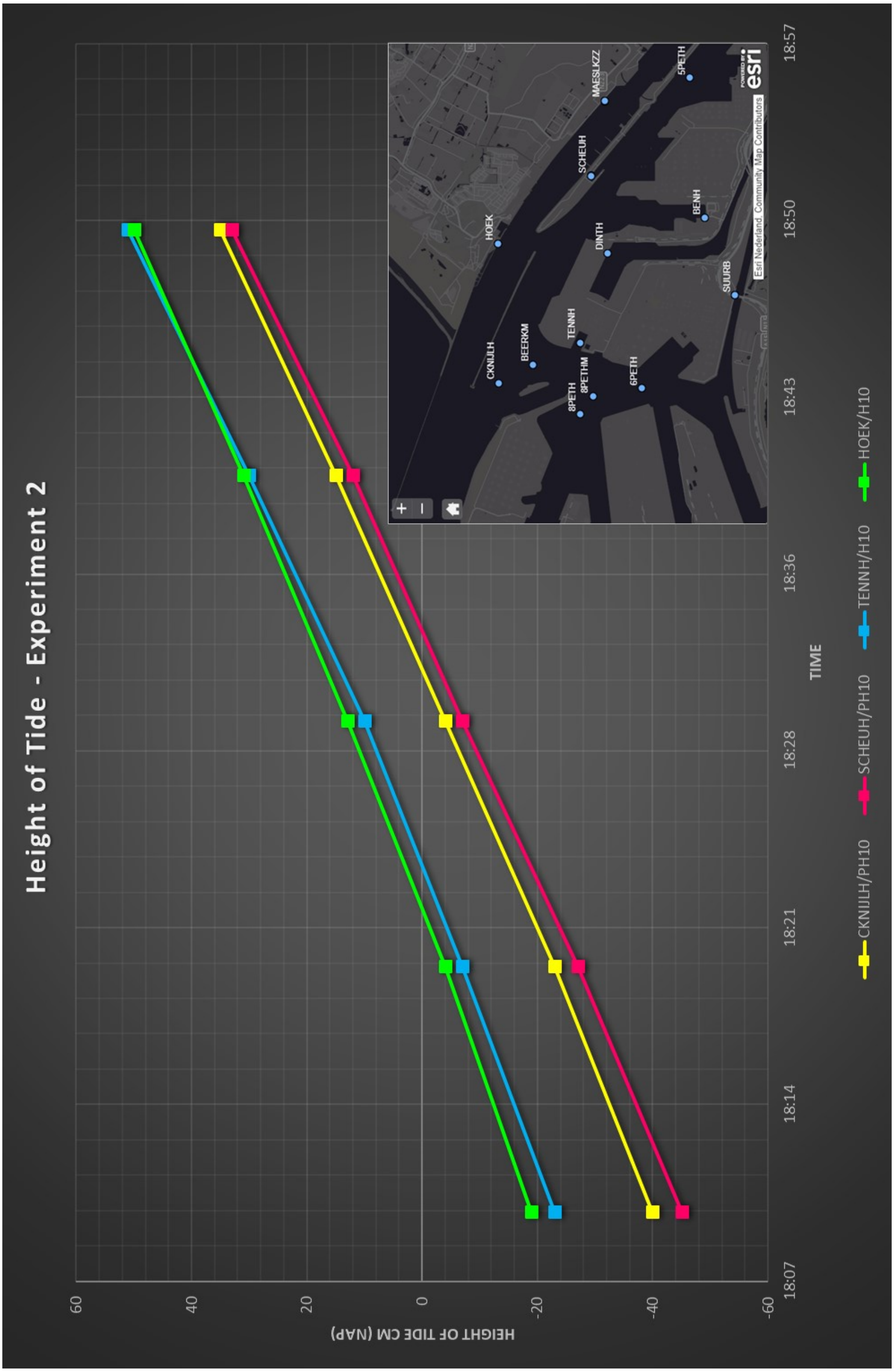

Figure B.4: Height of tide during field experiment 2

C

Field experiment 1

C.1. PPU Data

Figure C.1: Bow and stern velocities during manoeuver 1 & 2

(a) Velocities manoeuver 1

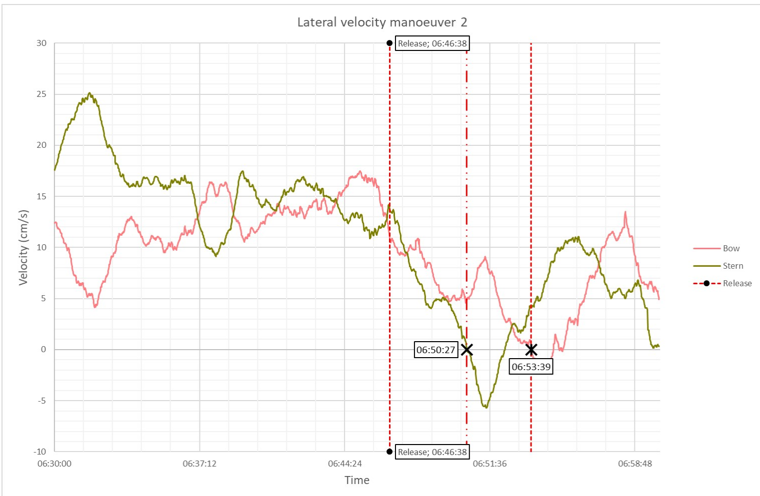

(b) Velocities manoeuver 2

C.2. RTK Data

Figure C.2: Position bow sensor ship 1

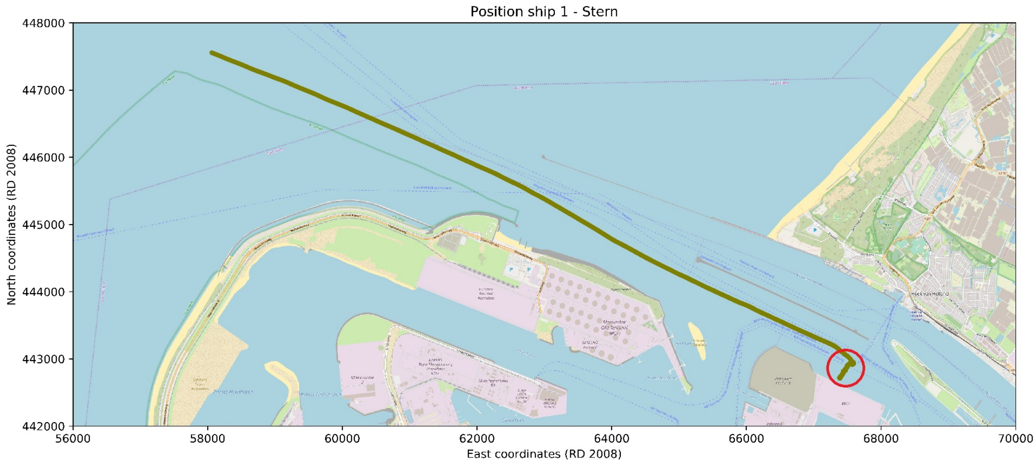

Figure C.3: Position stern sensor ship 1

Figure C.4: Bow and stern positions during manoeuver 1

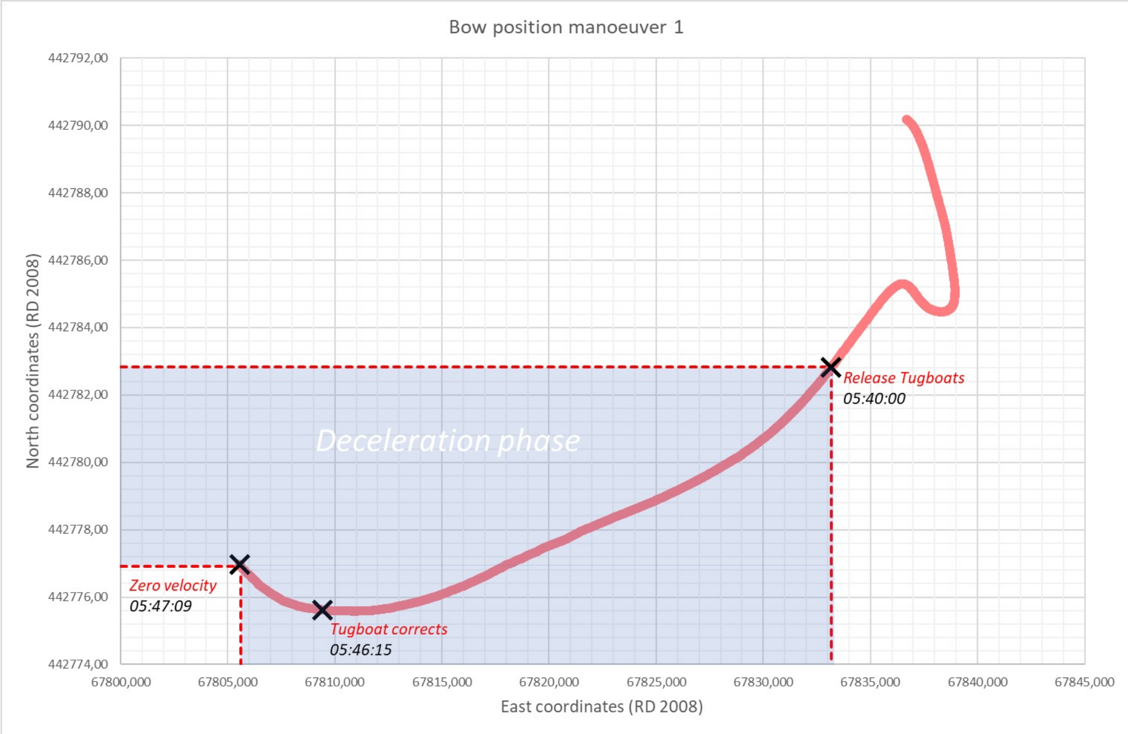

(a) Bow position manoeuver 1

(b) Stern position manoeuver 1

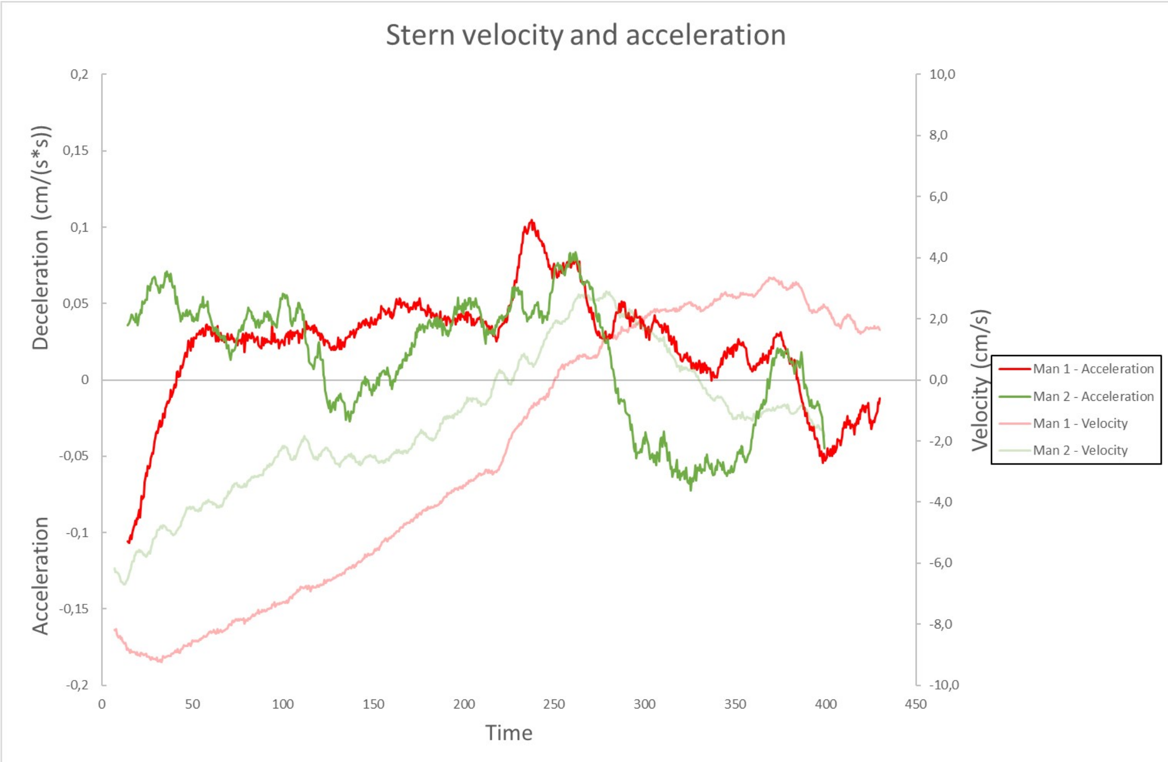

Figure C.5: Velocity and acceleration of the stern during both berthing manoeuvers

Figure C.6: Difference in maximum acceleration during both berthing manoeuvers - stern

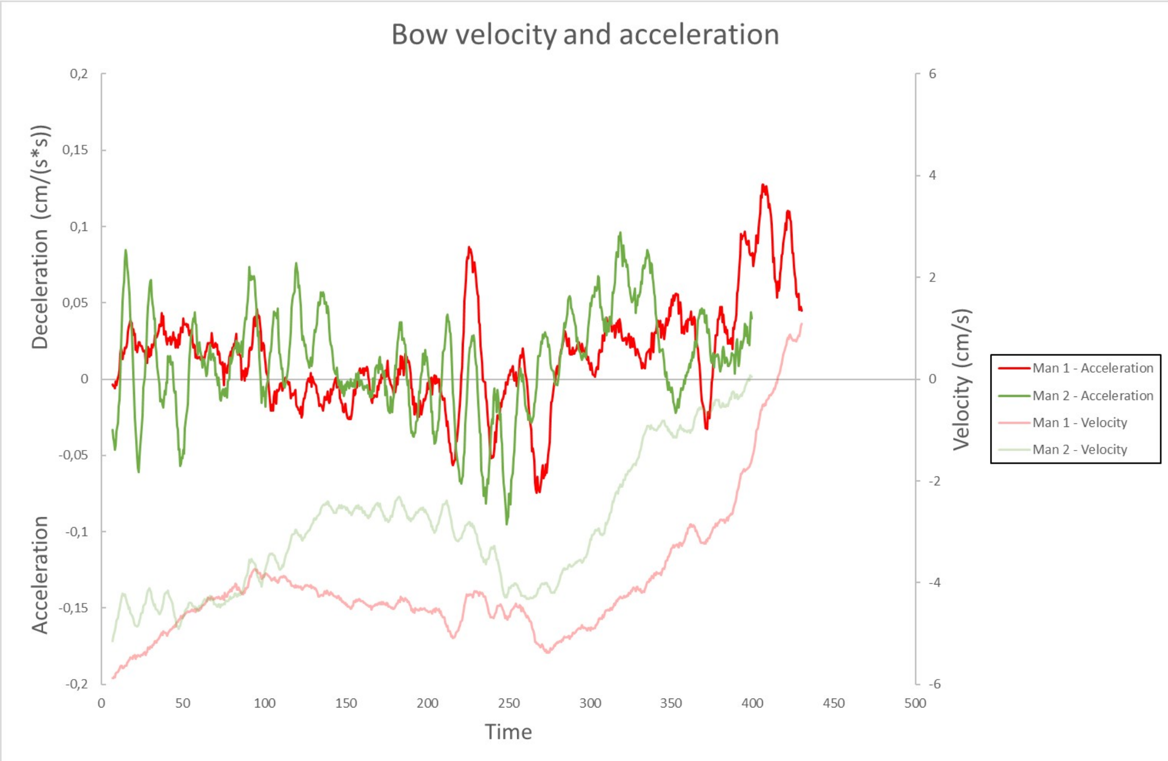

Figure C.7: Velocity and acceleration of the bow during both berthing manoeuvers

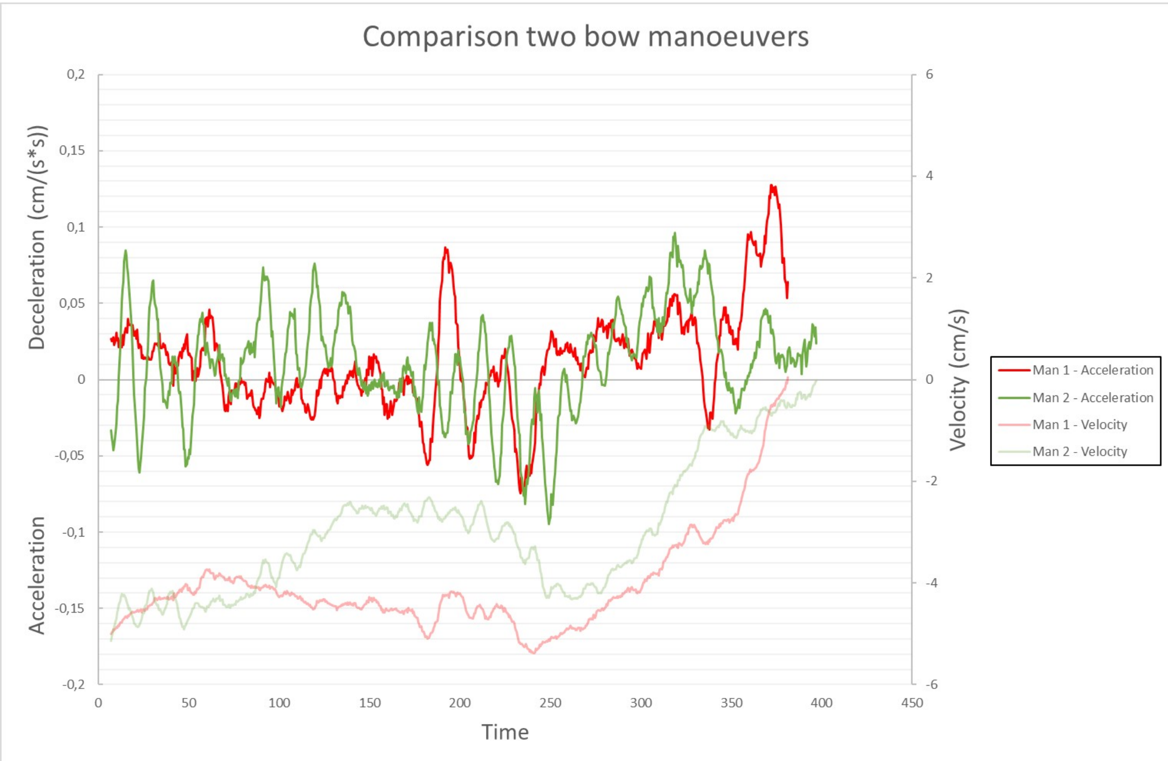

Figure C.8: Difference in maximum acceleration during both berthing manoeuvers - bow

D

Field experiment 2

D.1. PPU data

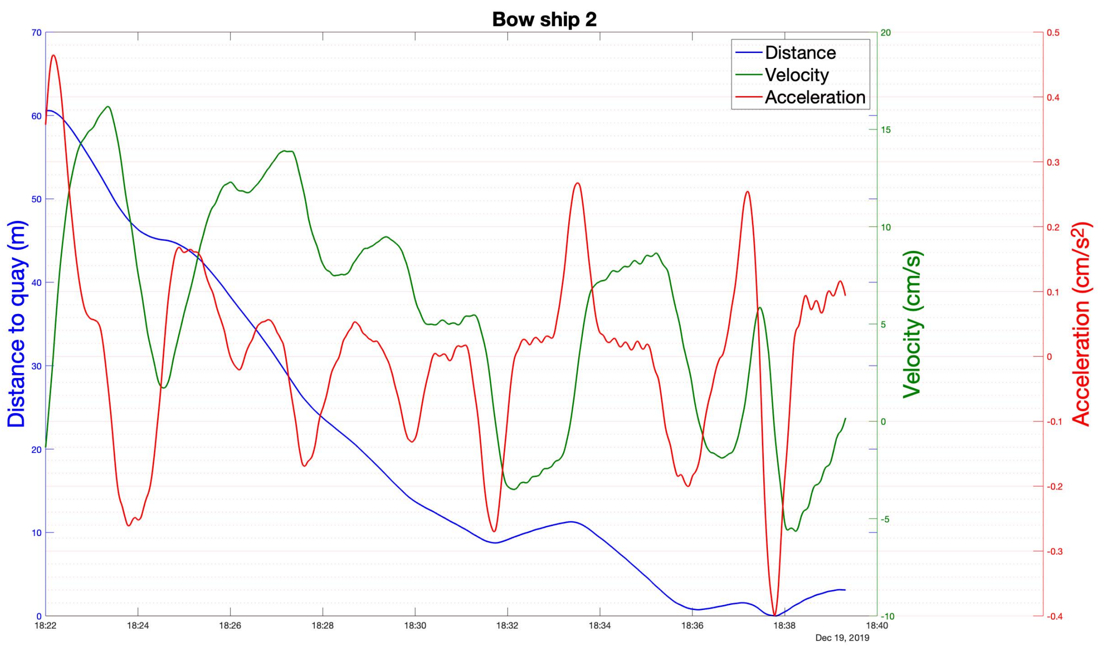

Figure D.1: Distance to the quay, lateral velocity and acceleration ship 2 - bow

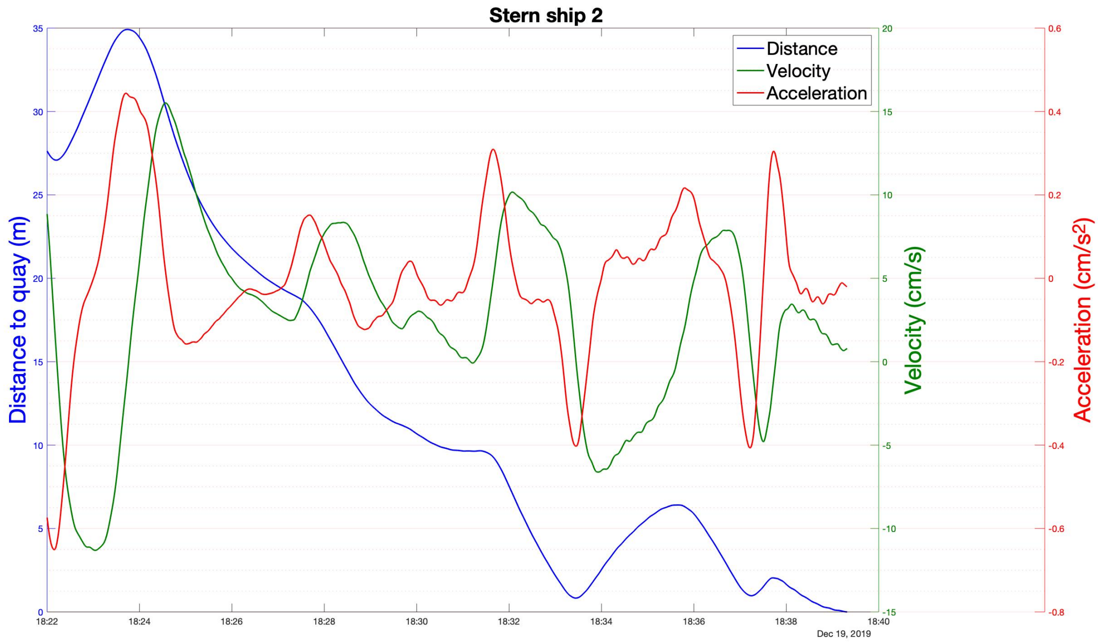

Figure D.2: Distance to the quay, lateral velocity and acceleration ship 2 - stern

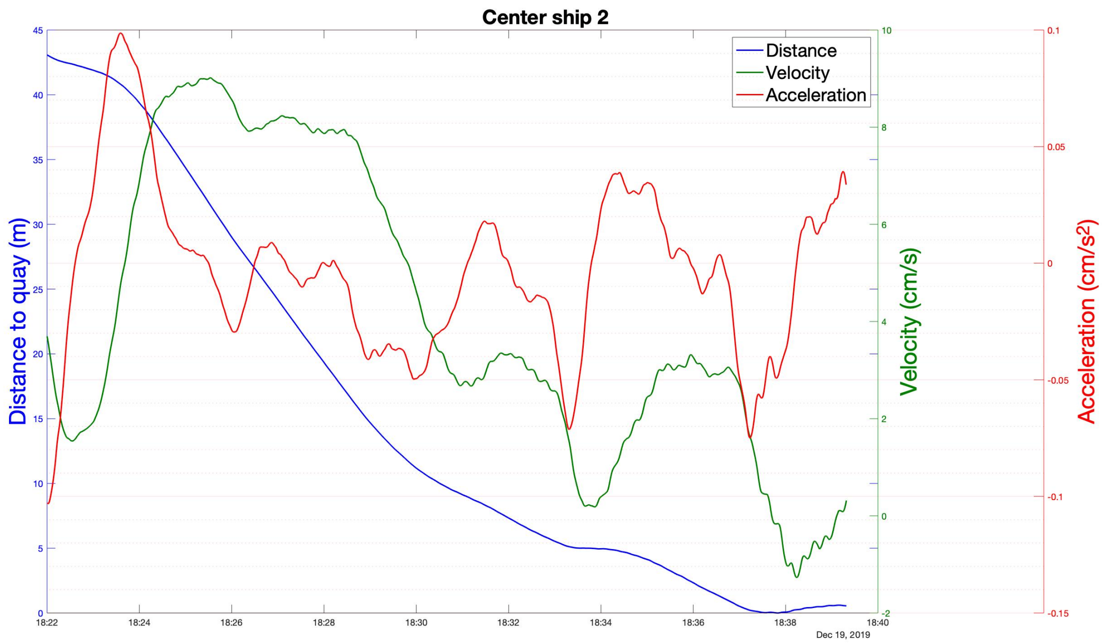

Figure D.3: Distance to the quay, lateral velocity and acceleration ship 2 - center

D.2. OTT, AWAC & Signature data

Figure D.4: AWAC - Velocity longitudinal to the quay per meter distance from the quay during the berthing manoeuver

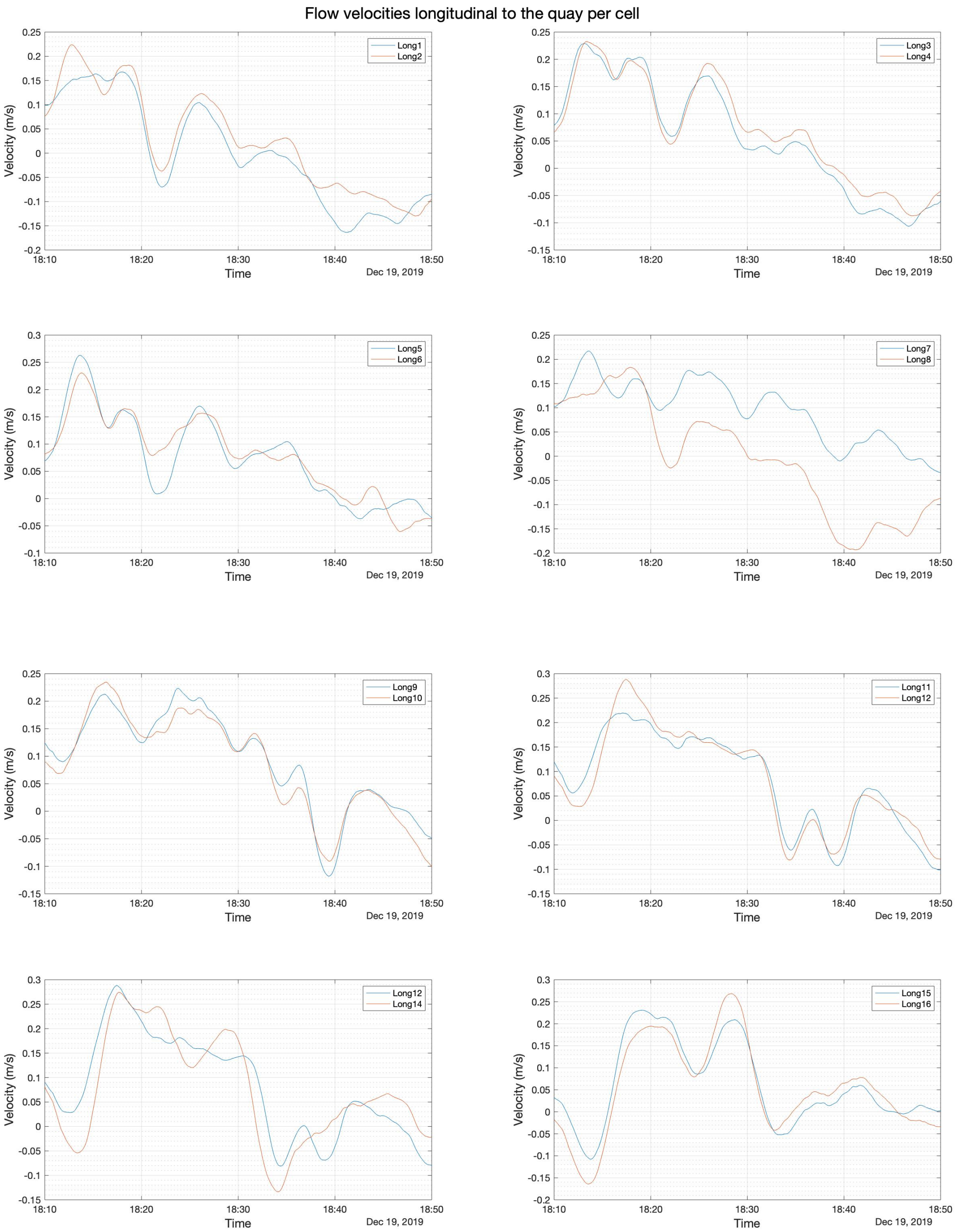

Figure D.5: AWAC - Velocity perpendicular to the quay per meter distance from the quay during the berthing manoeuver

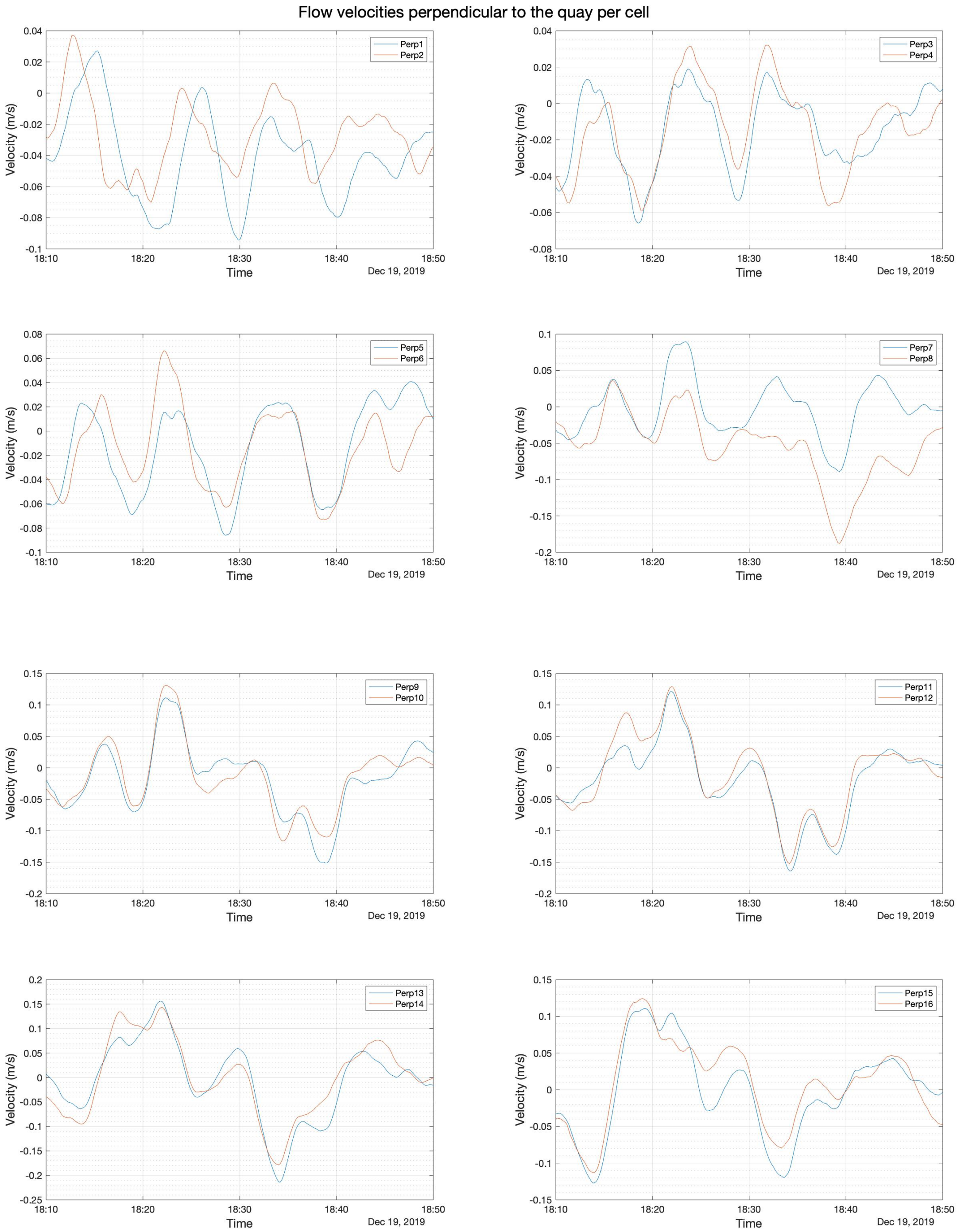

Figure D.6: AWAC - Velocity upwards per meter distance from the quay during the berthing manoeuver

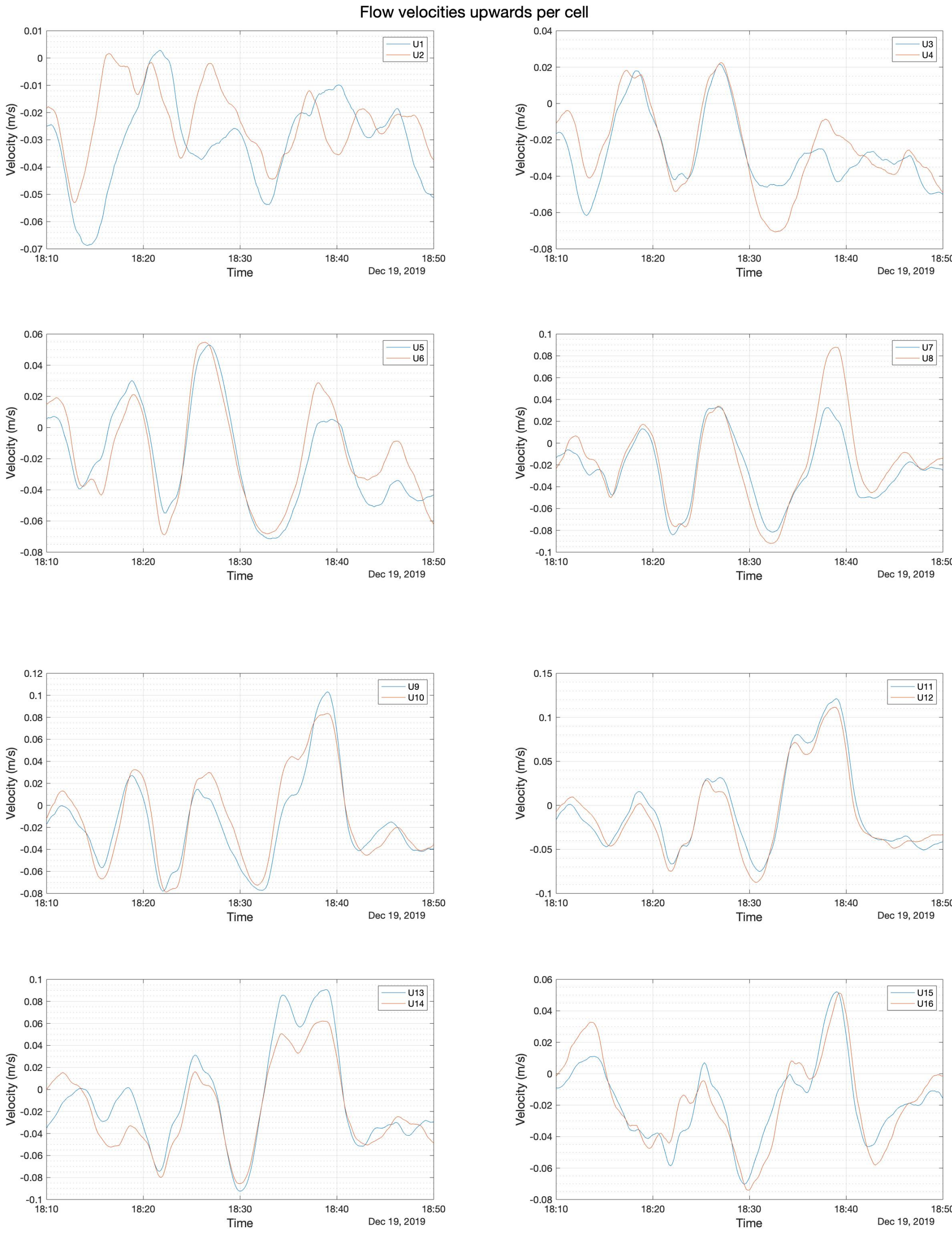

Figure D.7: Signature - Velocity longitudinal to the quay per meter distance from the quay during the berthing manoeuver

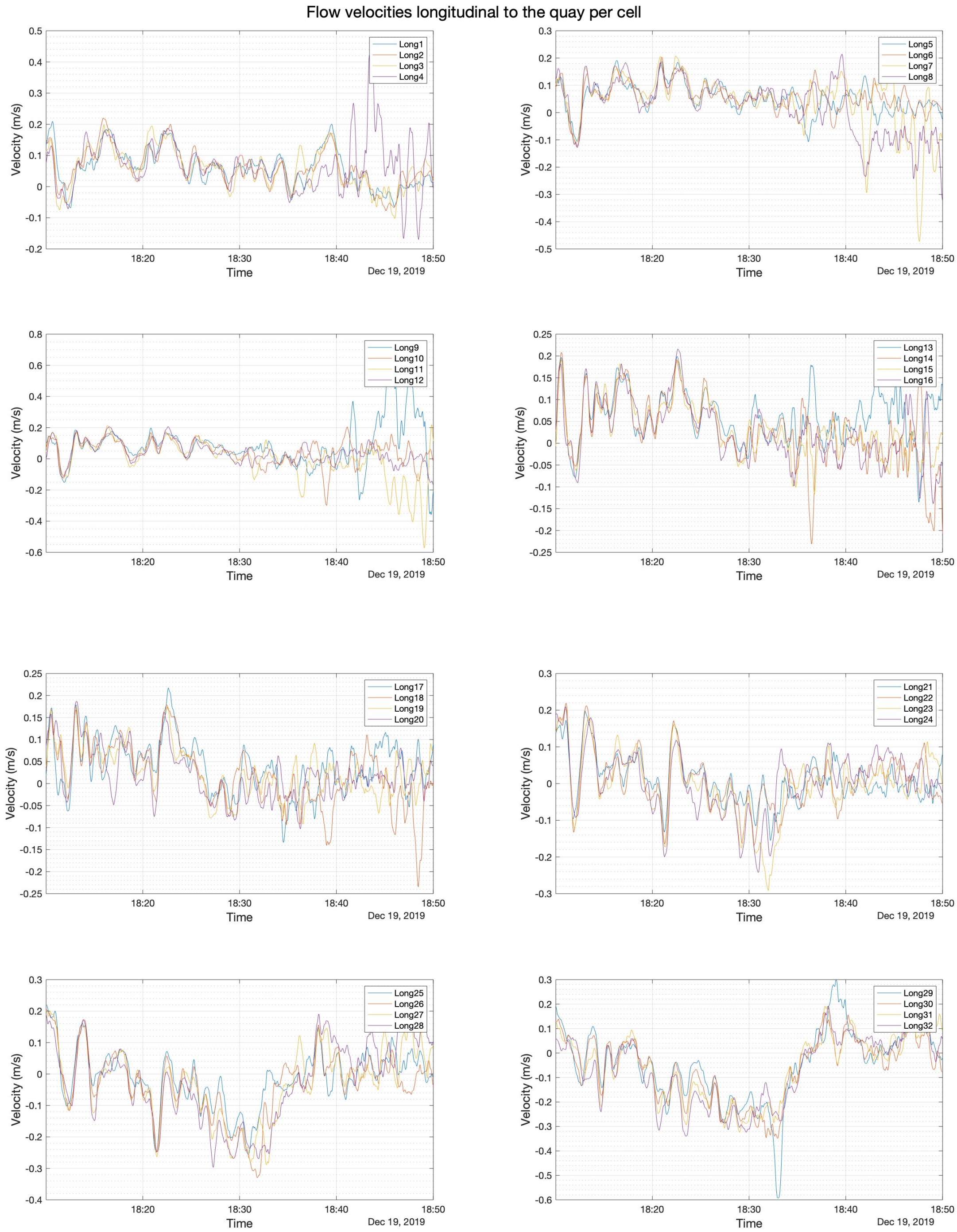

Figure D.8: Signature - Velocity perpendicular to the quay per meter distance from the quay during the berthing manoeuver

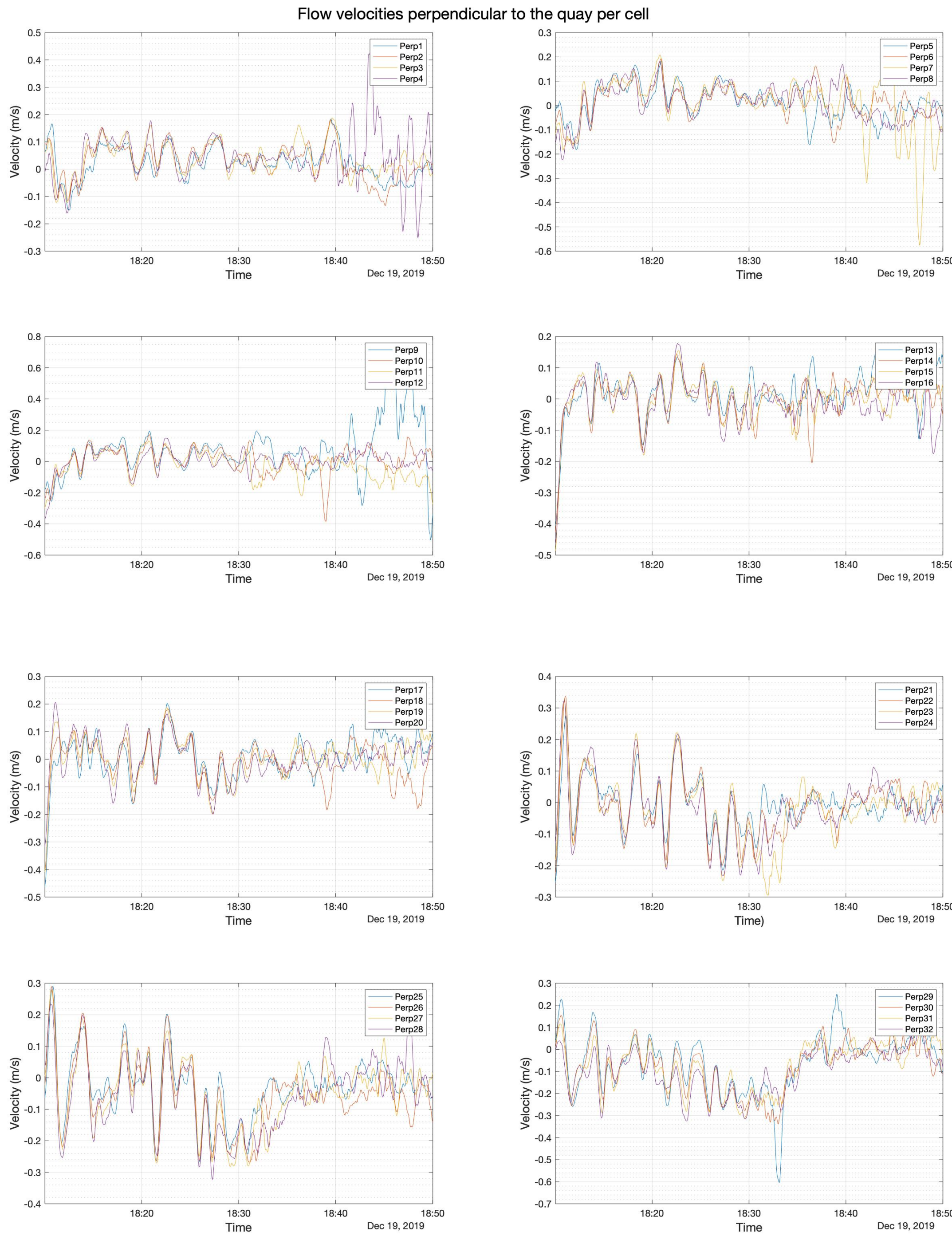

Figure D.9: Signature - Velocity upwards per meter distance from the quay during the berthing manoeuver

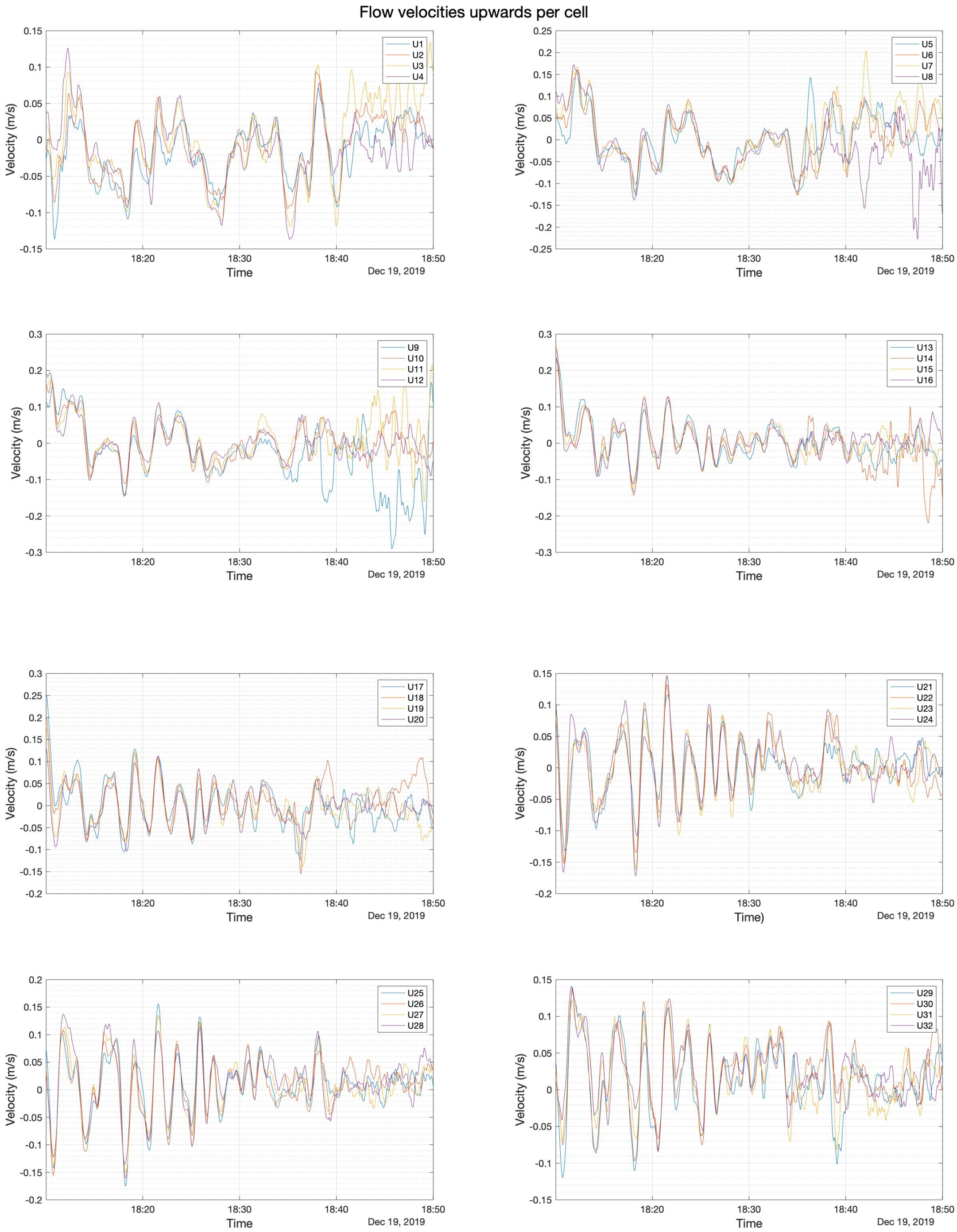

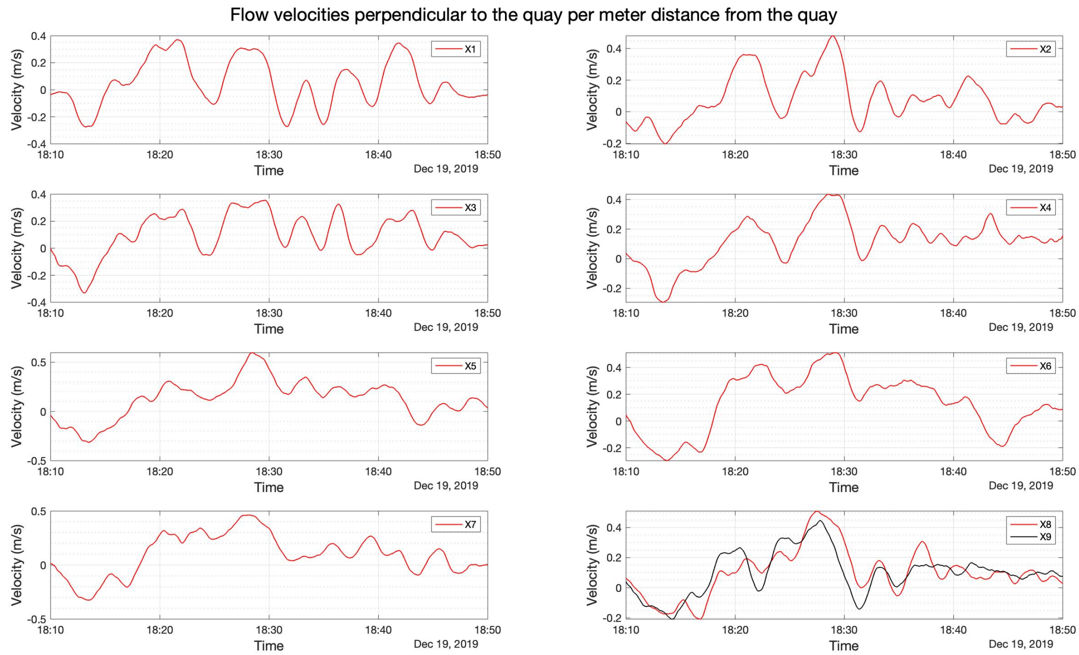

Figure D.10: OTT - Velocity longitudinal to the quay per meter distance from the quay during the berthing manoeuver

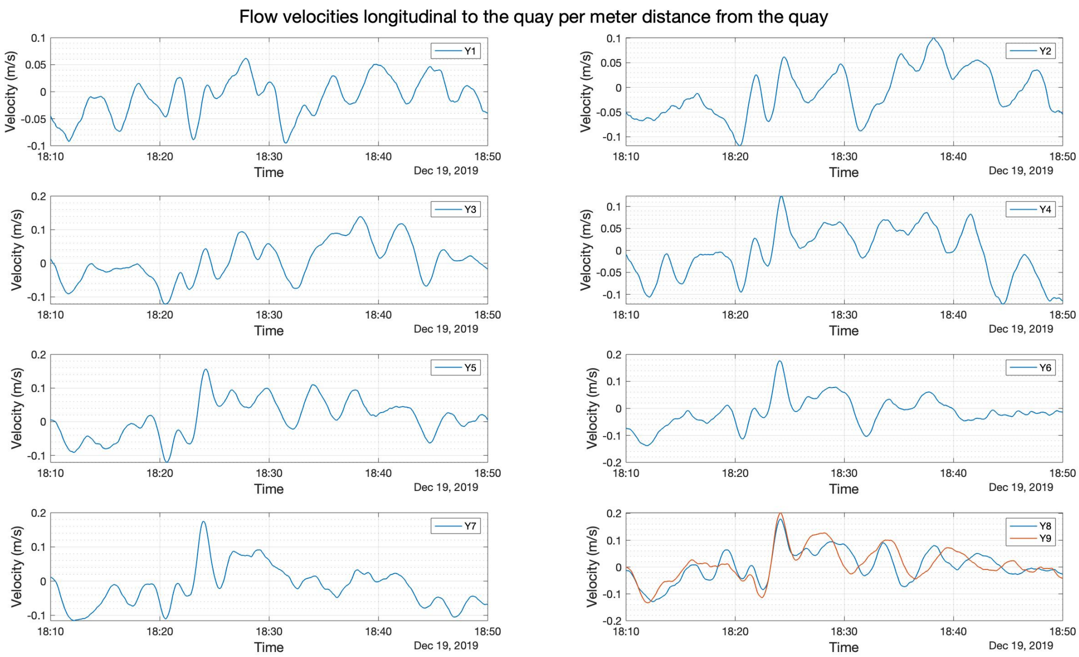

Figure D.11: OTT - Velocity longitudinal to the quay per meter distance from the quay during the berthing manoeuver

E

Reliability measurements

E.1. Reliability for AWAC

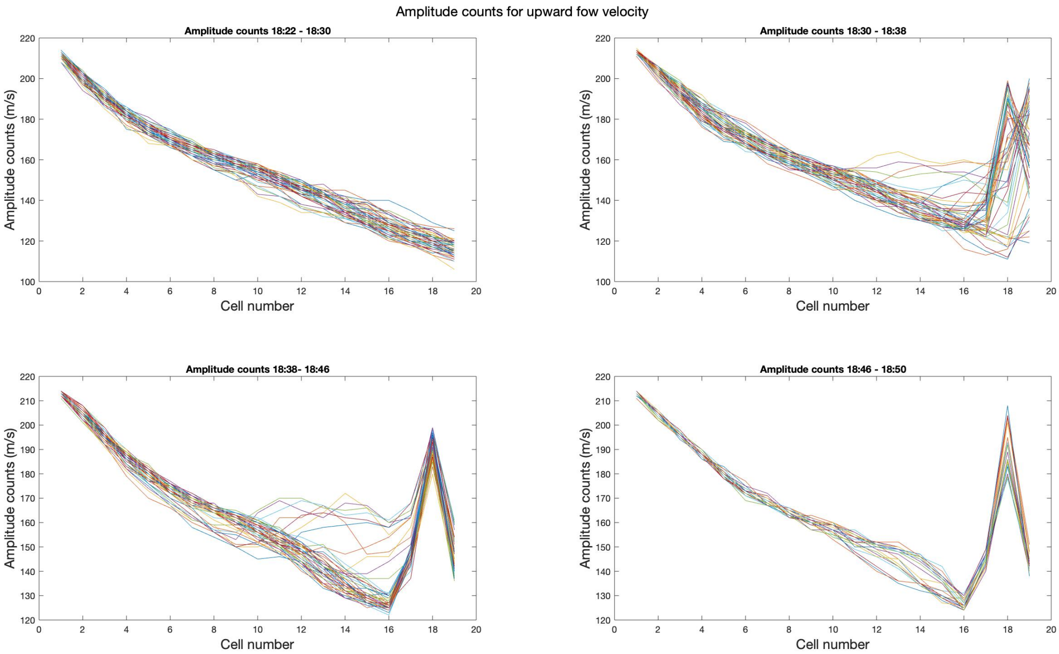

Figure E.1: Reliability for upward velocity

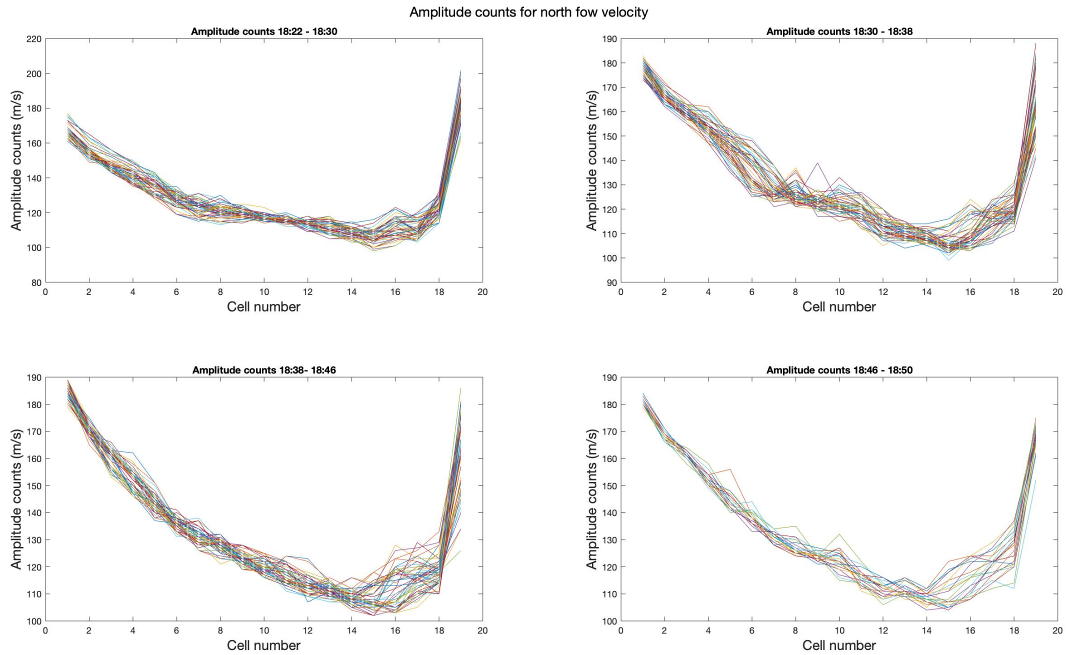

Figure E.2: Reliability for perpendicular velocity

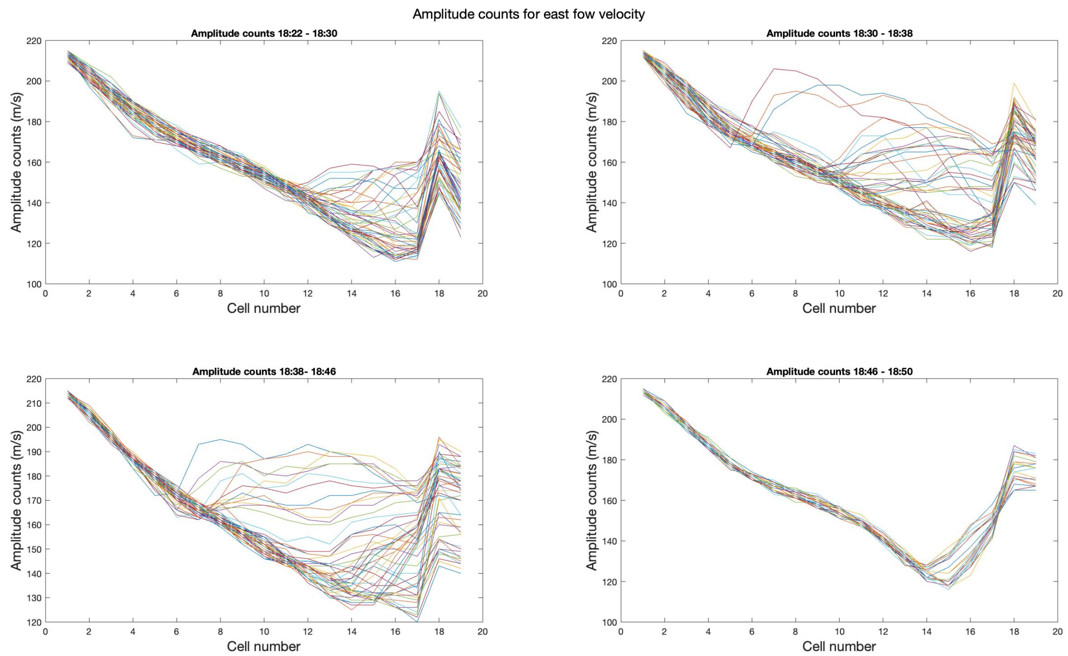

Figure E.3: Reliability for longitudinal velocity

E.2. Reliability for Signature

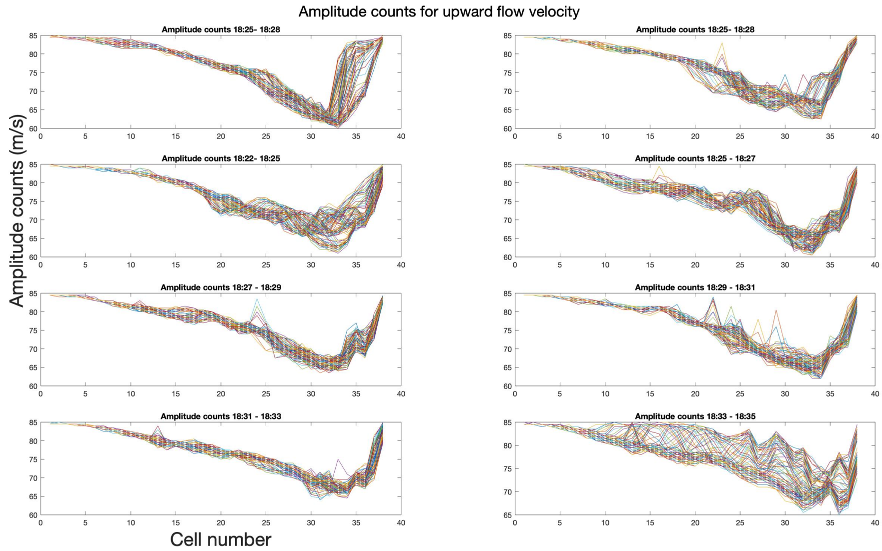

Figure E.4: Reliability for upward velocity

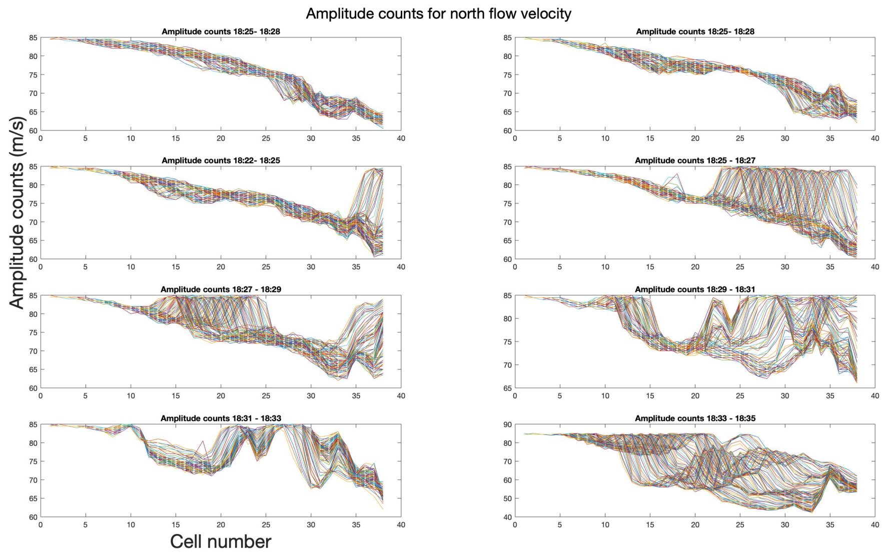

Figure E.5: Reliability for perpendicular velocity

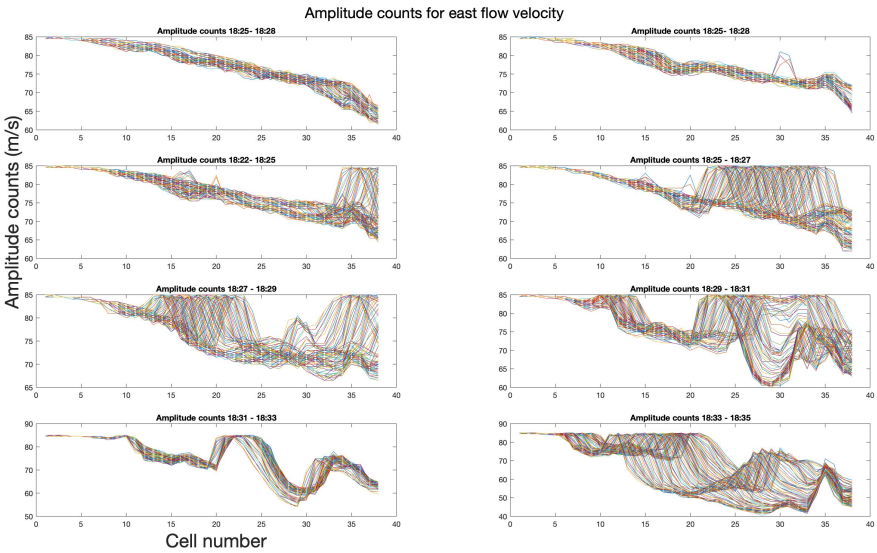

Figure E.6: Reliability for longitudinal velocity

E.3. Realiability for OTT

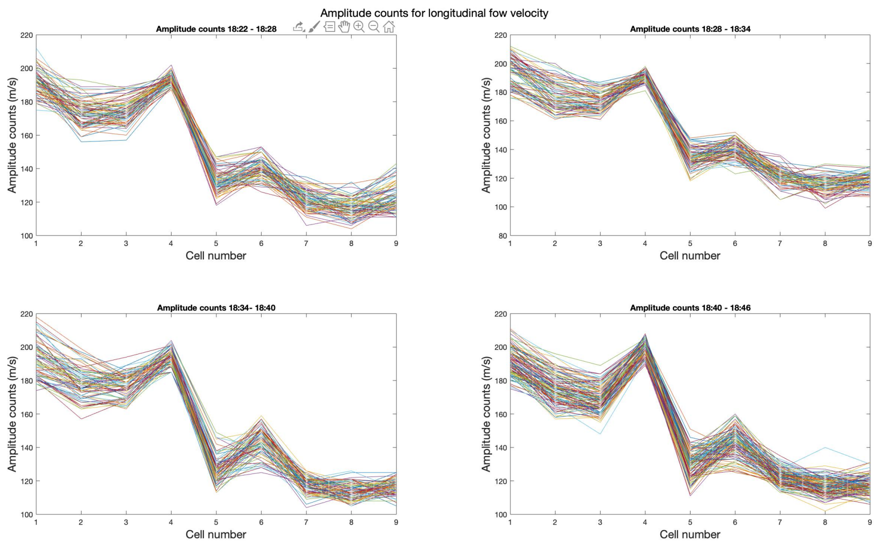

Figure E.7: Reliability for velocity longitudinal to the quay

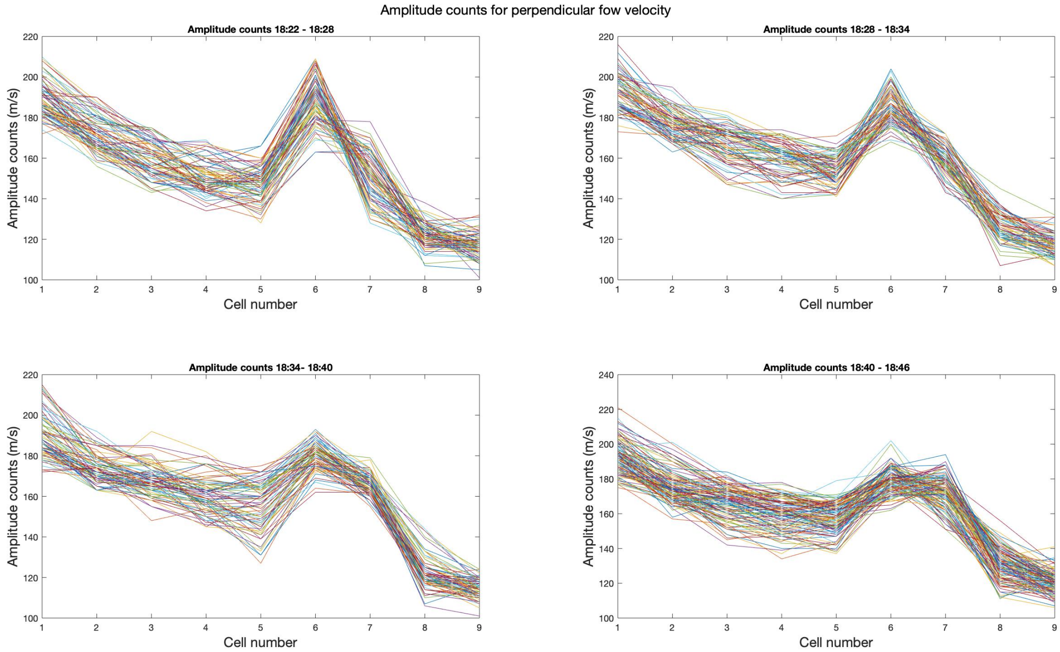

Figure E.8: Reliability for velocity perpendicular to the quay

E.4. Uniformity OTT

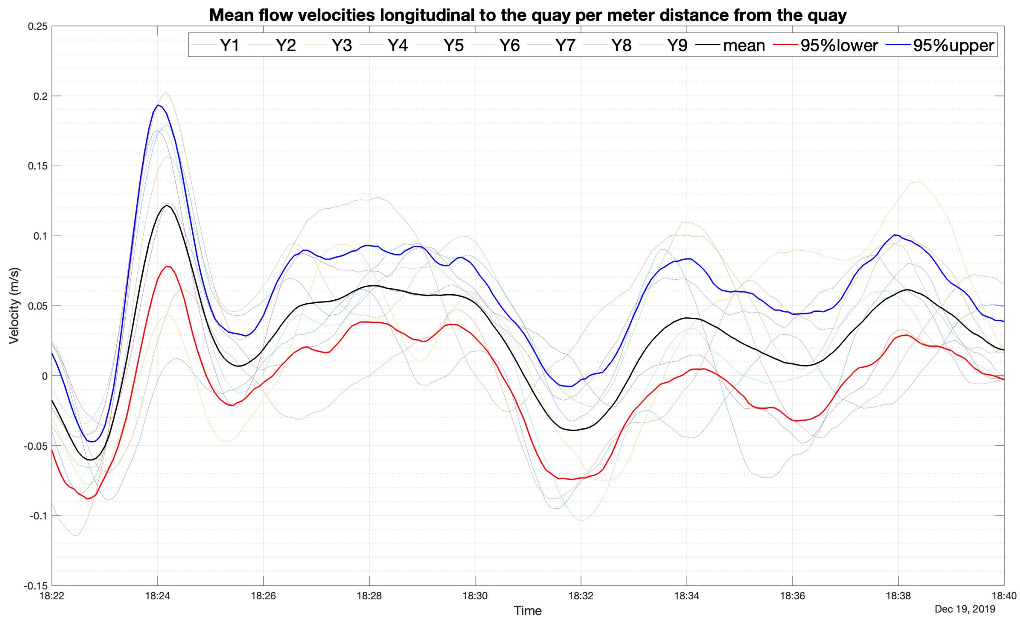

Figure E.9: Longitudinal uniformity investigation of the OTT

F

Comparison PPU and RTK

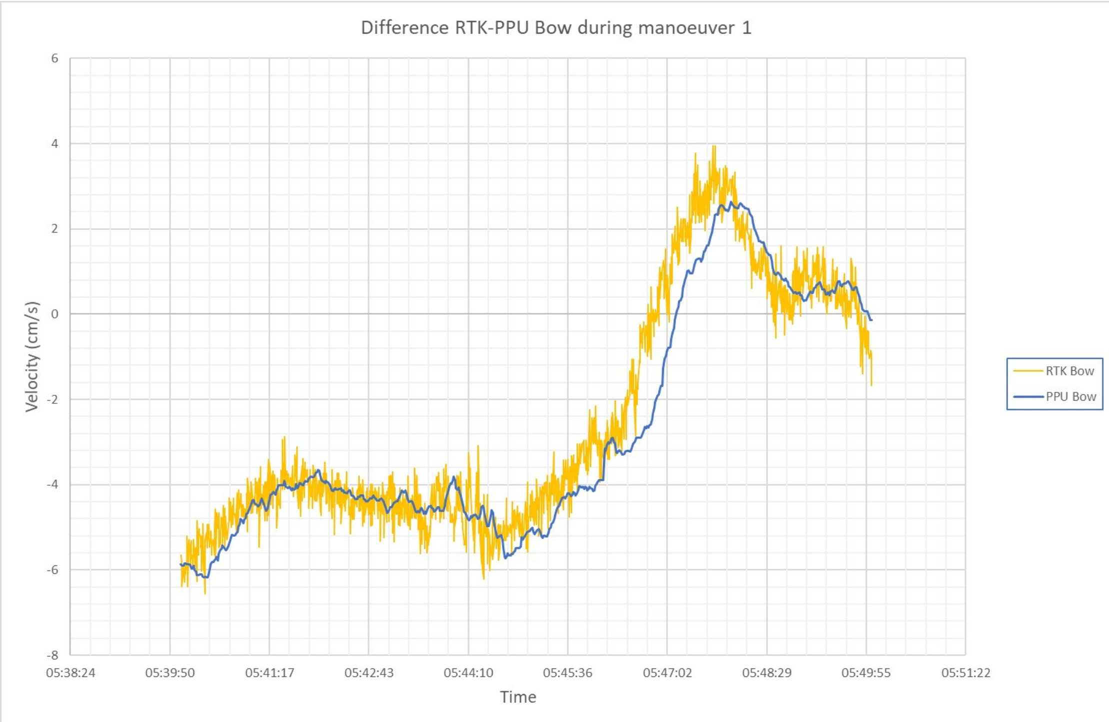

Figure F.1: Difference in velocity measurements between the PPU and the RTK - manoeuver 1 bow

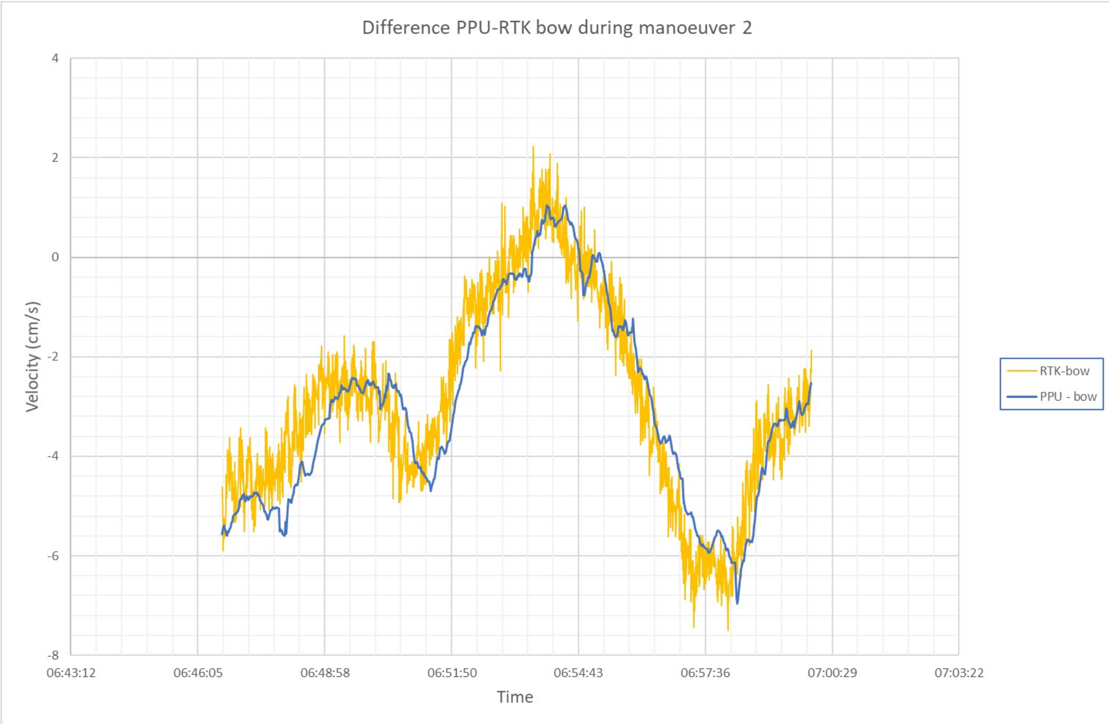

Figure F.2: Difference in velocity measurements between the PPU and the RTK- manoeuver 2 bow

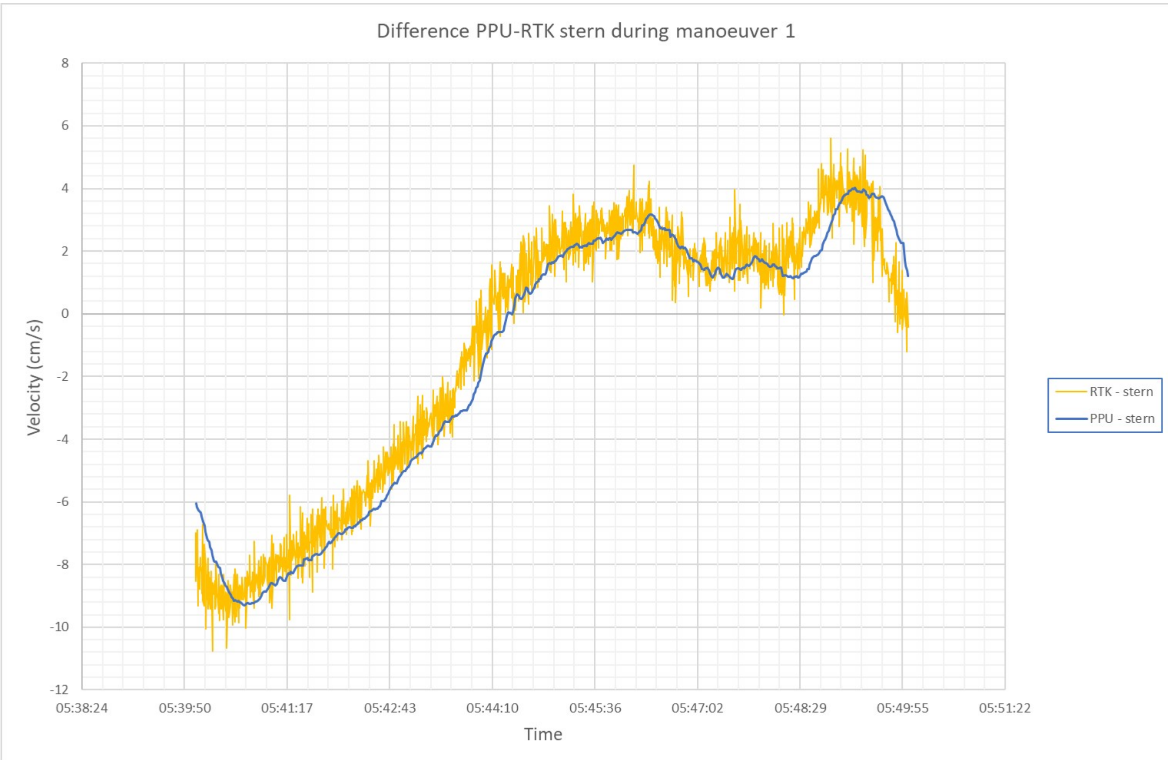

Figure F.3: Difference in velocity measurements between the PPU and the RTK - manoeuver 1 stern

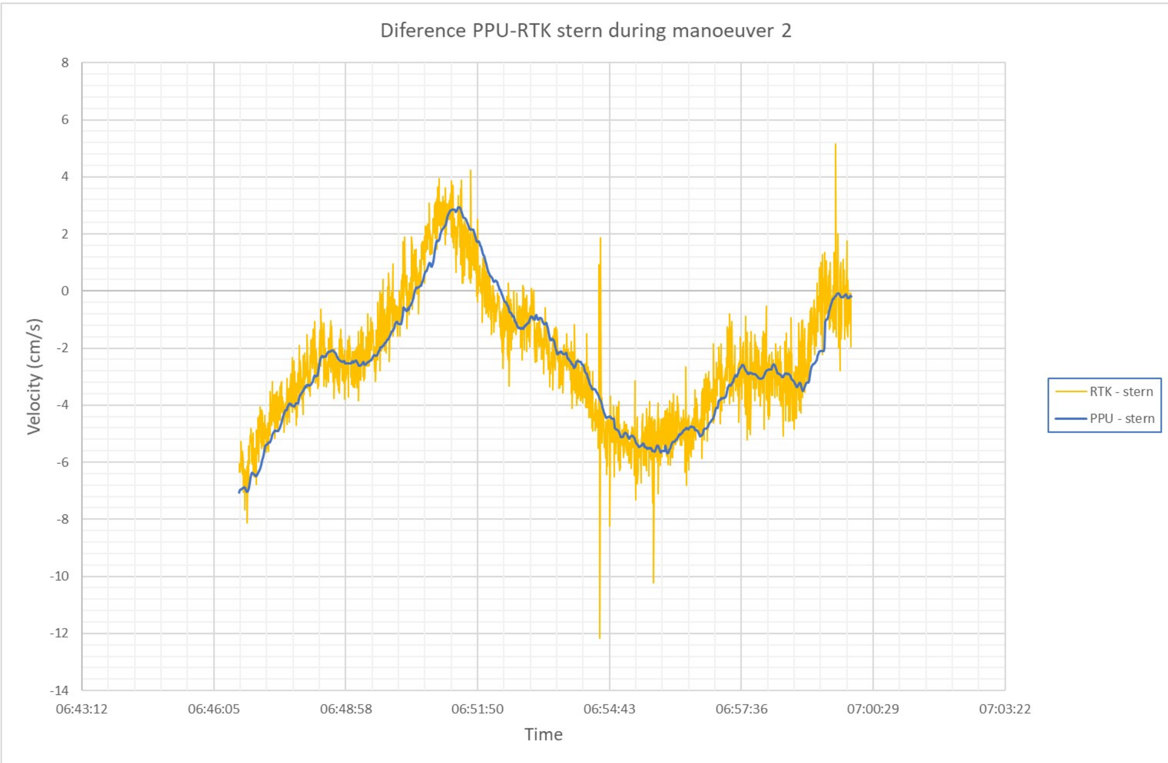

Figure F.4: Difference in velocity measurements between the PPU and the RTK - manoeuvre 2 stern

G

Energy losses due to friction

G.1. Estimating energy losses using a culvert

The second approach to estimate the energy losses in this model a comparison is made with a sunk culvert as shown in figure G.1. The elevation on the right side of the vessel is expected to be in the order of centimeters.With culverts the energy losses are expressed as entry losses, exit losses and a resistance coefficient. This resistance coefficient corresponds to the length of the culvert.

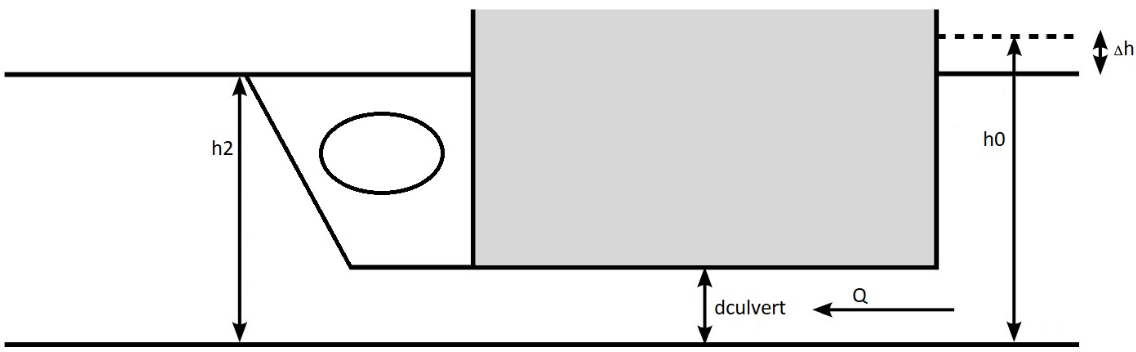

Figure G.1: Berthing manoeuver simplified to a fully submerged culvert

To explore the behaviour of culverts, the 'discharge relation' should be introduced (Kolkman, 1989). The discharge relation is as follows:

$$Q = f(h_0, h_2, geometry) \tag{G.1}$$

Or in terms of energy heads:

$$Q = f(H_0, H_2, geometry) \tag{G.2}$$

It is important that one keeps in mind that one section controls the entire discharge relation and therefore the control section should be chosen deliberately. According to Kolkman (1989) certain energy losses need to be implemented in the discharge relation as well. Examples of these 'hydraulic losses from different components' are losses from friction, entrance, exit, hydraulic jumps etcetera.
The discharge characteristics of free surface flow are considered, as the flow only has one vertical constriction and not two. The flow is only constricted by the bottom of the control area and has no constriction at the surface before and after the weir. In other words there is zero parallel stress. Free surface flow can be subdivided into three flows, free flow, fully submerged flow and intermediate flow. A concise explanation is given.

- Modular flow, only the upstream velocity (h_0) influences the discharge. Big difference is velocity heads.

- Fully submerged flow, only small head differences. Horizontal water levels form a boundary independent of velocity.
- Intermediate flow, in between the former two regimes. Discharge depends on h_0 and h_2.

The relation between the discharge and the water level for the three flow regimes is shown in figure G.2 (Kolkman, 1989).

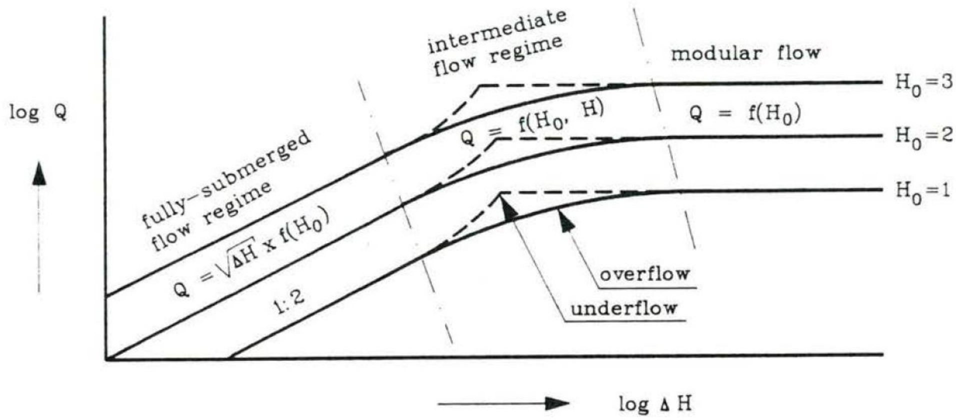

Figure G.2: Relationship between discharge and water level for a certain geometry (Kolkman, 1989)

The culvert considered is a sunk culvert or 'fully submerged' culvert. The water level differences between the right and left side are assumed to be so small that the culvert is considered to be 'fully submerged'. The culvert is now in the 'fully submerged' flow regime. This means that the flow velocities are very low, expressed in a low Froude number. The losses in energy heads are:

$$\Delta H = \varepsilon \frac{V^2}{2g} = \Delta H_{entrance} - \Delta H_{friction} - \Delta H_{exit} \tag{G.3}$$

The total loss is a summation of local losses. The only losses considered in this model are entrance loss, exit loss and friction loss. This gives the following expression:

$$\varepsilon = (\varepsilon_{entrance} + \varepsilon_{friction} + \varepsilon_{exit}) \tag{G.4}$$

$$V = \varepsilon^{-0.5}\sqrt{2g\Delta H} \tag{G.5}$$

$$Q = C_d A \sqrt{2g\Delta H} \tag{G.6}$$

Friction losses
Friction head loss is expressed as:

$$\Delta H_{friction} = f * \frac{L}{D_h}\frac{V^2}{2g} \tag{G.7}$$

For culverts the friction losses are calculated with the Moody diagram for circular pipe flow. The Moody diagram only needs a slight adaptation for this situation, the hydraulic diameter (D_h) is now calculated through the hydraulic radius (R_h) multiplied by 4. The culvert possesses the same dimensions as the ship that is used for the theoretical model parallel ship berthing. With these physical properties the friction loss can be determined. Because the model is 2D, the width of the culvert is set to 1 meter. First the hydraulic radius should be calculated:

$$R_h = \frac{A}{P} = \frac{d_{culvert} * w_{culvert}}{w_{culvert} + w_{culvert} + d_{culvert} + d_{culvert}} \tag{G.8}$$

This gives:

$$R_h = \frac{4 * 1}{1 + 1 + 4 + 4} = 0.4m$$

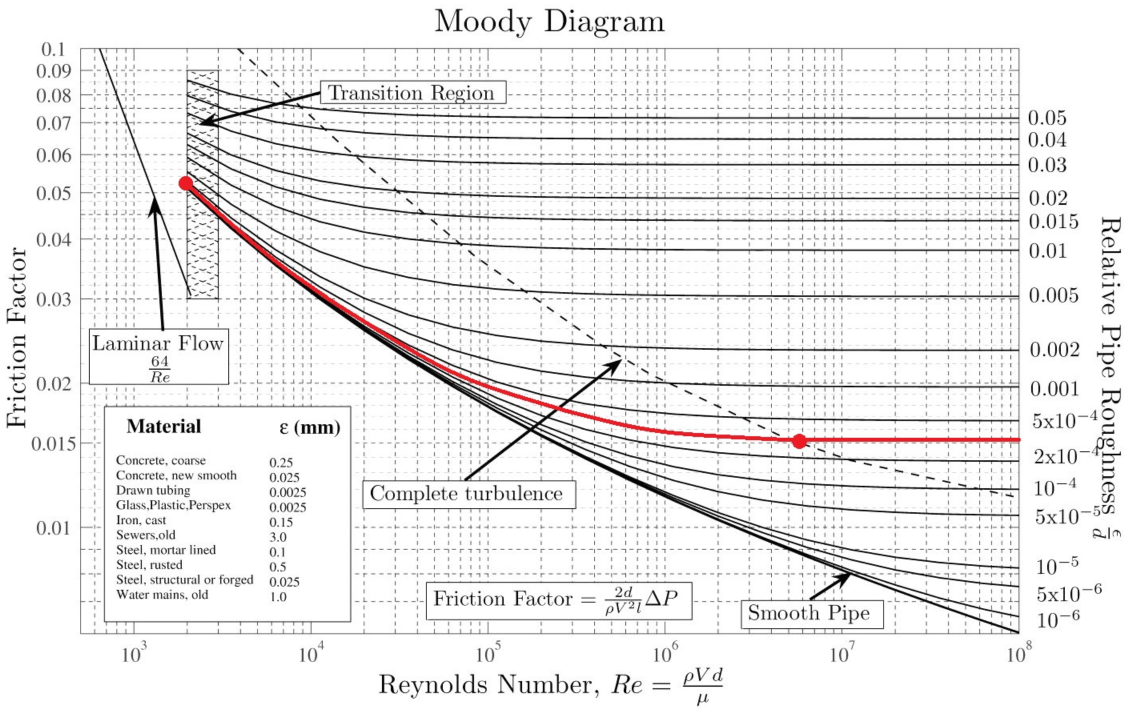

Figure G.3: Moody diagram

From the hydraulic radius the hydraulic diameter can be computed:

$$D_h = 4 * R_h = 1.6m \tag{G.9}$$

For the roughness 'steel rusted' is chosen because it is believed that this comes closest to the properties of a ship hull. Therefore, the relative pipe roughness is calculated with:

$$\frac{\epsilon}{D_h} = \frac{0.5 * 10^{-3}}{1.6} = 0.3125 * 10^{-3}$$

The Reynolds Number is calculated with:

$$Re = \frac{\rho * V * D_h}{\mu} \tag{G.10}$$

$$Re = \frac{1025 * 0.08 * 1.6}{0.00114} = 0.115 * 10^6$$

With this information the friction factor can be derived from the diagram and the **friction factor = 0.019**. This friction factor is based on a fluid velocity of 0.08 m/s, that is the ship's velocity as explained in section 5.1. On closer inspection it is more accurate to express the Reynolds number as a function of fluid velocity, this yields:

$$Re = 0.144 * 10^7 V$$

If one looks at the Moody diagram in the transitional flow regime with the relative pipe roughness of $.3125 * 10^{-3}$ the friction factor is:

$$0.015 < \text{friction factor} < 0.05$$

Because now the friction factor of a culvert with dimensions 1 x 4 is calculated a reduction is needed to approximate the friction factor of a culvert without sides. So the friction is only induced by the bottom and the top of the 'culvert', this is 20% of the total wet parameter. The friction factor is reduced with 80% to arrive at a more accurate friction factor:

$$0.0003 < \text{friction factor} < 0.001$$

In Kolkman (1989) it is stated that the friction coefficient is an averaged over distance friction coefficient. If fully developed flow is not possible in the culvert, the averaged friction coefficient changes slightly following figure 68 from Kolkman (1989). However the culvert considered is long enough to get to fully developed flow and there is no change in the friction coefficient. Besides, the bottom of the ship as well as the bottom of the basin is assumed to have the same roughness, namely of rusted steel. BED PROTECTION ROUGHNESS FACTORS Now, the head loss due to friction can be calculated:

$$\Delta H_{friction} = f * \frac{60}{1.6} \frac{V^2}{2 * 9.81}$$

$$5.7 * 10^{-4} V^2 < \Delta H_{friction} < 0.0013 V^2$$

In reality the bottom of the basin has a different roughness. However it is decided that this can be neglected due to the fact that the energy loss due to friction is very small.

Entrance losses

Entrance loss is calculated with formula G.3. Following Elger, Williams, Crowe, and Roberson (2013) the value for $\varepsilon_{entrance}$ for an abrupt inlet is 0.5. However, this value is for an inlet with two sharp edges as shown in figure G.4. The culvert considered only has one sharp edge, so the the value reduces to 0.25, so:

$$\varepsilon_{entrance} = 0.25$$

This gives a head loss of:

$$\Delta H_{entrance} = 0.25 * \frac{V^2}{2 * 9/81} = 0.01275 V^2$$

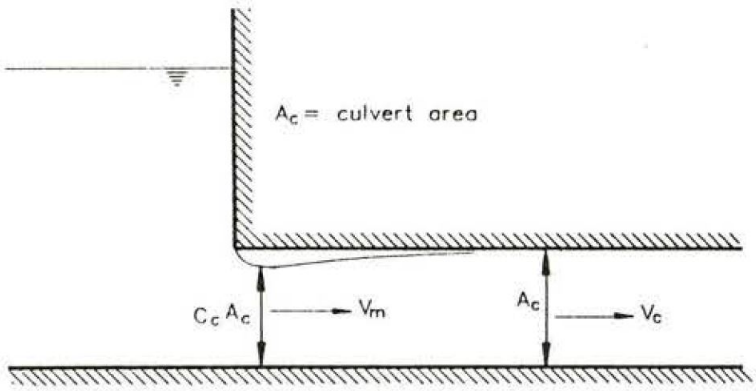

Figure G.4: Flow at sharp edged inlet (Kolkman, 1989)

Exit losses

The outflow of the culvert is abrupt. For an abrupt outflow a zone of separated flow is created. The head loss over the outflow section needs to be considered. With an abrupt expansion the velocity after the expansion is assumed to be 0. Therefore the loss is 1.

$$\varepsilon_{exit} = 1$$

This gives a head loss of:

$$\Delta H_{exit} = 1 * \frac{V^2}{2 * 9/81} = 0.051 V^2$$

Total loss

Now the loss in water head and therefore the loss in velocity under the culvert can be depicted. The total head loss is:

$$0.06432 V^2 < \Delta H < 0.06505 V^2$$

In conclusion, the energy loss in the intermediate flow regime is approximately 6.5 %. The exit loss is the biggest contributor to this, followed by the entrance loss, the friction loss is an insignificant amount.

Loss	Contribution
Exit	78 %
Entrance	20%
Friction	2 %

G.2. Estimating energy losses using ship hydrodynamics

Because the culvert is a representation of our theoretical model of the parallel berthing ship the friction factor is also derived using a ship resistance formula from and compared tot the friction factor derived with the Moody diagram. Ship resistance is usually calculated with the ITTC1957 method from the International Towing Tank Comittee (Kristensen & Lützen, 2012). The total ship resistance consists of friction, incremental and air resistance. Because the focus is on the friction of the ship's hull only the 'under water' part of the ship is into account. The air and incremental resistance are not taken into account. The frictional resistance formula is:

$$C_F = \frac{0.075}{(\log(Re)-2)^2} = \frac{R_F}{\frac{1}{2}*\rho*S*V^2} \tag{G.11}$$

The Reynolds number is calculated as follows:

$$Re = \frac{V_s * B}{\mu/\rho} \tag{G.12}$$

$$Re = \frac{0.08*60}{0.00114/1025} = 0.43*10^7$$

And the wetted surface of the simplified ship per meter is:

$$S = D*B*1 = 20*60*1 = 1200m^2 \tag{G.13}$$

This gives a frictional resistance of:

$$R_F = \frac{0.075*1/2*\rho*S*V^2}{(\log Re-2)^2}$$

$$R_F = \frac{0,075*1/2*1025*1200*0.08^2}{(\log(0.43*10^7)-2)^2} = 1373.664N$$

And a frictional resistance coefficient of:

$$C_F = \frac{0.075}{(\log(0.43*10^7)-2)^2} = 0.00349$$

H Recommendations for further research

The recommendations for further research regarding fender and quay wall design are outlined in this appendix. As seen from the recommendations in chapter 7 the water cushion effect is important for pilots and their berthing manoeuver. However, the water cushion effect is of importance before the first fender impact, from 10 - 1 meters before the quay wall. Therefore, it is expected that the magnitude of the impact on the fender is not influenced by the water cushion effect. The inertia of the vessel during fender impact is important in fender design since the fender decelerates the vessel and therefore inertial forces act on the fender as well, next to the force due to the vessels initial velocity on first impact. To investigate the inertia of the vessel, usually express as added mass or virtual mass, the following research is proposed.

H.1. Berthing manoeuvers - field experiments

To measure the difference in inertia of a vessel in deep water and in shallow water experiment 1 should be executed again. To investigate the influence of velocity on the inertia manoeuver 1 of experiment 1 should be executed twice. The first time with a large velocity such as 20 cm/s, the second time the velocity should be in the order of 6 cm/s. Manoeuver 2 should be executed with 6 cm/s just like in experiment 1. However, manoeuver 2 should not be done in vicinity of the quay wall. With these berthing manoeuvers the relationship between velocity and inertia en the relationship between water depth and inertia can be investigated.

H.2. Measuring tugboat forces - field experiments

To measure the inertia of the vessel during acceleration and deceleration of the vessel in a shallow basin, the most straight forward way is placing dynamometers on the tugboats that push the vessel laterally to the quay wall. To execute this two or three tugboats need to be adapted such that a dynamometer can be placed on the ship's hull. This should be a construction consisting of a large cushion or bumper that has a shape such that the total force is led to one contact force which can be led through the dynanometer. If one could measure the forces that are exerted by the tugboats on the lateral moving vessel and measure the position during these berthing manoeuvers through the PPUs two different forces are measured. The force from the tugboats pushing the vessel forward and the force derived from the deceleration and acceleration following Newton's second law and the mass of the vessel. The difference between those two forces are the counteracting hydrodynamic forces acting on the vessel, the inertia. A measurement campaign with these tugboats in combination with different vessels and different berthing sites should be prepared. When the inertia for different vessels with different velocities and different under keel clearances is measured, the results can be investigated and conclusions can be drawn on the inertia of the vessels and therefore the virtual mass of the vessels. The relation between the virtual mass and the actual mass of the vessel can be derived empirically to refine the virtual mass factor in the guidelines.

H.3. Measuring fender forces - field experiments

To measure the force acting on a fender during berthing, the fender displacement should be measured. If the fender displacement can be measured, using the material properties and their degradation curve over time, the force exerted on the fender can be calculated. This is difficult since there is no easy way to measure the fender displacement. An option could be cameras and using imaging techniques that are installed at the quay wall and send their information regularly to a computer. If this could be measured accurately, material property tests for each fender need to be done to obtain an accurate force acting on the fender. The material property guaranteed by the manufacturer and their degradation curve is usually not very reliable.

H.4. Inertia - scale experiments

Executing the field experiments with the berthing manoeuvers, the dynamometers on the tugboats or the fender forces is very expensive, time consuming and maybe not a realistic goal. A good alternative is scale experiments. Scale experiments for ship manoeuvering at for example Deltares are executed regularly. A scale experiment for the lateral berthing manoeuver to a closed-quay wall is an option for determining the force executing on the fenders or the hydrodynamic counteracting force acting on the vessel when pushed by the tugboats. Furthermore, the berthing manoeuvers in shallow and deep water without a quay wall can be investigated through scale experiments as well. Using the model rules of Froude the following dimensions are proposed. The Froude number should be the same for the model as for the actual size.

$$Fr = \frac{V}{g * L} \tag{H.1}$$

$$\frac{V_m}{g * L_m} = \frac{V}{g * L} \tag{H.2}$$

$$\frac{V_m}{L_m} = 0.0002 \tag{H.3}$$

Which means that if the model of the vessel is 1 meter long, the velocity of the vessel should be 0.02 cm/s. Using Froude scaling, the scale experiments could be executed accurately and reliable conclusions can be drawn.